FUNCTIONAL MAGNETIC RESONANCE IMAGING (fMRI) *STUDY OF* THE TRIGEMINAL SOMATOSENSORY SYSTEM IN HEALTHY VOLUNTEERS AND PATIENTS WITH TRIGEMINAL NEURALGIA

Thesis submitted in accordance with the requirements of the University of Liverpool for the degree of Doctor of Medicine by

SURAJIT BASU

SEPTEMBER 2010

UNIVERSITY OF LIVERPOOL

Faculty of Medicine

DECLARATION IN HIGHER DEGREE THESES

DECLARATION

This thesis is the result of my own work. The material contained in the thesis has not been presented, nor is currently being presented, either wholly or in part for any other degree or other qualification

I have conceived the hypothesis, obtained approval of ethics committee for undertaking the research, participated in data acquisition sessions, and have analysed and interpreted the obtained data.

The fMRI data acquisition was carried out in collaboration with Dr Arshad Zaman. Dr Zaman and clinical colleagues helped in volunteer and patient recruitment.

The research was conducted at the facilities of the Pain Research Institute, Liverpool University, United Kingdom.

Surajit Basu

September 2010

Acknowledgements

I express my thanks to all members of the staff at the Pain Research Institute of Liverpool University for their support during the preparation of this work and to the patients and volunteers who participated in this study. My thanks also go to Mrs Kate Maciver, Dr Arshad Zaman and Miss Caroline Hayhurst for their help, without which this study would not have been possible. I also sincerely thank Prof. T.J. Nurmikko and Mr. Paul Eldridge for their help and guidance. Finally, my wife, Mausumi and son, Souradeep, gave me the encouragement to pursue this research to its conclusion, I am thankful to have them by my side.

to my parents

my inspiration

Abstract

FUNCTIONAL MAGNETIC RESONANCE IMAGING (fMRI) STUDY OF THE TRIGEMINAL SOMATOSENSORY SYSTEM IN HEALTHY VOLUNTEERS AND PATIENTS WITH TRIGEMINAL NEURALGIA

Surajit Basu

Introduction: Neuropathic Pain originates from damage to the nervous system that maintains a painful perception without the presence of a continuous peripheral nociceptive cause. This study aimed to investigate such changes in the nervous system in patients with trigeminal neuralgia, an 'ideal pathological chronic pain' model from that of healthy volunteers by a comparative study of neural functions through a set of specific sensory stimulation and an fMRI based activation analysis. The comparative study was extended to include patients suffering from trigeminal neuropathy to generate an intrapathology comparison and an understanding of pathology specificity of the changes observed.

Materials and methods : Ten healthy volunteers and thirteen patients (11 neuralgia , 2 neuropathy)) in the age group of 40-75 years underwent fMRI based experiments consisting of serial stimulations of the three trigeminal areas of the face and ipsilateral thumb with air puffs and noxious heat. The fMRI data was pre-processed. We introduced a novel event identification technique- 'micromotion' by detection of 3D spatial movement from motion correction time course data. The micromotion identified patient movements due to an effect of a stimulus and was found to be a sensitive marker of allodynic and neuralgic events. Single and multi subject analysis were conducted on the data, and compared. Comparisons were made with homologous healthy volunteers' data. The neuralgia group was further divided on the basis of symptoms and micromotion and detailed analysis of activation through symptoms progression were made. A revised predictive protocol was used for analysis of the neuralgic attack event based on micromotion. We used False Discovery Rate (FDR) as error correction tool for multiple comparisons.

Results : Tactile innocuous stimulation activated predominantly the contralateral area 2 of the primary somatosensory cortex in healthy volunteers without any cingulate or insular stimulation. Thermal pain activated predominantly the contralateral area1 of the primary somatosensory cortex along with bilateral anterior insular and cingulate activations. In patients with trigeminal neuralgia, a shift of activation pattern was identified. The activations from the air puff stimulation drifted towards area1 of the primary somatosensory cortex along with the activation of anterior insula and cingulate gyrus. The noxious heat activation instead occupied the area 2 of the primary somatosensory cortex. Patients with trigeminal neuropathy maintained healthy volunteers activation pattern but were hypersensitive to thermal pain with formation of large activation clusters in anterior insula, bilateral S1 and the cingulate gyrus. Activation during allodynia showed a harmonic response from the whole of known pain neuromatrix . A neuralgic attack using the same airpuff protocol, demonstrated cortical activation to a predominantly contralateral primary somatosensory cortex area 1. The analysis undertaken following a 'revised predictive protocol' suggested a cortical spread of activity from a seed of previous activation focus on the SI cortex. This seed was the peak activation voxel during allodynic response and the only cluster that was visible during analysis of neuralgic attack data set using the uncorrected protocol. This activity at the point of neuralgic attack was not associated with brain stem or sensory thalamic activity, suggesting the neuralgic attack could be a cortical based phenomenon, like a sensory fit. Thus discrete activation of the primary somatosensory cortex with spread of cortical activity and a reproducible variation of fMRI activation pattern from a healthy state was demonstrated.

CONTENTS

CHAPTER 1: INTRODUCTION 3

CHAPTER 2: REVIEW OF LITERATURE 6

Anatomy of the trigeminal somatosensory system 6
- Trigeminal ganglion 6
- The brain stem nucleus of trigeminal nerve and central connections 7
- Somatotopy within trigeminal sensory system and its development 8
- Somatotopy : Cortex 10
- Somatotopy : Thalamus 12
- Somatotopy: Brain stem nucleus of trigeminal nerve 12

Components of the sensory nervous system 13
- Receptors and fibres 13
- The dorsal horn 14
- Ascending tracts 16
- The supporting cells of the nervous system 17

Pathophysiology of trigeminal neuralgia and neuropathic pain 18
- Changes in axon and dorsal root ganglion following chronic compressive injury of a peripheral nerve 20
- Changes in the dorsal horn 21

Principles of fMRI 21
- Physiological basis of BOLD signal 24
- Concepts of neurovascular coupling 27
- Anatomical basis of BOLD signal 28

fMRI in pain studies 29

CHAPTER 3: MATERIALS AND METHODS 34

Ethics 34

Subjects 34
- Inclusion and exclusion criteria 35
- Pre-scan screening 36

Equipments and set up 36

The experiment 37
- Functional imaging 37
- Report of pain experience and elicitation of tactile allodynia /unpleasantness or neuralgic attack 39

fMRI Data Analysis 39

CHAPTER 4: POST PROCESSING ANALYSIS AND RESULTS 45
Analysis of pre scan screen and post scan patient report 45
Identification and verification of unpleasantness/allodynia or neuralgic attack response from 3D motion correction algorithm 48
Analysis of activations in healthy volunteers 51
Analysis of activations in patients 61
Analysis of fMRI runs of trigeminal neuralgia patients classified by 'micromotion' 68
A single patient study through allodynia – neuralgia phase and correlation with micromotion 69

CHAPTER 5: DISCUSSION 80

CHAPTER 6: SUMMARY AND CONCLUSION 99

BIBLIOGRAPHY 101

Chapter 1: Introduction

Pain is an unpleasant sensory and emotional experience associated with or potential tissue damage. Pain is a polymodal sensation. The neural structure responsible for the sensation of pain not only carries discriminatory information about 'what and where' but also produces an affective response. The processing of a sensory stimulus including a painful stimulus in primates and humans take place at multiple levels of the central nervous system (CNS). In the CNS, the well-recognised synaptic stations are at the dorsal horn, brain stem, hypothalamus-thalamus and the cerebral cortex. The concept of a 'pain neuromatrix' was introduced to define all these parts of the central nervous system involved that are in processing of sensation of pain (Melzack 1990).

Neuropathic pain originates from damage to the nervous system that maintains a painful perception without the presence of a continuous peripheral nociceptive cause. Its prevalence is estimated at 7-8% of general population in Europe (Bouhassira et al., 2008). In the clinical setting, patients suffering from this kind of

pain will lack any anatomical or biochemical diagnostic criteria that would differentiate the painful from the non-painful forms of neuropathy. The diagnosis often hinges on clinical history alone and not uncommon to have significant differentials. To investigate neuropathic pain and appreciate the changes of the nervous system, it is imperative to understand how the function of the nervous system has altered in these conditions.

Functional Magnetic Resonance Imaging (fMRI) is a non invasive tool which can help investigate and demonstrate the anatomical substrates of the neuronal network which can be described as the pain matrix (Neuromatrix). fMRI has been used extensively to investigate activities of the human brain in the past decade. Most of these researchers investigated and confirmed the previous knowledge of classical anatomy, physiology and neural connectivity. There is also a current explosion of research into fMRI based investigations to identify brain areas involved in computation/actioning of tasks, designed to investigate motor, sensory and affective systems (event related fMRI). However fMRI has not become a routine 'function based' diagnostic tool. The activations of the brain areas manifested after an fMRI statistical analysis remained subtle and required multi subject analysis to achieve any meaningful statistical significance. Thus, this type of analysis precluded any single patient analysis with confidence for diagnostic purpose, where such an opportunity existed.

The wider availability of 3 Tesla MRI scanners raised the prospect of a higher signal to noise ratio for fMRI analysis and opened the prospect of a single subject analysis and investigation of functional disease states like neuropathic pain in a clinical context.

Trigeminal neuralgia is a chronic neuropathic pain condition. The diagnosis of trigeminal neuralgia is clinical. There is no confirmatory diagnostic investigation available for trigeminal neuralgia. The differentials of other painful facial conditions, especially trigeminal neuropathy has to be considered in patients with atypical symptoms even in the presence of a well recognised structural cause (vascular contact at root entry zone). A successful outcome following treatment, particularly surgical decompression is reliant on an accurate diagnosis of the condition. Trigeminal neuralgia is a model pathological neuropathic pain condition. Gaps in the

knowledge about the pathophysiology of trigeminal neuralgia exist, as well as a clinical need to understand the pathophysiology and availability of a diagnostic test.

The research aimed to address the above issue by investigating the functional pathophysiology of the trigeminal somatosensory system in healthy volunteers and patients suffering from trigeminal neuralgia and other facial pains (like trigeminal neuropathy), using fMRI as a tool.

The research proposed that a difference in the activation pattern of the trigeminal somatosensory system exist between healthy volunteers and patients suffering from chronic facial pains, particularly trigeminal neuralgia and trigeminal neuropathy in the context of this research. This research aimed to demonstrate this difference in activity through experimentally evoked sensations, and use of fMRI as a detection tool, in an effort aiming to characterise the differences and develop an fMRI based diagnostic criteria for clinical use.

This research also explored the development of methodology and fMRI analysis protocol to administer the above as a diagnostic tool.

Chapter 2: Review of literature

Anatomy of the trigeminal somatosensory system

Trigeminal Nerve is a mixed nerve and the major sensory nerve of the face. It also innervates the muscles of mastication. It has ophthalmic (V1), maxillary (V2) and mandibular (V3) divisions. The three divisions converge at the trigeminal ganglion, located at the Meckel's cave, in the middle cranial fossa. The unified sensory root leaves the trigeminal ganglion and traverses the pontine cistern to enter brain stem through the middle cerebellar peduncle.

Trigeminal ganglion

The trigeminal ganglion is the sensory ganglion of the trigeminal nerve, similar to the dorsal root ganglion (DRG) of the spinal nerves. The ganglion houses cell bodies of the sensory neurons and supporting glial cells along with the

sympathetic fibres. There are around 25000-35000 neurons present in the trigeminal ganglion (Laguardia JJ,Cohr RJ, Gilden DH, 2000). The neurons of the trigeminal ganglion are morphologically classified as bipolar. Except for a few proprioceptive neurons, which have their cell body at the mesencephalic nucleus of the trigeminal brainstem nucleus complex, the trigeminal first order sensory neurons all have their cell body at the trigeminal ganglion. Trigeminal ganglion does not contain any synapse of the sensory or motor system. The capillary architecture of the ganglion is similar to that of the central nervous system (Smoliar et al., 1998)

The brain stem nucleus of trigeminal nerve and central connections

The central processes of the trigeminal sensory neurons, carrying information about pain, temperature and crude touch dips into the substance of pons and medulla to synapse with the second order neurons at the spinal nucleus of the trigeminal nerve. The spinal nucleus of the trigeminal nerve extends up to upper border of the lamina of second cervical vertebra and is homologous of substantia gelatinosa of the cervical cord. Some fibres from the lower cranial nerves and upper cervical root also synapse at the spinal nucleus of the trigeminal nerve. The spinal nucleus is somatotopically arranged with the fibres originating farthest from the mouth relaying at lowest part of the nucleus. This arrangement of facial innervations is popularly termed as 'onion skin'. The second order neurons from the spinal nucleus cross the midline and ascend as the ventral trigeminal tract (homologous to lateral spinothalamic tract in the spinal cord) to reach ventro-posterior medial (VPM) nucleus of the thalamus. The third order neurons from thalamus, relay to cortical areas.

The fibres carrying discriminatory information of light touch and two point discrimination relay at the main sensory nucleus of the trigeminal nerve at the upper border of pons, above the level of entry of the trigeminal root and rostral to the spinal nucleus of the trigeminal nerve. The second order neurons (homologous

to spinal dorsal column) ascend in the dorsal trigeminal tract as both crossed and uncrossed fibres (Rengachary SS , 1996). They relay at VPM on both sides and project to corresponding cortical areas.

Proprioceptive sensation from muscles of mastication and jaw are relayed at mesencephalic nucleus.

Fig 2.1 Brainstem nucleus complex of the trigeminal nerve

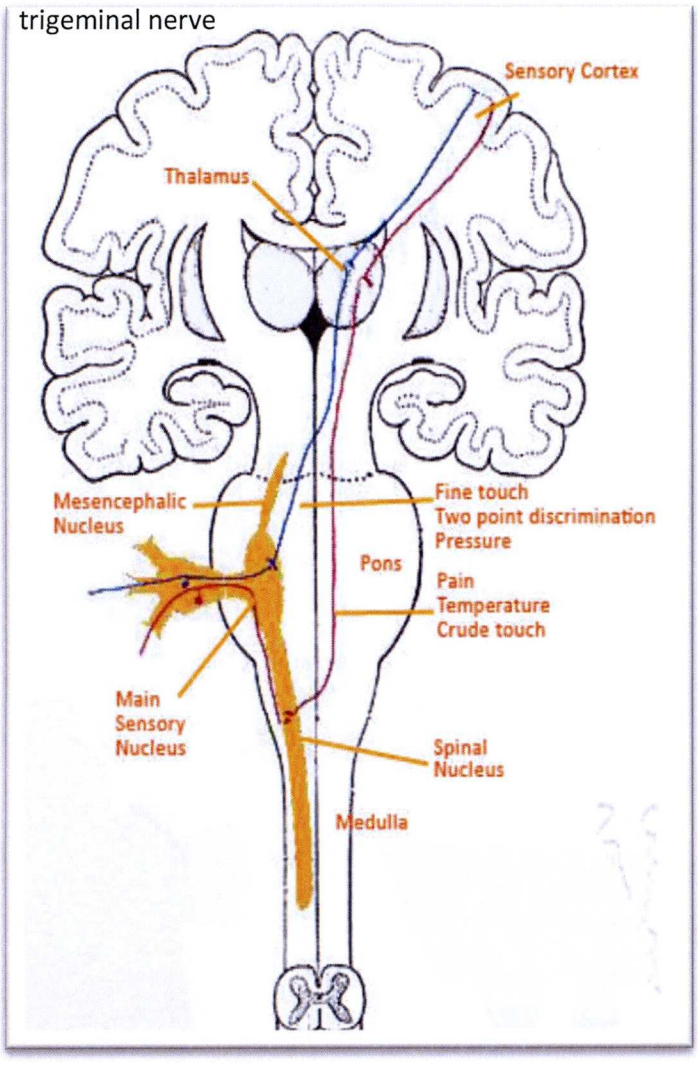

Somatotopy within trigeminal sensory system and its development

Trigeminal sensory system, carrying somatosensory information from the face is somatotopically organised. Somatotopic organisation of the trigeminal ganglion , the descending nucleus of trigeminal nerve, VPM and the somatosensory cortex has been proven by staining studies (Rengachary SS , 1996), electrophysiology and more recently by functional neuroimaging.

The study of the development of trigeminal sensory system in rodents and the recent discovery of the role of molecular signalling in the establishment of somatotopy has helped in understanding how a sensory signal is processed. It has been shown that during embryonic development there is a dorso-ventral

differential expression of genes in the trigeminal ganglion. Retrograde signalling by bone morphogenetic protein (BMP), helps in the

differential expression of the genes in trigeminal neurons, that in turn, codes spatial distribution of these neurons to topography of the face (Hodge et al., 2007). The central processes of these labelled neurons establish a somatotopic map of the face in the brain stem second order neurons by positional patterning of the gene expression. This becomes the first somatotopically defined structure in the developing trigeminal pathway within brain (Erzurumlu et al., 2010). This map is serially copied at each level and finally on to the neocortex by matching molecular signals from the periphery (face) and from the cortical neurons (Inan and Crair, 2007). The neurons of the developing cortex carries neighbour relationship molecular cues derived from the parent ventricular zone neurons (O'Leary and Borngasser, 2006). The guidance cues from the neurons help thalomocortical neurons to connect appropriately (Catalano and Shatz, 1998). This may be in the form of pioneer neurons that had dilineated the path of migration or by the gradient of patterning molecules (Fukuchi-Shimogori and Grove, 2001). The continuing activity of the cortical neurons are necessary for appropriate connections to be made by the thalamocortical neurons (Catalano and Shatz 1998). The development of thalamocortical neurons and cortical neurons are independent at the start but that is lost once cortical connections are made (Cohen-Tannoudji et al.,1994). Rodents develop 'Barrels', which are sensory units, in the somatosensory cortex. Each barrel receives information from only one whiskers, thus establishing a precise somatotopic pattern (Inan and Crair,2007). The maturation and refinement of these connections and development of the inter area connections are determined greatly by continuing influence of the thalamocortical neurons (Jensen and Killackey 1987). It is shown that continuing expression of barrel cortex specific marker post-natally is dependant on active innervation of the cortex by thalamocortical neurons (Gitton Y et al., 1999).

The developing somatosensory cortex shows plasticity. The area subserving a particular part develop bigger representation in the cortex if sensory input from the periphery increases and vice versa. The neighbouring represenations enlarge

to take up the space if any row of whiskers are denervated during development (Van der Loos and Woolsey 1973).

Somatotopy : Cortex

Somatotopic organisation in the somatosensory cortex has been well studied. Penfield (Penfield and Boldrey 1937) described the sensory and motor homonculus on either side of the central sulcus in the parietal cortex by direct cortical stimulation. Somato sensory evoked potential was used by Woolsey (Woolsey et al., 1979) to describe a similar representation. This area, receiving somatosensory afferents was designated as primary somatosensory area. This classical simplistic description has been challenged by later investigators. Direct cortical recordings in primates (Kaas et al., 1979; Pons et al., 1985), and functional imaging studies suggest a more complex and multiple representative areas of the body in the primary somatosensory cortex (Iannetti et al., 2003; Servos et al., 1999). Four anterior parietal somatosensory fields have been now described along with atleast two other maps in lateral parietal cortex, Somatosensory Area II and Parietal Ventral PV) area (refer to table 2.1) in the primates. The non human primate work was extrapolated to humans (Disbrow et al.,2000; Geyer et al.,2000). These two areas occupy the upper bank of lateral sulcus and thought to be involved in the tactile discrimination. Somatosensory somatopic maps have also been described in the insular cortex (Ostrowsky et al., 2002)

Somatosensory area		Function	Reference
Primary Somatosensory Cortex (SI)	Area 1	Cutaneous Receptors	(Kaas et al. 1979)
	Area 3b	Cutaneous Receptors	(Kaas et al. 1979)
	Area 2	Deep receptors Directional stimulus	(Pons et al. 1985)
	Area 3a	Deep sensation and muscle spindle	(Wiesendanger M, Miles TS, 1982)
Secondary Somatosensory cortex (S II)	Area S2	Moving stimulus Microgeometric or roughness discrimination Bilateral activation	(Krubitzer et al.,1995) (Disbrow E, Roberts T, Krubitzer L, 2000)
	Parietal Ventral area (PV)	Complex processing Moving stimulus Bilateral activation	(Krubitzer et al.,1995) (Disbrow E, Roberts T, Krubitzer L, 2000)
Somatosensory maps in insular cortex		Pain, Visceral Pain	(Ostrowsky et al., 2002)

Table2.1: Somatosensory body maps in parietal cortex

Nguyen (Nguyen et al 2004) used magnetoencephalography (MEG) and found that the area of upper face covered with skin is represented in a very small area between that of thumb and lips, which dominated the facial representation in the somatosensory cortex. The thumb occupies a more superior, posterior and medial position compared to the lower lip as was suggested by Penfield. However he was unable to find consistency in the location of rest of the facial topography. The extensive representation of thumb and lips in humans are not contrary to expectations considering their role and mechanoreceptor density (Stohr M, Petruch F, 1979). Manger (Manger et al., 1997) suggested that in the homunculus, there is a limiting boundary between representative area of body-

hand-neck- lower jaw (innervated by spinal roots) and face (innervated by trigeminal nerve). He showed that the inter-connections exist between cortical areas representing structures innervated by the spinal dermatomes or by the trigeminal but not in between these two areas. This finding has implication on how cortical reorganisation could happen following deafferentiation or how a cortical based stimulation would spread (Manger et al., 1997).

Somatotopy : Thalamus

The ventro- posterior thalamus (VPL and VPM) contains well developed representation of the body. VPM relays sensation from the trigeminal receptive zone. The somatosensory thalamus contains columns of neuron that are organised antero-posteriorly parallel to its lateral border. The anterior dorsal part transmits joint position and muscle stretch sensations, the middle part is utilised for cutaneous sensations. Each column communicates with specific cortical units (Apkarian et al., 2000). Sensory thalamus also has mediolateral somatotopic organisation. The face and upper body segments are represented in the medial part while lateral part relays sensation from the trunk and the lower limbs. Apkarian suggested presence of nociceptive and nonnociceptive neurons in the thalamus, which are segregated. He demonstrated by multi unit recordings, the population properties, interneuronal connectivity and inter-dependancy of the thalamic neurons. He demonstarted a 'centre-surround' organisation within the thalamus and suggested this to be one of the mechanisms that cause large cortical inhibition associated with painful sensations. (Apkarian et al., 2000).

Somatotopy: Brain stem nucleus of trigeminal nerve

The central processes of trigeminal afferent neurons carrying pain and temperature sensations enter the brain stem and project caudally as the spinal trigeminal tract. They synapse with the second order neurons in the spinal nucleus of the trigeminal brainstem nucleus complex. The sensory neurons, originating

from the perioral area synapse more rostrally than the neurons originating farthest from the mouth (Bushnell et al.,1984; Kunc Z, 1970). This arrangement is popularly called the 'Onion Skin' somatotopy. The arrangement may not be very strict and it can only be said that the ophthalmic division fibres may not terminate as low as mandibular division and vice versa (Lee J, 2008). The determinants of this somatotopic organisation have been described in the previous section. The main sensory nucleus of the trigeminal nerve sub serves light touch and two point discrimination. This nucleus is much more compact and a large nucleus situated in pontine tegmentum (Lee J, 2008). The somatotopy in trigeminal brain stem nucleus has been demonstrated with the help of fMRI (Borsook D, Burstein R, Becerra L, 2004).

Components of the sensory nervous system

Receptors and fibres

Cutaneous receptors transduce environmental information and present them to the CNS. It is practical to classify these receptors according to the conduction velocity of the nerve fibres they are associated with. This depends upon axon diameter and myelination. In hairy skin (like skin of face), large diameter, myelinated fibres (A-alpha) are associated with low threshold mechanoreceptors. The low threshold mechanoreceptors can be rapidly adapting type, responding to movement of the skin only and slow adapting type, that responds to movement and distortion of the skin surface.

A-delta fibres have smaller axon diameter and are thinly myelinated. They can be low threshold mechanoreceptor of D hair type or high intensity mechano-nociceptor (Adriaensen et al., 1983). Described by Brown and Iggo (Brown and Iggo, 1967), the D hair receptors, taking its name from 'Down Hair', are very low threshold mechano receptors. Mechano nociceptors are thinly myelinated A-delta fibres. They form free nerve endings in the epidermis (Kruger L, Perl ER, Sedivec

MJ, 1981). These fibres can be subdivided into those who additionally respond to noxious heat and cold sensation. This additional character is present in around 20% of the population of these fibres in rodents (Cain et al., 2001; Caterina et al., 2000).

The unmyelinated and thin nerve fibres are called C fibres. They have slow conduction velocities. They form 60-70% of the primary afferent neurons originating from the skin (Lewin GR, Moshourab R., 2004). C fibre receptors have been classified by the modality by which they can be stimulated. Some C fibre nociceptors are called 'sleeping nociceptors'. They are found in the skin as well as joint and on the visceral surface (McMahon SB, Koltzenburg M, 1990). Some of them are insensitive to both mechanical and heat stimulation in normal conditions. In humans they can be 15-20% of C fibres nociceptors in the skin (Weidner et al.,1999). They are classified as C-MiHi (C mechano insensitive and heat insensitive). C fibres can be sensitised by capsaicin, prostaglandins, and bradykinins. C-MiHi fibres can be rapidly sensitised to heat and mechanical pressure stimuli on exposure to capsaicin and other algogens (Meyer et al., 1991; Schmidt et al.,1995; Kress et al., 1992). This demonstrates the reserve capacity of C fibre nociceptors to become alive in disease conditions or when algogens are present in the environment.

The dorsal horn

Dorsal horn of the spinal cord and its homologous (the brain stem trigeminal nucleus) receive sensory exteroceptive, proprioceptive and interoceptive afferent inputs (Lee J, 2008) and act as a gate-way for the afferent information to arrive at the spinal cord (central nervous system). Spinal cord grey mater, of which dorsal horn is a part, is arranged in layers (called Rexed's lamina) on the basis of cell type, size, staining characteristics, connectivity and position within the spinal cord. Layers I-VI together form the dorsal horn (please see table 2.2).

Lamina layer	Morphology (Lee J, 2008)	Receives	Neuron type (Lee J, 2008) (Scadding J, 2000)
I	Variable size cells, meshed in fibres of differing diameters	Cutaneous Nociceptive C fibres	High threshold
II	Dense packed, small neurons, No myelinated fibres	Cutaneous Nociceptive C fibres	High and low threshold
III	Larger neurons, loosely packed, myelinated fibres	Cutaneous , non nociceptive	WDR, Low threshold
IV	Cells of variable size, intermingled with fibres	Cutaneous, non nociceptive A fibres, A-delta	WDR, High threshold, Low threshold
V	Cells of variable size and bundles of fibres	Cutaneous, muscle and visceral afferents	WDR, High threshold, Low threshold
VI	Cells of variable size and bundles of fibres	Cutaneous and Proprioceptive afferents	WDR and both low and high threshold neurons, low threshold muscle afferents
VII and VIII (Ventral Horn)		Deep somatic muscle and joint sensation also some Cutaneous sensation	High threshold, WDR, low threshold neurons, interneuron

Table 2.2: Lamina of the dorsal horn

The deeper layers of dorsal horn receive afferents from the layers dorsal to them, in a 'cascade' fashion, causing more complex connectivity in deeper layers (Scadding J, 2000). Dorsal horn processes the afferent signal most of the time, than transmitting it upstream unmodulated. Gate control theory of pain (Melzack R, Wall PD, 1965) is a classical example of dorsal horn modulation of sensory afferent impulse. It was proposed that myelinated afferents terminating in deeper lamina of dorsal horn (lamina IV) are also excitatory to interneurons that terminate at lamina I or II (substantia gelatinosa of Rolando). These inhibitory interneurons, when excited, cause presynaptic inhibition of forward propagation of any afferent signal to spinothalamic tract, effectively closing the gate for

afferent input through the dorsal horn. The afferent impulse through dorsal horn also gets modulated by descending control from, for example reticulospinal, rubrospinal tracts. The complexity of function of dorsal horn is not fully understood. Four functional states of dorsal horn have been described (Scadding J, 2000). They are physiological, suppressed, sensitised and reorganised. The last two states will be discussed later.

Ascending Tracts

The ascending tracts in the spinal cord and the homologous tracts of the trigeminal system carry sensory information to the brain. They are the second and third order neurons of the system with two synaptic nodes on their pathway before reaching the post central cortex. The two main tracts are the spinothalamic tract and the dorsal column. (Lee J, 2008)

The dorsal column is the first order neuron with uncrossed fibres in the spinal cord. They relay at nucleus gracilis and cuneatus in medulla. The second order neuron decussate and ascend in the medial leminiscus to reach contralateral ventro-posterior thalamus. The third order neuron from thalamus projects to the somatosensory cortex.

The spinothalamic tract ascends in the anterior and lateral part of the spinal cord. They convey sensation of pain, temperature and non-discriminatory touch. The cells originate from lamina I, IV –VIII but mostly from VI and VII. Spinothalamic tract relays at ventral –posterior thalamus like dorsal column fibres. They project to somatosensory cortex. A minor percentage of the spinothalamic tract fibres, mostly from lamina I of the dorsal horn may terminate within the parabrachial area and project to limbic structures. These fibres may generate an affective response (Hunt PS, Mantyh PW, 2001).

The spinoreticular tract originates from the cells in lamina VII and VIII, and the spinomesencephalic from lamina I. They are concerned with generation of affective response from a sensory stimulus.

The spinothalamic and dorsal column tracts show somatotopic arrangement and lamellar organisation. Somatotopy in the thalamus has been described before.

The supporting cells of the nervous system

(Astrocytes, Oligodendrocytes and Microglia)

The cellular components of the nervous system can be divided into two categories, neuronal and non-neuronal. Neuronal component – neurons are the electrically excitable cells that can generate action potentials while the glial cells cannot. The conventional concept of organisation of nervous system places glial cells in a supporting role while neurons are the active cells of the nervous system. However recent evidence and understanding of the glial cell function, complexity of their structure and their regulatory role has put the glial cells in a

	Astrocytes	Oligodendrocytes	Microcytes
Developmental	Neuro and gliogenesis Synaptogenesis and maintenance of synapses		
Structural	Scaffolding cells in CNS	Formation of myelin	CNS scavengers
Vascular	Regulator of cerebral microcirculation and neurovascular coupling		
Metabolic	Provides energy substrate to neuron and removes waste and excess		
Homeostasis	Maintenance of extracellular homeostasis		
Signalling	Modulation of synaptic transmission Volume transmission		Sensitisation following CNS damage

Table 2.3: Functions of the glial cells (Verkhratsky and Butt, 2007)

central role of generation, maintenance and regulation of the nervous system.

The glial cells have two lines of origin. Astrocytes (star-like cells with multiple processes), oligodendrocytes (cells with fewer processes) and ependymal cells originate from neural progenitors. The microglia is mesodermal in origin, they invade CNS during development. The function of the glial cells reflects their cellular lineage. In humans, glial cells form around 50% of the volume and 60% of the cellular population of the nervous system. Description of the glial cell functions are summarised in table 2.3. The astroglial function of synaptogenesis, maintenance, and removal of synapse along with their function of modulation of synaptic transmission assumes importance in the perspective of neural plasticity and chronic pain. The microglia has recently been implicated with changes in the dorsal horn following nerve injury and the genesis of chronic pain (Verkhratsky and Butt 2007).

Pathophysiology of trigeminal neuralgia and neuropathic pain

Trigeminal Neuralgia (TGN) is a chronic neuropathic pain condition characterised by intense brief sharp painful episodes (often described as electric shock) in the face area innervated by the trigeminal nerve branches. It has also been called 'tic douloureux' because of the typical facial movement that a patient will do when the painful episode strikes. 'International Association for the Study of Pain' (IASP) has defined TGN as 'sudden, usually unilateral, severe, brief stabbing and recurrent in nature along the distribution of one or more branches of the Vth cranial nerve' (Merskey and Bogduk, 1994). International headache society has elaborated the disease in their definition or diagnostic criteria and mentioned trivial peripheral triggers as well as the spontaneous episodes and the feature of long periods of spontaneous remission. Nurmikko and Eldridge classified TGN into two variants to encompass the clinical spectrum that is encountered. The 'Liverpool Criteria' classifies TGN into typical and atypical. The neuralgic pain in the atypical variant lasts longer with appearance of some residual constant

discomfort in the face. Trigeminal neuralgia may be symptomatic or idiopathic. The symptomatic TGN happens in association with multiple sclerosis (MS), cerebello-pontine angle tumour or in presence of a vascular compression of the nerve at or near the trigeminal root entry zone. In idiopathic TGN, no cause can be found (including vascular compression).

The presence of a vascular compression at the trigeminal nerve root entry zone in a patient with symptoms of TGN provides a definitive way of management of these patients. Though the concept of vascular compression as a causative feature was introduced earlier, decompression of the trigeminal nerve root was seriously undertaken by Gardner and Miklos (Gardner and Miklos,1959) and later popularised by Jannetta (Jannetta PJ, 1977). It is undisputable that a large volume of patients seen in the clinical practice with features of TGN will have a vascular compression at the trigeminal nerve root entry zone and will benefit from a decompression of the nerve (Barker et al., 1996; Sarsam et al.,2010). It is fair to conclude simply from the surgical experience that the process of decompression of the nerve at the root entry zone causes a change that delivers the longest symptomatic relief. A further observation that a MS plaque at trigeminal root or near its intraparenchymal part (Gass et al., 1997) can cause TGN, adds to the fact, that it is the peripheral nerve that possibly is the generator of the pain rather than any other part of the trigeminal system.

TGN does not cause clinical sensory impairment. However in experimental setting, it has been proved that there is a raised threshold to touch and temperature sensitivity on the affected side (Bowsher et al,. 1997) which normalises following decompression (Miles et al., 1997). Electron microscopy of trigeminal ganglion in TGN has shown hypermyelination and microneuromata formation (Beaver DL, 1967). The pathophysiology of spontenuous neuralgic attacks or following triggering has been attributed to changes following chronic constrictive injury. It is now shown that following chronic constrictive injury (CCI) of a peripheral sensory nerve, spontaneous ectopic subthreshold and spike potentials are generated in the corresponding dorsal root ganglia (Amir et al.,1999). The molecular explanation for these spontanuous activities is now well understood. A

vascular compression at root entry zone or an MS plaque can well be considered as a chronic compressive agent on the trigeminal root.

Changes in axon and dorsal root ganglion following chronic compressive injury of a peripheral nerve

Injury to a peripheral nerve can produce spontaneous pain, tactile allodynia, heat hyperalgesia; the features of chronic neuropathic condition. In experimental model of chronic neuropathic pain (nerve ligation model causing chronic constrictive injury), spontaneous activity of the injured nerve fibres are observed. Chaplan et al., (Chaplan et al., 2003) demonstrated that the increased spontaneous firing is due to increased activity of hyperpolarisation-activated; cyclicnucleotide modulated (HCN) channels on the cell body of the damaged axonal fibres present in the dorsal root ganglia. Accumulation of HCN channel proteins are since been demonstrated at injured axonal site (Jiang et al.,2008) and peripheral mechano- receptors (Meissner's corpuscle, Merkel Cells) from the territoy of the injured fibre (Luo et al.,2007). Four subtypes of HCN channel proteins have been identified. HCN1 is expressed in the large diameter fibres (A and A-delta). HCN4 is expressed in the small diameter C fibres. Following a CCI, abundance of HCN1 expression was seen in DRG, suggesting expression in the somata of large and medium sized fibres. Similar expression is seen at the constriction site, again suggesting involvement of mylinated fibres. HCN4 expression is not reported to be increased in the experiment (Wan Y, 2008). Which suggest C fibres neurons may not be participating in the hyperpolarisation mediated ectopic discharge at the peripheral level.

In neuropathic pain models (like CCI) only a proportion of the fibres will be damaged by the injury. It was shown by Obata et al. that the symptoms of thermal hyperalgesia and tactile allodynia is related to the proportion of cells or fibres of the nerve damaged by the injury. He used an activating transcription factor 3 (ATF3) as marker of the neuronal injury in an experiment of CCI in rats.

Depending upon ATF3 expression, the rats were divided into three groups. Group 1 (< 12.5%), group II (12.5-25%) and group III (>25%) expression of ATF3. Only the rats in Group II developed tactile allodynia. Both II and III showed hyperalgesia. Group I had no effect. Immunolabelling at DRG showed molecular expression change in both injured and intact neurons with increased expression of BDNF in ATF3 negative neurons (Obata et al., 2003).

Changes in the dorsal horn

Peripheral nerve damage acts as a trigger for the microglial response in the spinal cord dorsal horn. A large number of studies have confirmed the microglial and astroglial involvement in the event that threatens CNS internal milieu. The microglial response includes an increase in number and size. Following peripheral nerve injury, the number of microglia can increase by twofold in the dorsal horn. The microglial response is specific to the area of the dorsal horn receiving the damaged afferent fibre. A number of molecules have been suggested as a signal from the damaged neuron that initiates this event.

The morphologically changed – activated microglia – express a host of molecules that modulates synaptic function, and neuronal excitability. Purinergic receptor $P2X_4RA$, chemokines and chemokine receptors, cannabinoid receptors, protein kinases (TNF), immunological molecules are all implicated. Microglia mediated dorsal horn sensitisation has become a key research interest for the process of generation of neuropathic pain and possible target for pharmacological manipulation.

Principles of fMRI

Magnetic Resonance Imaging (MRI) exploits the fact that living organisms are made up of molecules that act as micro magnets. Hydrogen atom nucleus (H1 isotope) with one proton is the smallest atomic dipole that exists aplenty in the human body (70% of human body is water). The proton has a polarity because of

its spin along the axis. The axis is not static, but wobbles like a spinning top. The frequency of wobble is called precess frequency. During an MRI scan, these dipoles get aligned parallel to the primary magnetic field of the bore (B_0). This is the most stable, low energy state. The strength of the primary magnetic field commonly used in clinical practice is 1.5 or 3 T (Tesla).

An extraneous radiofrequency (RF) pulse - energy, of appropriate frequency and direction will increase the energy of the protons and will flip them at an angle from the B_0 vector. The protons will also precess in phase under the influence of RF energy.

When RF energy is withdrawn, protons dissipate the acquired energy to realign themselves along B_0. This realignment along the static magnetic field is called longitudinal relaxation (T1). The protons also start precessing in a dephased manner with each precessing proton influencing its neighbour. Due to magnetic field inhomogeneities in physiological tissue, the dephasing rate is inhomogeneous. The dephasing process is called transverse relaxation (T2). The energy released during these two types of relaxation is captured by the receiver coil of the MRI scanner. The source of the energy is encoded with a position (in a two dimensional plane) to generate an image. Stacks of two dimensional images generate a 3D volume data.

Local field inhomogeneities cause dissimilar precession frequencies of the protons once the RF pulse is withdrawn, thus accounting for quicker dephasing of the proton population. Magnetic field passing through biological tissue is bound to have local magnetic field inhomogeneities as biological volume is not homogeneous. Also the field homogeneity in biological volume is not static but is a function of changing physiological state. This changing local magnetic field homogeneity is the basis for functional magnetic resonance imaging (fMRI).

Ogawa (Ogawa et al.,1990) while experimenting with anaesthetised rodents in high magnetic fields recognised that increased presence of deoxyhemoglobin in

blood vessels made them appear as dark lines in gradient echo pulse sequence with spatial resolution of 65X65 micron and slice thickness of 700 microns. He noted that when blood vessels have excess of oxygen (oxyhemoglobin) or carbon monoxide, both diamagnetic molecules, this contrast is not manifested. He attributed this to magnetic susceptibility effect of paramagnetic deoxyhemoglobin.

In a further paper in 1990, Ogawa first mentioned the possible application of this Blood Oxygen Level Dependant (BOLD) MRI signal in studies of regional neuronal activity similar to Positron Emission tomography (PET) (Ogawa S, LeeTM, Kay AR, Tank DR, 1990).

Hence local presence of oxyhemoglobin, which itself is a marker of neuronal activity in brain, improves local magnetic field homogeneity compared to deoxyhemoglobin. Measurement of this change of magnetic field homogeneity develops BOLD contrast and the application of fMRI studies of brain neuronal activity.

BOLD signal change following neuronal activity is in the range of 1-5%. (Goebel R, 2007). fMRI data analysis requires pre-processing to remove noise and multistep statistical analysis to extract and present this data buried in noise artefacts. In spite of these constraints, fMRI has been taken up by the scientific community as perhaps the investigation of choice for investigating the function of the nervous system in humans. The advantages of fMRI over similar other methods like PET, are many. fMRI is non invasive. fMRI does not require radioisotopes and hence relatively easy to conduct. Subject can participate in longitudinal studies without any known risk of harm. The spatial resolution is better compared to PET, MEG or EEG. fMRI has been able to discriminate between two points, 2 mm apart in studies related to human visual cortex (Engel SA, Glover GH,Wandell BA, 1997).

Physiological basis of BOLD signal

BOLD MRI signal is a surrogate representation of neuronal activity in the brain. A cortical region in baseline phase will have a reference oxyhemoglobin /deoxyhemoglobin ratio in the capillary beds, venules. During neuronal activity, at the initial phase, there is an excess extraction of oxygen from the capillary bed, causing increase in the ratio of deoxyhemoglobin. However soon, the area is flooded with oxygenated blood, that wash away the deoxygenated haemoglobin and surplus oxyhemoglobin abounds in the area (Goebel R, 2007). Oxyhemoglobin, being diamagnetic, produces less local magnetic field inhomogeneities and thus returns a stronger T2*signal (Ogawa et al.,1990).

A typical time course of evoked fMRI signal (Hemodynamic Response Function, HRF) from human visual cortex (V1) following a short visual stimulus of 100ms will show an initial dip in signal followed by a hemodynamic response, which starts around 2-4 seconds following the stimulus. The peak signal is reached by 5-6 seconds with a return to baseline around 10 seconds later (Goebel R, 2007). This response profile is sluggish compared to visual evoked potential. However BOLD MRI signal does not only reflect evoked potentials or an action potential in neuronal networks (Logothetis NK. Wandell BA, 2004).

Central Nervous System (CNS) is a network of conductive elements (neurons and their processes), supporting cells (astrocytes, oligodendrocytes and microglia) in an extracellular medium, permeated by vasculature. Action potentials (AP) are the signal with which the network communicates within and with the extra-neural targets. Most of our previous understanding of the functional properties of the substrates of the neuronal network, connectivity, and representative cortical maps are from animal studies using direct recording/stimulation based electrophysiology techniques.

Such methods involve placement of intraparenchymal electrodes in the extracellular space and recording of a variety of electrical signals like Extracellular Field Potential (EFP) when electrode is located in CNS extracellular space. Spike

Potential (SP) when electrode tip is located on or near an axon or a cell body of a neuron identifying an action potential, summation of all SPs from nearby spiking neurons as Multi Unit Activity (MUA). Local Field Potential (LFP) when the signal is filtered to demonstrate a summation of non action-potential related electrical activities, like subthreshold synaptic potentials, dendro-somatic electrical gradients, after potential and hyperpolarisation after a soma dendritic spike, voltage dependant membrane oscillations, and subthreshold interneuron signals (Bullock TH, 1997).

Logothetis (Logothetis NK, 2002) acquired simultaneous BOLD fMRI signal and direct intracortical recording from anaesthetised monkey following visual stimulation. The BOLD response could be matched to local mEFP and there was a linear relationship between stimulus strength, mEFP and BOLD response within a limited range. The study demonstrated that hemodynamic BOLD signal can be estimated more accurately by LFPs than MUAs (Logothetis NK, Pauls J, Augath M, Trinath T,Oeltermann A, 2001). Further research (Mathiesen C, Caesar K, Lauritzen M, 2000) where MUAs and LFPs were dissociated and their relationship with BOLD were examined, confirmed that fMRI is more representative of collective background synaptic activity that facilitate generation or modelling of an AP rather than AP itself.

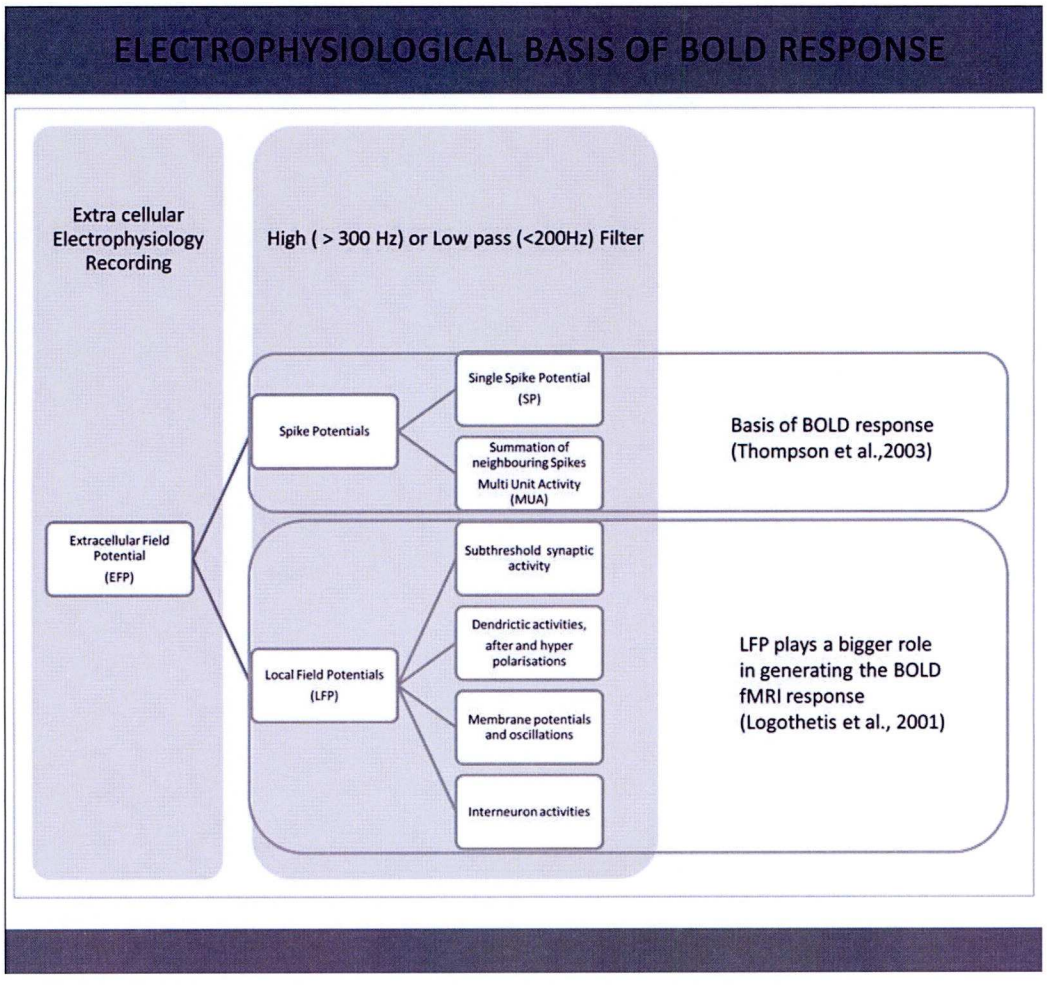

Fig 2.2 The electrophysiological basis of BOLD response. *The BOLD response predominantly represents local field potential. Thompson et al., 2003 has shown a part played by spike potentials in its development in an active area.*

When translating the above in the perspective of neuronal network, it can be deduced that when conventional electrophysiology will identify only those part of a network that will ultimately generate an action potential. The part of the network, involved in preparation, modelling, processing and modulating by sub threshold activities may only be identifiable by BOLD signal through fMRI. This is the case was shown by Tolias and colleagues in visual cortex of primates processing motion encoded information (Tolias As, Smirnakis SM, Augath AS, Trinath T, Logothetis NK, 2001).

Concepts of neurovascular coupling

Synaptic activity and thus metabolism driven increase in localised cerebral blood flow (CBF) is an established fact. The mechanism underpinning the hemodynamic response is a topic for discussion. Though many parallel mechanism of actions exist (as mentioned below). The temporal demand of the relationship negates many of the mechanisms proposed as the prime mover. The CBF increases within 1 second of the neuronal activity and is confined to 250 micrometer around the location of the activity (Silver IA, 1978). The metabolic control of local cerebral blood flow through chemical products of cerebral metabolism does not fit the time constrain of the effect observed. PCO_2, H^+, K^+, adenosine, glycolytic intermediates have been proposed. These factors could maintain a change in CBF, however they are unlikely to be the initial mechanism involved.

Neurogenic control through perivascular innervation has been proposed as a mechanism. Direct or Indirect stimulation by a collateral axon can alter vessel diameter and regulate local CBF (Selman RW, Lust WD, Ratcheson RA, 1996). A rich plexus of adrenergic sympathetic nerves exist on the cerebral vasculature. Neocortical layers IV and V have abundance of adrenergic receptors, which are the most vascularised layer of cerebral cortex (Bowler JV, 2000), having the highest density of synapses. Cerebral vasculature is now accepted to have dual sympathetic innervation. The larger vessels are innervated by sympathetic fibres originating from ipsilateral superior cervical ganglia and smaller vessels are innervated from sympathetic fibres originating from Locus Ceruleus (Bowler JV, 2000).

Role of astrocytes is taking centre stage as neurovascular coupler for regulation of local CBF. Araque et al. highlighted the role of astrocytes in a synapse and rightly called 'tripartite synapses, glia the unacknowledged partner' (Araque A, parpura V, Sanzgiri RP, Haydon PG,, 1999). A synapse is not only a junction between processes of two neurons; it is completely encapsulated by astrocytes making a

synapse an anatomical 'astrocyte-neuron' unit. Astrocyte interacts with the neuron and the synaptic cleft, and expresses appropriate transporters, receptors and uptake channels for neurotransmitters released during synaptic transmission. Astrocytes also surround adjoining brain capillaries with specialised end feet (Kacem et al., 1998). Hence astrocytes are uniquely placed to detect synaptic transmission and initiate appropriate change to vasculature through their end feet and bring about changes to energy metabolism.

Cerebral cortex contains excitatory neurons which makes around 80% of the neuronal population. The excitatory neurotransmitter is glutamate. When glutamate is released from the presynaptic membrane, it is predominantly removed by adjoining astrocytes from the synaptic cleft by glutamate transporter along with two to three Na^{+i} ions. The excess intracellular Na^{+} in astrocytes activates Na^{+} K^{+} ATPase, which in turn promotes glucose uptake from capillaries and utilisation (Magistretti et al.,1999). This explains the coupling of synaptic activity and glucose metabolism identified in ^{18}F –2DG glucose PET scan. The arrangement also goes a long way in explaining the neurovascular hemodynamic response and BOLD effect following a synaptic activity.

Anatomical basis of BOLD signal

The hemodynamic response for BOLD signal following activation of an area of brain requires presence of appropriate density of capillaries to generate enough signals. Low vascularity areas like white mater does not have enough capillaries to generate a substantial hemodynamic response that can be confidently detected by a BOLD signal change (Logothetis NK. Wandell BA, 2004). Cortical layers are highly vascularised and density of capillaries is most in layers harbouring most synapse and perisynaptic cells (Duvernoy HM, Delon S, Vannson JL, 1981).

Cerebral vasculature was described by Duvernoy as having three levels of organisation, the leptomeningeal vessels, the pial vessels and the intracortical vasculature. The intracortical vasculature has been divided in to four layers by density. The most dense capillary network is present in the layer IV. This is the layer that contains most synapse and perisynaptic cells. Layer I on the contrary has twice the number of cell bodies but less synapse and have the most sparse capillary density amongst the six layers of neocortex (Duvernoy HM, Delon S, Vannson JL, 1981). This distribution of intracortical vasculature give credence to the anatomy-physiology concordance to the basis of the hemodynamic response, as seen in BOLD signal change, described above.

The cerebral intracortical vascular bed lacks any precapillary arterio -venous communication channels (Ravens, 1974). The vasculature is armed with arteriolar sphincter that can redistribute blood according to need. The capillary branching points have constriction, housing a sphincter, which can regulate blood flow to a capillary bed (Reina-De l, Rodriguez-Baeza A, Sahuquillo-Baris J, 1998). A caution during interpretation of BOLD signal is that the vascular dilatation seen with hemodynamic response is shown to incorporate proximal vessels, which may lie adjacent the activated area (Iadecola et al., 1997).

fMRI in pain studies

The advantages of fMRI and ability to compute and display the results in novel 2D and 3D representations enabling easier visualisation fuelled an explosion of functional neuro-anatomical and neuro-psychological research in past 15 years. The researchers are focusing on reconfirming the conventional knowledge of anatomy or refuting it with the new tool. There is enough confidence in the scientific community to venture into using the fMRI for probing functions and network beyond what is known. The visual pathway and visual sensory cortex has been extensively studied, followed by the somatosensory pathway. Scientists have tried to understand the parts of the brain that gets involved in processing of a

sensory stimulus including nociception. Most notable of the pioneering observations was the appreciation of the role of cingulate gyrus in nociception and strengthening of the concept of a network or 'neuromatrix' and in case of nociception – the 'pain matrix'.

fMRI used to investigate anatomy and comparison of findings with knowledge from conventional neuroanatomy

One of the first investigators to focus on fMRI activations of somatosensory cortex was Hammeke and his team. They stimulated palm of right hand in six volunteers periodically undergoing echoplanar imaging in a 1.5 Tesla (1.5T) MRI scanner. They were able to demonstrate activation around contralateral central sulcus. This raised the possibility of studying somatosensory network of human brain and fMRI investigation of painful conditions/states (Hammeke et al., 1994).

Lin et al described activations around central sulcus in subjects made to appreciate a textured surface by rubbing with finger tips (Lin W et al., 1996).

Gelnar et al. described cortical activations in the multiple somatotopic sensory maps in the post central gyus, upper bank of post sylvian cortex and parietal operculum in an exhaustive early investigation involving vibrotactile fingertip stimulation in the humans. These were in congruence with traditional neuroanatomy as known in humans and in non-human primates. He also suggested variations in somatotopic arrangement in the different sensory areas investigated (Gelnar et al.,1998).

Using fMRI as early as 1999, Servos et al, managed to locate facial activations from post central gyrus, confirming the anatomical knowledge of the existence of sensory homunculus, but they thought that the facial representation being inverted (Servos et al., 1999).

Disbrow et al. used a directional stimulus protocol over several body areas and was able to demonstrate activations in the upper bank of lateral sulcus. He

demonstrated existence of at least 4 sensory body maps and attributed differential functional properties for these. He suggested modality specificity in the activation pattern (Disbrow et al., 2000).

Iannnetti et al. demonstrated activation of somatosensory cortical areas in the post central gyrus, and was able to demonstrate both primary and secondary somatosensory areas; he demonstrated bilateral activations from upper face and showed that the face is located in a much more compact territory (Iannetti et al., 2003) than what had been demonstrated by Penfield (Penfield and Boldrey 1937).

DaSilva et al. focussed on the trigeminal somatosensory system was easily identifiable in a MRI scan. He was not only been able to demonstrate activations in all the synaptic stations in the trigeminal sensory system, but somatotopy as well. This was one of the poineering study, investigating a specific somatosensory territory, describing a methodology for investigation of activations in the trigeminal ganglia through region of interest analysis and demonstrated somatotopy as it has been described in the visual and auditory pathway nearly half a decade earlier. This study confirmed knowledge of conventional anatomy (DaSilva et al.,2002). The confidence in the robustness of fMRI as a technique for the study of specific brain activations was confirmed by reproducibility of the result, that agreed with previous knowledge and outcome from similar studies using other functional imaging techniques.

fMRI to identify anatomical substrates involved in a function (task/event/conditions)

Rainville et al., in a PET study used hypnosis to dissociate painful experience from a noxious sensory input and concluded that anterior cingulate gyrus is involved in the appreciation of the sensation of pain and not somatosensory cortex (Rainville et al., 1997). Researchers using fMRI started looking beyond somatosensory cortex to evaluate other structures of the brain involved in computation of

different sensory stimulation and especially painful stimulation. The team from Massachusetts reported activation pattern in the trigeminal system following noxious and non noxious stimulation in healthy volunteers and raised the possibility of investigating the trigeminal system in patients with facial pain (Borsook et al., 2003; Borsook et al., 2004). Similar result was demonstrated following, event related painful electrical stimulation by Fitzek and his team (Fitzek et al., 2004) and capsaicin induced thermal hyperalgesia and sensitisation of trigeminal nociceptive pathway (Moulton et al, 2007; Maniero et al., 2007). These studies and similar other studies identified the brain areas that commonly gets activated in painful conditions. The areas are SI, SII, insular cortex (IC), anterior cingulate cortex (ACC), prefrontal cortex and thalamus (Peyron et al., 2000; Apkarian et al., 2005; Treede et al., 2000; Baumgartner et al., 2010). On moving from experimental pain states to patients with disease conditions, it has been realised that there may be specific neural representations of chronic pain states in the central nervous system which may not have been reproduced during fMRI studies of experimental painful conditions in healthy volunteers (Bingel and Tracey ,2008). Chronic back pain, migraines, fibromyalgia, phantom limb pain are chronic pain conditions that are extensively investigated with fMRI. In chronic migraine, hypometabolism and hypoactivation of extensive cortical areas were reported in several studies with normalisation following successful therapy (May and Matharu 2007; Chiapparini et al.,2010). In a study on patients sufferring from trigeminal neuralgia, fMRI study was undertaken following tactile stimulation of the face over trigger area. Neuralgia was elicited in 7 patients out of 15. When comparing the difference between the areas in the two groups, it was found that patients, who did not experience pain, had only ACC, brainstem and spinal nucleus of trigeminal activated. Painful stimulus involved activation of SI, S II, ACC, IC, premotor cotex, prefrontal cortex, hippocampus and brainstem (Moisset et al., 2010).

From task based - event related fMRI, research has moved into investigation of functional connectivity of brain when it is not involved in interaction with outside world or engaged in any goal based task. A network of brain areas remains active

to introspect (gather thoughts). This network is defined as Default Mode Network (DMN). DMN is a collection of connected brain areas that are active in introspective state. Some of the areas are medial temporal lobe, medial prefrontal cortex, posterior cingulate cortex, precuneous, medial lateral and inferior parietal cortex (Buckner RL, Andrews-Hana JR, Schacter DL, 2008). DMN will deactivate at the initiation of a goal based task and another network gets activated (Task Positive Network TPN). Recent fMRI studies have suggested that resting brain network activities may be altered in patients suffering from chronic pain, manifested as alteration in brain's default mode network along with impaired switching from the default to active state (Baliki et al., 2008). Alteration in DMN was shown in fibromyalgia with increased connectivity between DMN and insular cortex at resting state (Napadow et al.,2010).

fMRI is a very useful tool to investigate function of the brain in chronic neuropathic pain conditions. Its application has widened, and along with morphological studies like structural imaging, cortical volumetric study, spectroscopy, a more comprehensive understanding of changes that happen in chronic pain condition is being understood.

CHAPTER 3: MATERIALS AND METHODS

Ethics

The Local Research Ethics Committee (Liverpool and Mersey side) of the NHS (National Health Service) Research and Ethics Committee approved this research which forms a part of a wider study on trigeminal neuralgia, facial pain and use of MRI based applications. The research met the national data protection guidelines.

Subjects

Ten healthy volunteers and fourteen patients were recruited in the present study. Recruitment of healthy volunteers was done through advertisement circulated in the Liverpool University campus and related departments.

Before being enrolled in the study, each prospective participant underwent screening to identify any contraindication for participation in a MRI based research, including the presence of claustrophobia.

Three patients were excluded from the analysis. One had more than 5 mm movement artefact and did not complete the scanning session. A further two sets of patient data were lost due to significant susceptibility artefact before the unwarping technique was implemented. (Please see below)

The age of the patients varied from 41-75 years with the duration of trigeminal pain from 6 months to 8 years. Patients were not asked to stop medication before the experiment because of constraints of the ethics.

The volunteer group is fairly age matched, ranging between 41 to 62 years.

Inclusion and exclusion criteria

Healthy volunteers

Adult healthy male or female volunteers, who were able to understand the practicalities of the experiment and could judge the risk involved in taking part in the research, were included in the study.

Patients

Adult Patients with clinical diagnosis of trigeminal neuralgia or neuropathy, being treated at the Walton Centre for Neurology and Neurosurgery, Liverpool, were approached for participation in the study. The trigeminal neuralgia patients had a partially controlled symptoms who were getting occasional but muted neuralgic attacks and were being worked up for neurosurgical management. Trigeminal neuropathy patients were on pharmacotherapy for their symptoms.

Patients with acute intractable symptoms, requiring inpatient treatment were excluded from the study as triggering pain in them would have been inhumane. Patients with established diagnosis of dementia, or severe learning difficulties, with major systemic or cerebrovascular disease, brain tumour and multiple sclerosis were also excluded from the study.

Every patient and volunteer signed a consent form before participation in the research. They were informed about 'what to expect' during the scanning session and the time required.

Pre-scan screening

Thermal pain threshold temperature

The thermal pain threshold temperature was determined in each subject prior to fMRI. This was done with a peltier thermode (Medoc, Haifa, Israel). A 1.6cm square MRI compatible thermode was placed in contact with the facial skin over the maxillary eminence (corresponding to V2 area of the trigeminal nerve dermatome) on the side opposite to the proposed experiment. The temperature was then raised from a baseline of 32^0C till patient complained a level of discomfort that was painful, scoring 6-7 on Visual Analogue Scale (VAS). This threshold temperature (T^{pain}) was used to elicit a thermal pain response later during the experiment.

Laterality of the symptoms in patients and clinical diagnosis

The side of the symptoms was recorded with the clinical diagnosis. For volunteers, the preferred site of stimulation was 'right' side of the face and right thumb unless the left side was preferred by the volunteer.

Equipments and set up

MRI scanner

The study was conducted on a Siemens Trio 3 Tesla MRI scanner which was optimised for neurological use.

Air puff applicator

A custom made air puff applicator was assembled locally using four narrow bore polyurethane tube. A sequential air flow-jet generator (CACTUS , Compressed Air Controlled Tactile Universal Stimulus) was used to generate air puffs. During the experiment, the ends of the tubes were taped on to the MRI head coil and to the thumb. The air puffs were triggered by the appropriate time locked sequence of the MRI scanning protocol (TTL signal). The air was directed through different

tubes from the connector-distributor which was placed outside the bore of the scanner and operated manually. This allowed us to stimulate different segments of the facial skin and thumb, and continue with the scanning protocol with air puffs, without moving the patient or repositioning. The air puffs produced an innocuous tactile stimulation with a direction, with minimal distortion of the facial skin.

Thermode

A peltier thermode (Medoc, Haifa, Israel) 16 mm X 16 mm in dimension was used to apply thermal nociceptive stimulation. The thermode maintained a baseline temperature of 32^0C. The thermode could support a temperature rise of 5^0C per second and a fall of 4.5^0C per second. During scanning sessions, the temperature change was controlled by the TTL signal within the scanning time protocol.

fMRI analysis software

The pre processing and statistical analysis of the fMRI data, and presentation was done using BrainVoyager^{TM} QX version 2.6 of Brain Innovation B.V. Appropriate software licence was obtained for the purpose.

The experiment

Functional imaging

Each subject had a total of nine MRI runs in the Siemens Trio 3 tesla neurooptimised MRI scanner. Eight of them are fMRI sequences to specific targeted stimuli.

The fMRI image slices were constructed using a gradient echo (GE) echo planar imaging (EPI) pulse sequence. This GE-EPI pulse sequence has extreme sensitivity to magnetic field (B^0) inhomogeneities. The inhomogeneities were most pronounced at tissue interfaces and for example, between skin and air, skin and thermode. This produced image distortion, known as susceptibility artefact. The distortion of the image caused imperfections during structural-functional image

co-registration and error in labelling of the activated voxels. We faced this susceptibility artefact in our fMRI datasets in early part of the study. Following its recognition, we implemented an unwarping technique as suggested by Jenkinson (Jenkinson, 2001) by acquiring a measurement of field in homogeneity. 'The field map' consisted of a T2 weighted phase and magnitude data acquired by non EPI spin echo sequence which was further normalised by Gaussian smoothening.

The fMRI images were acquired in 3.5mm isometric voxels in a 64X64 matrix. Each volume acquired had 36 slices.

Runs 1-4

The air puff fMRI paradigm was a box design consisting of 10 pairs of 'OFF and ON' epoch, each of (12 X 2) 24 seconds duration. The data was collected in 80 volumes with 36 slices per volume over a total duration of 240 seconds. There were four runs of the air puff paradigm, one each for the stimulation of the skin of forehead, cheek, mandible and thumb, corresponding to V1, V2, V3 segments of the trigeminal nerve innervation and the palmer surface of the thumb. The point of air puff stimulation was approximately 6cm from the midline of the face, along a longitudinal axis of the face, as restricted by the head coil. This distance from the midline remained constant for every subject.

Runs 5-8

The nociceptive thermal stimulation was delivered to the same locations as the air puffs with the peltier thermode described above. The fMRI paradigm was a box design with base line being at 32^0C for 30 seconds followed by stimulation at threshold temperature for 24 seconds. The stimulation at threshold temperature was preceded and followed by ramps of 4.5 seconds duration to account for temperature change. Three epochs were obtained over 189 seconds acquiring 63 volumes. This paradigm was used for V1, V3 and thumb. For V2, the ON state was prolonged to 48 seconds. A 24 seconds innocuous thermal stimulation (sub threshold) at 42^0C was added, as a priming sequence. Three epochs were obtained over 261 seconds and 86 volumes.

It was not possible to gain access and hold the thermode in place over V2 segments in two patients because of bigger dimension of the head. It left no space for the thermode to fit in below the head coil. In these two patients, thermal pain data from V2 segment were not obtained.

Run 9

A final T1 weighted, 1 mm isometric, high resolution sagittal volume scan of whole head was obtained, with a matrix of 256 X 256, with contiguous slices.

During each run, subjects were requested to keep still. The head was padded within the head coil with sponge wedges to restrict movement. They were also requested to keep their eyes shut and relax while the scanning took place.

Report of pain experience and elicitation of tactile allodynia or unpleasantness or neuralgic attack

Patients were asked to rate their pain experience or unpleasantness on a visual analogue scale (VAS) of 0-10, '0' being no pain and '10' being the worst pain felt following the nociceptive thermal stimulation with the thermode. Similarly patients were asked to report verbally at the end of each run with the tactile stimulation (air puffs), whether the stimulation was felt to be painfully- unpleasant only (allodynic) or whether a triggering of a neuralgic attack had happened.

fMRI Data Analysis

A multistep data analysis was undertaken using BrainVoyager^{TM} QX 2.6 (BVQX2.6) software developed by Brain Innovation BV.

Step1

The MRI image datasets were converted to software readable DICOM files.

Step2

The high resolution structural image was transposed into Talairach (Talairach J, Tournoux P, 1988) space by a trilinear interpolation algorithm. This brain volume was later used to coregister and display transposed activation maps. The Talairach transposition was useful for inter-subject comparison and group analysis.

Step3

The fMRI data was pre-processed, by a number of mutually independent corrective steps to improve signal to noise ratio (SNR), prior to the statistical analysis.

3D Motion correction was applied to reduce noise from small movement of the head. The first volume was taken as reference followed by alignment of the rest of the stack with the reference volume by rigid body transformation. This includes 3 translations and 3 rotational corrections. The 3D motion correction parameters were displayed in the BVQX2.6 in a time course graph. Any movement of less than 3-4 mm any axis was taken as 'acceptable' data. A dataset with a movement of more than 4mm in any axis was discarded.

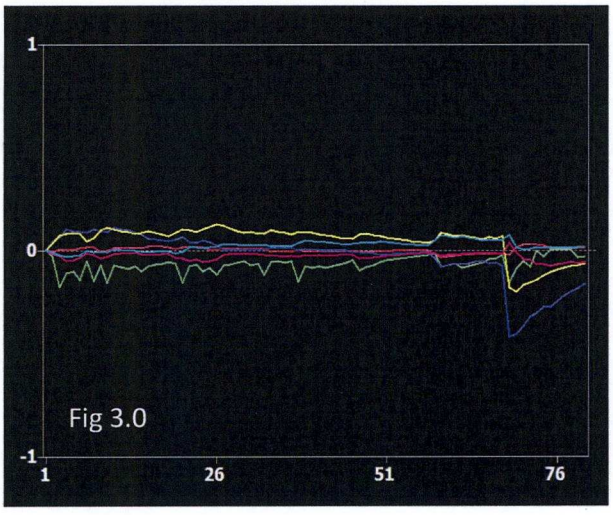

Fig 3.0 3D motion correction time course graph. Motion is detected in 6 planes of movement. 3 translations. Red denotes translation in X axis, green denotes translation in Y axis, blue denotes translation in Z axis. Yellow is representing rotation around X axis, magenta is rotation around Y axis and cyan representing rotation around Z axis. The X axis of the graph denotes volume counter of an fMRI scanning sequence, Y axis is displacement in mm.

The 3 D motion correction time course graph was analysed for each fMRI run and correlated with the time course of the sensory stimulus to unearth any phasic 'micromotion' (reflex or involuntary) related to the stimulus. Patients who

experienced tactile allodynia, unpleasant sensation or had a neuralgic episode triggered during the experiment were expected to demonstrate this micromotion. Details are described later.

Slice scan time correction was necessary for each functional volume data to interpolate the header scanning time of each of the slices of the volume to one time point, though they were acquired sequentially. The scan time correction algorithm required the slice scanning order protocol, which was available from the header file. Siemens Trio MRI scanner used an ascending 'interleaved 2' slice scanning option, which was checked during slice scan time correction.

Temporal filtering of each dataset was undertaken to remove noise from linear and nonlinear drifts by passing through a temporal high pass filter (GLM-Fourier). These noises originate from physiology and MRI hardware.

Spatial Smoothening using a 3D Gaussian kernel of 4mm width was undertaken for each of the fMRI dataset. For multi subject analysis, pre-processing of the VTC files were done with an 8 mm kernel. Spatial smoothening compromises spatial resolution of the data and hence a smaller kernel was used for the single subject analysis.

Step 4

The processed fMRI dataset (FMR) was co registered with the structural MRI volume scan (VMR). The FMR-VMR file was then linked with the Hemodynamic Response Function (HRF) predictor model to create a volume time course (VTC) file. Patients with left sided pathology had their FMR dataset flipped at this point to enable multisubject analysis at a later stage. A non flipped copy of the FMR was also generated for single subject analysis. A total of four patients needed flipping of sides.

The predictor models (protocols)

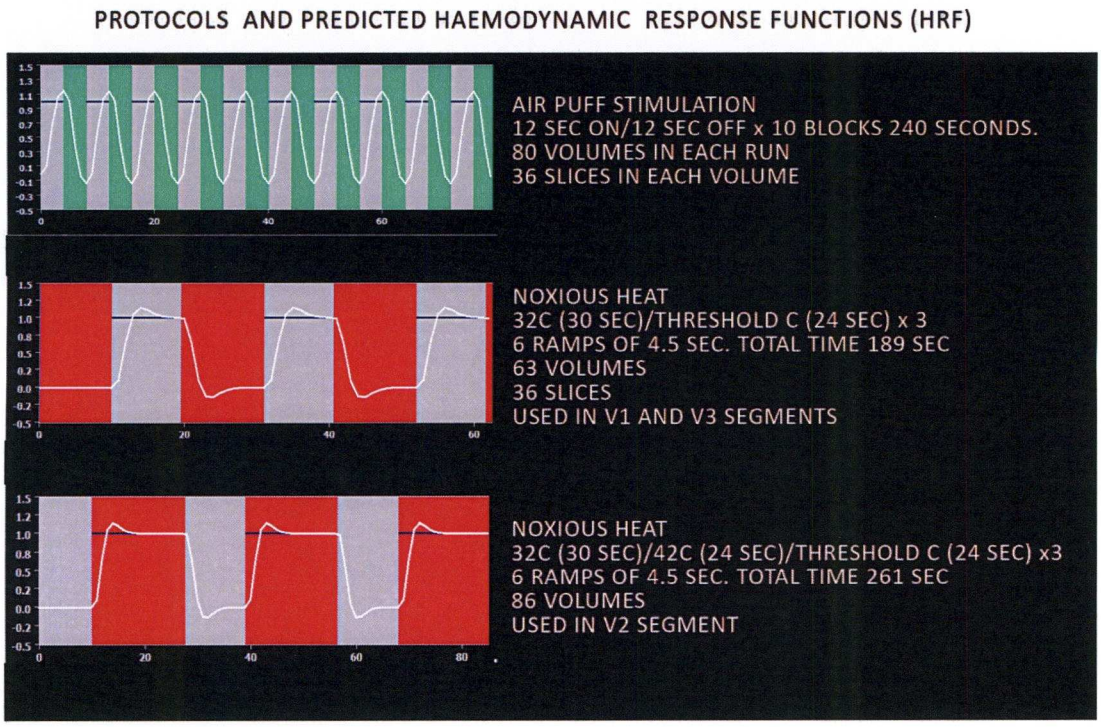

Fig 3.1 ***The Predictors*** *of the fMRI experiments (see text please)*

Step 5

The General Linear Model (GLM) was used to analyse the fMRI dataset. GLM analysis compares the model shape of the hemodynamic response (HRF) curve with the experimental HRF response derived from the BOLD signal change. It generates a statistical map for each voxel on how well the data fits that model. A 't' map was obtained for each voxel in the dataset.

Step 6

The statistical analysis of fMRI dataset, which runs the analysis for each voxel in the volume, is liable to suffer from multiple comparison error. Bonferroni Correction for multiple comparisons could adjust but is deemed to be too strict and though can reduce the alpha errors, can massively increase beta errors as well. However the activations of the voxels in an fMRI dataset involving human brain are not independent of each other and similar activations are seen in neighbouring voxels within functional areas. BrainVoyager™ QX uses False Discovery Rate (FDR) approach (Genovese et al 2002). FDR aims to restrict the

error rate of false positive voxels in a subset of voxels that are labelled as significant (suprathreshold and are called the 'discovered' voxels). Here a q value of .05 would suggest that the false positive voxels will be restricted to 5% of the suprathreshold (discovered) voxels in the activation map.

Step7

In a selected group of dataset a 'Region of Interest' (ROI) analysis was undertaken on selected clusters of activations in the anatomically important and functionally eloquent areas. The temporal analysis of the HRF and the signal change in the cluster selected provided an insight into how the area responded to the stimulus and comparison of that response with the neighbouring clusters or other clusters in the activation map. This particular aspect of ROI analysis was done to examine temporal relationship in activation amongst the activated ROI clusters.

Step 8

The activation maps were displayed in two dimension or inflated brain surface

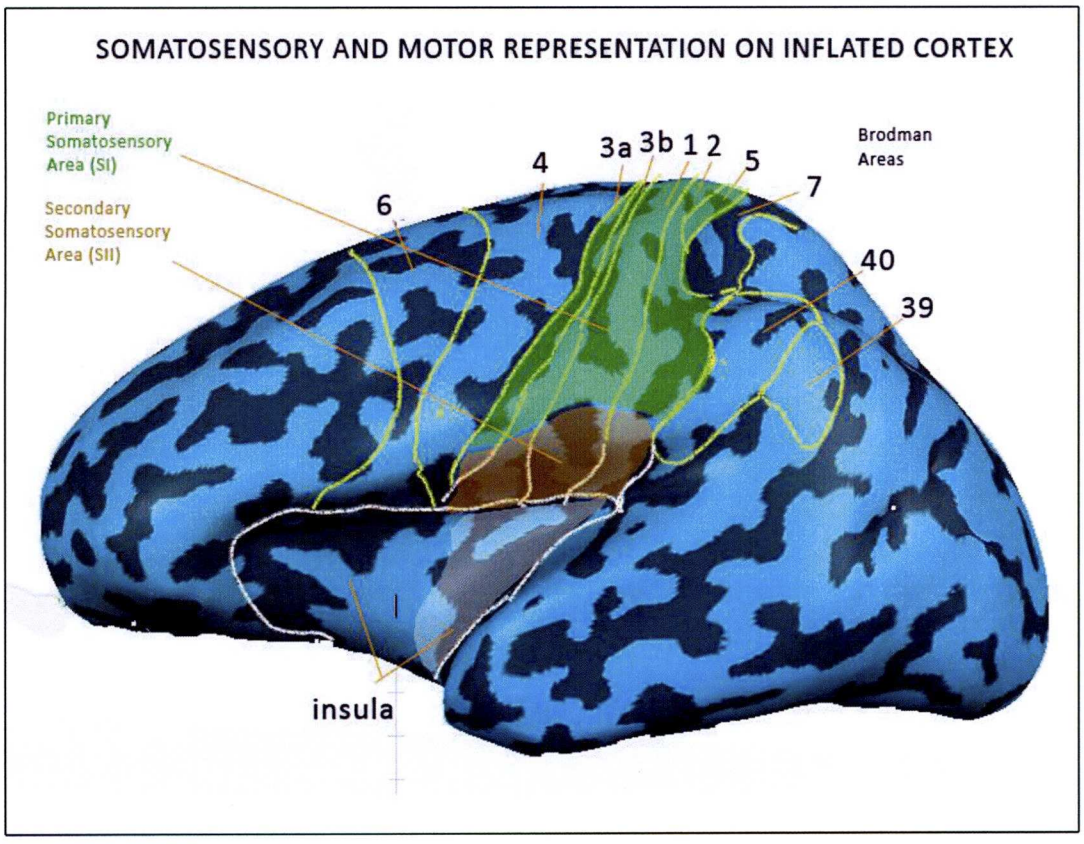

Fig 3.2 Inflated brain with the surface mark *of conventional landmarks and areas*

maps. Table 3.1 explains the parameters used to generate activation maps and. tools used for thresholding. A Talairach transformed structural brain volume from one of the volunteers was inflated by trilinear interpolation. This inflated and reconstructed cortex was used to develop surface maps for pictorial representation and visual comparison of the data.

All activations were anatomically correlated. In case of comparatively sparse activation maps, a less strict multiple comparison correction was accepted ($q>0.05$), but with an acceptable cluster corrected *p* value of >0.01. The strictness of declaring a voxel as active was to similar fMRI studies (Borsook et al.2003; Brooks et al., 2002; Mainero et al., 2007). The activated clusters were there-after designated as 'Volume of Interest' (VOI).

Step 9

The 3 D talairach coordinates of the peak voxel in the VOIs were ascertained, and tabulated with an anatomical label along with p –value and intensity. This formed the full activation map along with other 2D and 3D representations for the analysis.

	Statistical method t test	Multiple comparison error correction False discovery rate (FDR)	Z value	Time course	Cluster threshold
Orthogonal representation 2D	P < 0.01	q < 0.05	>2.5	Visual check of congruency	>5 voxels
Volume representation 3D	P < 0.01	q < 0.05	>2.5	Visual check of congruency	**>50mm^3** applied to very busy datasets and mentioned in the text when this was used

Table 3.1 Parameters used for thresholding and creation of activation maps. In case of datasets with very sparse or no activation, a less strict parameters were used and highlighted in the adjoining text.

CHAPTER 4: POST PROCESSING ANALYSIS AND RESULTS

Analysis of pre scan screen and post scan patient report

The results from ten healthy volunteers and eleven patients were analysed in this study. Except one, all healthy volunteers had stimulation on the right trigeminal skin (face and forehead) and the ipsilateral thumb. One volunteer preferred the left side and left thumb. No volunteer data was excluded in this clinical part of the study. The thermal pain threshold (T_{pain}) estimated on contralateral maxillary eminence was within the range of 48^0 -49.5^0 C and a reference VAS of 6-7.

The air puff experiment did not evoke any unpleasantness, allodynia or precipitate any neuralgia like symptoms in the volunteers group. The thermal stimulus evoked a sensation of pain or unpleasantness in all volunteers. The reported degree maximum unpleasant sensation or pain felt from the thermal stimulation was tabulated in table 4.1. The reported maximum pain felt was highest at the thumb

compared to that when stimulation was on the facial skin for any individual subject. The difference of pain perception was highly significant ($p < 0.0009$).

Volunteer	Side of stimulation	Thermal pain intensity reported during experiment (VAS)				Thermal pain threshold (^{0}C)
		V1	V2	V3	Thumb	
1	L	8	8	8	9	49.5
2	R	8	8	8	9	48
3	R	6	6	6	6	49
4	R	6	6	6	6	48
5	R	6	6	6	7	49.5
6	R	6	6	8	9	49
7	R	6	6	7	9	48.5
8	R	5	6	7	9	49.5
9	R	6	6	6	8	48
10	R	6	6	6	8	48.5
Mean		6.3	6.4	6.8	8	48.6
Probability of a true difference between perceived evoked pain scores between face areas and thumb P<0.0009						

Table 4.1 ***Results of pre-scan screening and assessment of thermal pain threshold amongst the volunteers and post-scan report of maximum pain felt in the V1, V2, V3 segment of the trigeminal nerve and thumb.*** *Note that following thermal stimulation at respective thermal pain threshold temperature, a higher degree of pain was felt over the thumb than on the face in seven out of nine subjects who could recall their experience.*

Of the eleven patients, nine had a clinical diagnosis of trigeminal neuralgia. Two patients had the diagnosis of trigeminal neuropathy by Liverpool Criteria (Nurmikko and Eldridge, 2001). Seven patients had neuralgic symptoms on the right side of face while two had it on the left. Both the patients suffering from trigeminal neuropathy had their symptom on the left side. All patients were on medications to control symptom. Despite being on symptom controlling medications, the mean T_{pain} in the patient group (48.6^{0}C) matched well with the healthy volunteers but with a wider distribution 47.5-50^0 C.

Contrary to the observation in the volunteers group, the perceived thermal evoked pain intensity in the patient group showed a differing trend (Fig 4.1 a&b). All patients who suffered from trigeminal neuralgia, and could report, recorded the maximum pain score from a facial dermatome rather than the thumb, with the score from the thumb was significantly less ($p<0.01$). The two patients with the diagnosis of trigeminal neuropathy showed no specific trend. Trigeminal neuralgic pain episode was not triggered by the thermal stimulation in any group.

Patients	Side	Clinical diagnosis	Thermal pain intensity (VAS)				Report of tactile allodynia	Allodynic response during fMRI identified by motion correction paradigm				Thermal pain threshold (°C)
			V1	V2	V3	Thumb		V1	V2	V3	Thumb	
1	R	Neuralgia	8	8	6	7	no	no	no	no	no	50
2	R	Neuralgia	8	8	8	6	no	no	no	no	no	48
3	L	Neuralgia	7	7	3	4	yes	no	yes	no	no	48
4	R	Neuralgia	9	8	9	6	yes	yes	yes	yes	no	48.5
5	R	Neuralgia	5	6	8	3	no	no	no	no	no	47.5
6	R	Neuralgia	9	8	8	6	no	no	no	no	no	49.5
7	R	Neuralgia	5	7	3	7	yes	no	yes	trigger	no	48
8	L	Neuropathy	7	6	6	9	yes	no	no	no	no	49
9	L	Neuropathy	9	8	8	6	no	no	no	no	no	49
10	R	Neuralgia	X	X	X	X	no	no	no	no	no	X
11	L	Neuralgia	X	X	X	X	no	no	no	no	no	X
Mean			7.4	7.4	6.5	6						48.6

Table 4.2 **Results *of pre-scan screening and assessment of thermal pain threshold amongst patients and post-scan report of degree of pain.*** *Note the pain reported from thumb was less in patients with neuralgia. Also note that some patients reported allodynia or significant unpleasant response and a triggering of neuralgic attack. This allodynia was also unmasked by motion correction algorithm during pre-processing of the fMRI data.*

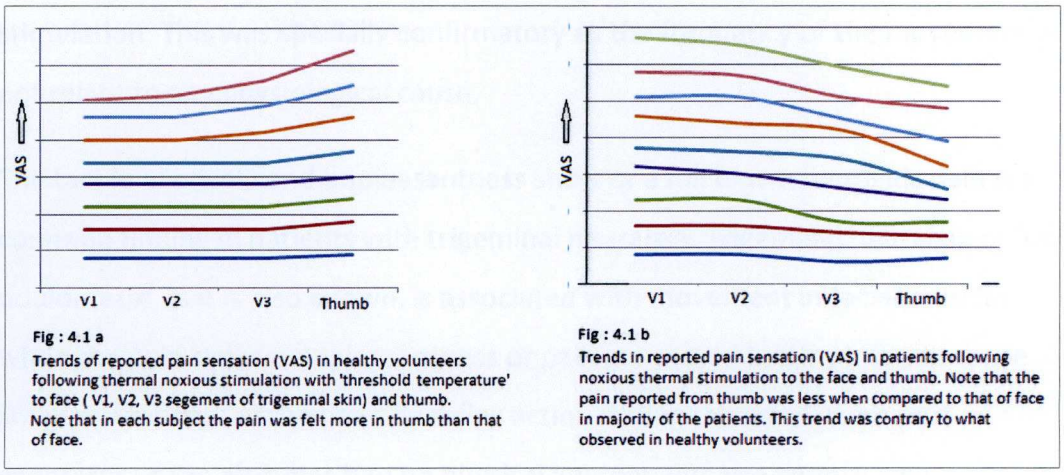

Fig : 4.1 a
Trends of reported pain sensation (VAS) in healthy volunteers following thermal noxious stimulation with 'threshold temperature' to face (V1, V2, V3 segement of trigeminal skin) and thumb. Note that in each subject the pain was felt more in thumb than that of face.

Fig : 4.1 b
Trends in reported pain sensation (VAS) in patients following noxious thermal stimulation to the face and thumb. Note that the pain reported from thumb was less when compared to that of face in majority of the patients. This trend was contrary to what observed in healthy volunteers.

Fig 4.1 a&b *Trends in reported maximum pain sensation score in healthy volunteers and patients following thermal nociceptive stimulation at* T_{pain}.

Four patients (P3,P4,P7,P8) reported experiencing tactile allodynia or unpleasantness(short of a neuralgic attack) during some of the runs of the air puff experiment. P7 reported triggering of a neuralgic attack. The signature of these reported events were visible during subsequent pre processing and 3D motion correction of the dataset. P8, who suffered from trigeminal neuropathy and reported an allodynic response but did not show the periodic micromotion mentioned above.

Identification and verification of unpleasantness/allodynia or neuralgic attack response from 3D motion correction algorithm

The pre processing of fMRI data to improve signal to noise ratio is a well established technique. Three dimensional (3D) motion corrections had been used to compensate for small head motion during the scan. The origin of these motions could be physiological like breathing movement and cardiac output. Subjects in the scanner could develop muscle fatigue to hold a certain head position and drift with time. However a periodic, regular head movement in one direction with a frequency matching with the application of the tactile sensory input (air puff), clearly suggested that the origin of the movement was triggered by the

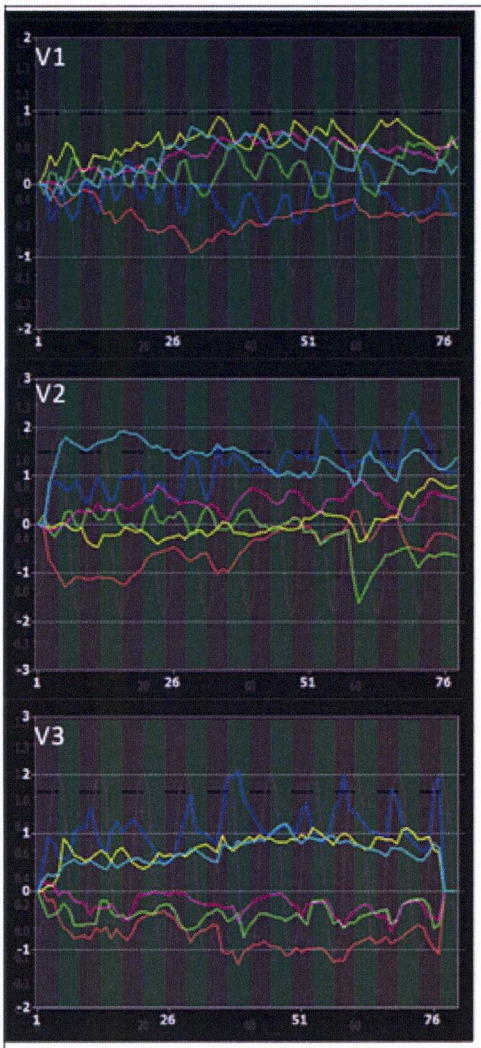

Fig 4.2 **Identification and validation of tactile allodynia from 3D motion correction time course graph**

Patient 4 reported mild tactile allodynia in V1, V2 and V3 segment following air puff stimulation of the face in post scan report.

During 3D motion correction, the 6 axis correction time course graph displayed a phasic micromotion. The air puff stimulation paradigm had ten 12sec on/12sec off stimulus cycle, applied in a block design. The micromotion, specially that of V2, V3 and later half of V1 matched the onset of airpuff stimulation or the block design. This phasic motion didnot match any physiological cause and the movement was away from the stimulus site. It was accepted that in presence of true allodynia, it would be impossible for the patient to keep still and reflex contraction of muscles following the sensation would cause this type of movement, which would be entirely involuntary.

This observation was used to validate the patient report of allodynia in neuralgia patients to categorise the air puff runs for further analysis. Please see text and table 4.3

3D motion correction time course graph of FMR volume data. The graph is superimposed on the airpuff time course block design to highlight the ***congruency*** *of micromotion and stimulus 'ON' state. Here the grey columns are ON state and greens columns are OFF*

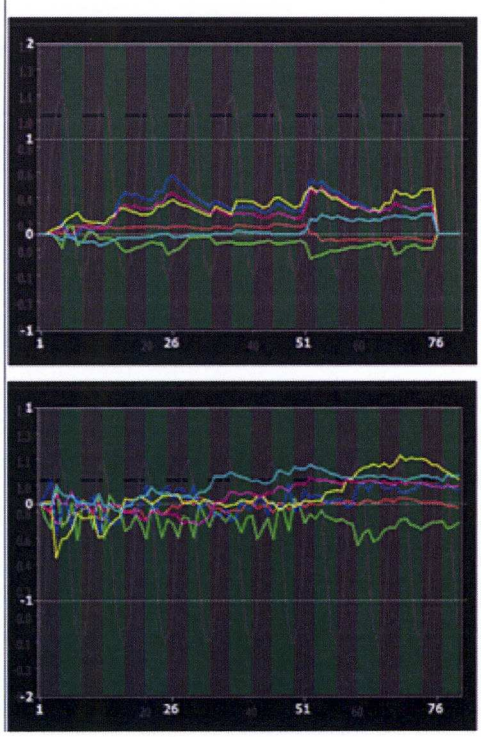

Fig 4.3 **Examples of 3D motion correction graphs which do not show phasic micromotion.**

Two motion correction time course graphs are displayed. These graphs do not show allodynic micromotion as the graphs in Fig 4.2. The movements demonstrated here are not phasic, donot match the air puff stimulus paradigm.

3D motion correction time course graph of FMR volume data. The graph is superimposed on the airpuff time course block design to highlight the ***incongruency*** *of micromotion and stimulus 'ON' state. Here the grey columns are ON state and greens columns are OFF*

Defining groups for the analysis of the activation maps

The runs which had the appropriate micromotion signature and had been reported earlier by the patients thus formed a group of fMRI runs where a definite unpleasant or allodynic response had been confirmed. This group of fMRI runs will be called as 'trigeminal allodynia group' runs for the purpose of the study. The run which captured the triggering of the neuralgic attack will be a separate entity, and the sterile runs where no allodynia or triggering had been reported by the patients formed the third subgroup amongst neuralgia patients.

Subjects	Stimulation	Clinical correlation/condition
Healthy Volunteers	Thermal nociceptive	Pain
Healthy Volunteers	Tactile stimulation	No allodynia/unpleasantness
Patients	Tactile stimulation	No allodynia/unpleasantness
	Tactile stimulation	Tactile-allodynia or unpleasantness
	Tactile stimulation	Triggering neuralgia
Patients	Thermal Nociceptive	Pain

Table 4.3 **List of groups for designated fMRI runs used later in the study**

Analysis of activations in healthy volunteers

The healthy volunteer group formed the control arm of the study. The primary angle of examination of the data from this group was to validate the methodology of the present research by being able to replicate results of other groups engaged in similar study on the healthy volunteers (Servos et al., 1999; Borsook et al.,2003; Iannetti et al., 2003). Hence we looked at the group data from two aspects; first, the activation maps and their content and second, variation in activation pattern amongst the modality. This was followed by single patient analysis of regions of interest (ROI).

Volunteer group analysis: air puff

The air puff stimulation produced an innocuous tactile stimulation on the facial skin. Group analysis of the activation patterns in healthy volunteers following the air puff stimulation of the three facial trigeminal dermatomes showed significant activation of the whole of the trigeminal somatosensory system upstream from the brain stem complex. At a q value of < 0.05, which meant a confidence that 95% of the discovered voxels were true activations, we were able to demonstrate discrete activations in the bilateral primary somatosensory cortex (SI), secondary somatosensory cortex (SII), and contralateral parietal ventral area (PV) which straddles parietal operculum and contralateral sensory thalamus. The ipsilateral activations of SI, SII, and thalamus were also well demonstrated. Activations were demonstrated in the trigeminal brain stem nucleus complex at a lower p value of 0.01, during the stimulation of the V2 segment of the face. Similar activations had been described by other authors (Servos et al., 1999; Borsook et al.,2003; Iannetti et al., 2003; Maniero et al.,2001). The activations in the SI area demonstrated somatotopy. The segregation of SI and SII activations and the loci of activations during noxious thermal stimulations (described later) matched our current knowledge of function of these areas in parietal neocortex (Table 2.1). For an anatomical correlation of the activated peak voxels during air puff stimulation of the V1, V2, V3 segment of the skin of the face innervated by the trigeminal nerve and the skin of thumb in healthy volunteers, please refer to Table 4.4. The activation clusters in Area1 &2 of SI and SII area showed a higher number of voxels activated, thus stronger activations, compared to the other clusters. These areas were known to compute for vector and texture of a stimulus rather than location (Kaas et al., 1979). The surface maps, represented over an inflated left hemisphere showed that the SI activations were located on the summit of the post central gyrus and the gyral cortex behind it (area 1 &2 of SI). The group activation map demonstrated thumb with respect to lower face (V3). This somatotopy was easily identifiable because of wide distance between their representations within the homunculus, interposed by a large area of the cortex, represented by the lip.

The somatotopic arrangement within the facial area activated following the tactile stimulation was also visible on the surface map represented on inflated brain.

Table 4.4 A sample list of activated clusters following air puff stimulation (BrainVoyager QX auto generated) Talairach Coordinates, the 't' value signifying measure of signal and 'p' the statistical probability of the voxel being a true activation

Cluster activation list of V1 air puff stimulation in volunteers from Talairach Coordinates						
	"Peak X"	"Peak Y"	"Peak Z"	"t"	"p"	
"Cluster 1"	48	-31	25	5.135584	0.000000	Inferior Parietal Lobule (40)
"Cluster 2"	33	-37	28			
"Cluster 3"	24	-58	-20	3.793790	0.000161	Cerebellum
"Cluster 4"	21	-13	28	3.646516	0.000285	Caudate
"Cluster 5"	15	-61	-42	4.287697	0.000021	Cerebellum
"Cluster 6"	-24	-58	-20	4.084918	0.000049	Cerebellum
"Cluster 7"	-30	-1	25	4.012239	0.000067	Insula (13)
"Cluster 8"	-45	-34	25	6.921857	0.000000	Insula (13)
"Cluster 9"	-42	-16	22	3.622471	0.000313	Insula (13)
"Cluster 10"	-54	-1	37	5.774021	0.000000	Precentral Gyrus (6)
"Cluster 11"	-48	-52	10	3.971533	0.000079	Superior Temporal Gyrus (39)
"Cluster 12"	-51	-22	37	4.365704	0.000015	Postcentral Gyrus (2)
"Cluster 13"	-57	-19	19	4.118744	0.000043	Postcentral Gyrus (40)
"Cluster 14"	-64	-43	-5	3.879585	0.000114	Middle Temporal Gyrus (21)
"Cluster 15"	-60	-31	22	5.007671	0.000001	Inferior Parietal Lobule (40)
Cluster activation list of V3 air puff stimulation in healthy volunteers from Talairach Coordinates						
	"Peak X"	"Peak Y"	"Peak Z"	"t"	"p"	
"Cluster 1"	60	-28	19	3.482916	0.000526	Postcentral Gyrus (40)
"Cluster 2"	63	14	1	2.941569	0.003372	Superior Temporal Gyrus (22)
"Cluster 3"	57	-1	-14	2.989519	0.002891	Middle Temporal Gyrus (21)
"Cluster 4"	48	14	-14	3.149842	0.001702	Superior Temporal Gyrus (38)
"Cluster 5"	42	41	22	3.066737	0.002246	Middle Frontal Gyrus (10)
"Cluster 6"	21	-4	16	3.545558	0.000417	Lentiform Nucleus
"Cluster 7"	-27	-4	7	3.220667	0.001337	Lentiform Nucleus
"Cluster 8"	-24	20	1	3.635673	0.000297	Claustrum
"Cluster 9"	-30	-4	52	2.845452	0.004563	Middlefrontal gyrus (6)
"Cluster 10"	-39	-1	-20	3.386788	0.000746	Fusiform Gyrus (20)
"Cluster 11"	-42	-4	43	3.183604	0.001518	Precentral Gyrus (6)
"Cluster 12"	-52	38	13	4.440786	0.000010	Inferior Frontal Gyrus (46)
"Cluster 13"	-42	-37	25	4.564845	0.000006	Insula (13)
"Cluster 14"	-57	-25	28	4.836226	0.000002	Inferior Parietal Lobule (40)

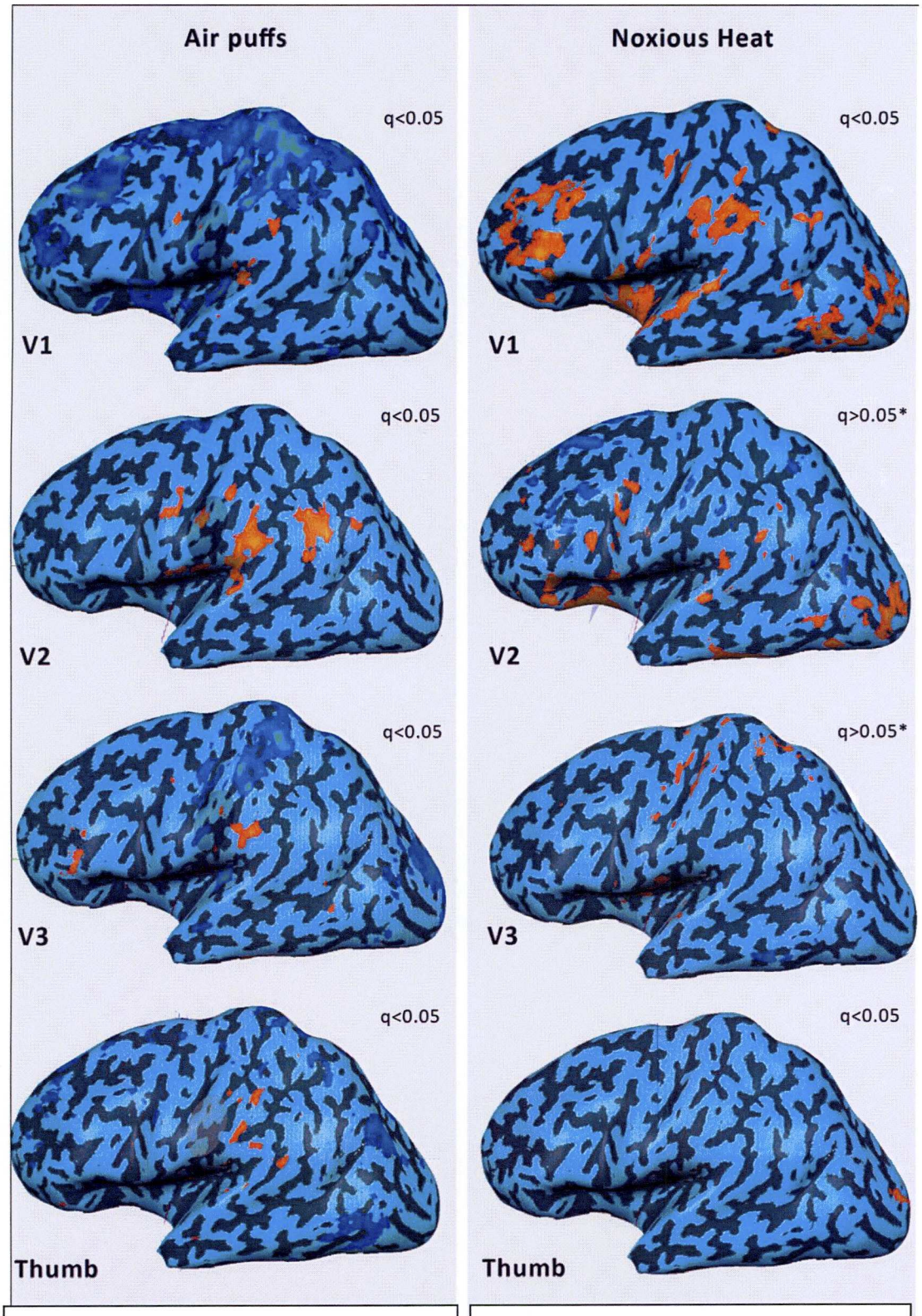

Fig 4.4a Activation maps from healthy volunteers during stimulation with air puffs. This is a contralateral cortical inflated map. Discrete activation from air puff is seen at area 2 of SI. Note no insular activations.

Fig 4.4b Activation map from healthy volunteers following thermal pain on contralateral cortical inflated map. Note the more anterior placed activations, towards the valley of the central sulcus, compared to air puff. Area 1 and 3b. Anterior insular activation is present

These activations were within a small area, representing the non-lip skin of face. Interestingly, cingulate gyrus and bilateral anterior insula were not activated. These areas did not get incorporated in the activated part of the map following the innocuous stimulation.

Volunteer group analysis: noxious heat

Noxious heat stimulation at T_{Pain} produced a thermal pain sensation. The pattern of activations following the thermal pain sensation showed bilateral S I and part of SII forming parietal operculum, but more consistently anterior cingulate and contralateral anterior insular cortex. The contralateral activations in the deep nuclei and the brain stem complex were also demonstrated. The threshold of the activation map needed to be relaxed for demonstrating brain stem activation. However the ROI time course graph and the anatomical location confirmed this to be a true activation and were retained. Anterior insula and cingulate cortex showed activations at a higher level of confidence during thresholding ($q< 0.05$) in all the four series, confirming these as integral substrates of the pain neuromatrix.

The activation of SI, when it was present, reflected a deeper location in the posterior bank of central sulcus or on its floor. This corresponded to deeper part of area 3b or area 1 in the primary somatosensory cortex. The activation in S I was on the summit or upper part of the posterior bank of the central sulcus when the air puff stimulation was used. This difference was consistent throughout the series. The analysis of the surface activation map, specially the map following V1 thermal pain stimulation (which had a FDR $q<0.05$) when compared with the map from air puff stimulation, showed remarkable non overlapping activation pattern between these two modalities (Fig 4.4 a&b). The anterior cingulate and anterior insular cortex were active during painful stimulus and were silent during innocuous tactile stimulation, and forms part of this disparate activation pattern

noted above. Fig 4.5 looked into the activation of the deeper structure and contralateral hemisphere activation patterns. The findings were commensurate with previous published data. A list of significant peak activation voxels following thermal pain sensation and their anatomic locations are described in table 4.5

Cluster activation list of V3 Noxious Heat stimulation in healthy volunteers From Talairach Coordinates						
	"Peak X"	"Peak Y"	"Peak Z"	"t"	"p"	
"Cluster 1"	67	5	19	5.265065	0.000000	Precentral Gyrus (6)
"Cluster 2"	58	-31	43	4.403517	0.000013	Inferior Parietal Lobule (40)
"Cluster 3"	51	-1	10	6.020925	0.000000	Precentral Gyrus (6)
"Cluster 4"	51	35	-14	5.084118	0.000001	Inferior Frontal Gyrus (47)
"Cluster 5"	51	-22	22	4.236774	0.000027	Insula (13)
"Cluster 6"	45	-7	46	4.721927	0.000003	Precentral Gyrus (6)
"Cluster 7"	42	-37	55	5.427365	0.000000	Inferior Parietal lobule (40)
"Cluster 8"	33	2	10	4.960322	0.000001	Claustrum
"Cluster 9"	39	-16	55	4.377997	0.000014	Precentral Gyrus (4)
"Cluster 10"	33	-25	65	5.475774	0.000000	Precentral Gyrus (4)
"Cluster 11"	21	-16	22	4.771019	0.000002	Caudate
"Cluster 12"	24	-31	13	5.059853	0.000001	Caudate
"Cluster 13"	3	-4	67	4.813731	0.000002	Superior Frontal Gyrus (6)
"Cluster 14"	3	8	37	3.815236	0.000151	Cingulate Gyrus (24)
"Cluster 15"	-3	-7	22	4.008857	0.000069	Cingulate Gyrus (24)
"Cluster 16"	-12	8	37	4.705225	0.000003	Cingulate Gyrus (24)
"Cluster 17"	-6	-76	40	4.412542	0.000012	Precuneus (7)
"Cluster 18"	-9	-55	68	3.917722	0.000100	Postcentral Gyrus (7)
"Cluster 19"	-18	-58	-14	4.368533	0.000015	Cerebellum
"Cluster 20"	-24	-25	22	3.886675	0.000114	Insula (13)
"Cluster 21"	-36	-37	62	4.477687	0.000009	Postcentral Gyrus (2)
"Cluster 22"	-42	5	7	4.243769	0.000026	Precentral Gyrus (44)
"Cluster 23"	-42	-16	49	4.066098	0.000055	Postcentral Gyrus (3)
"Cluster 24"	-45	-1	7	4.795839	0.000002	Precentral Gyrus (44)
"Cluster 25"	-63	8	7	5.389153	0.000000	Precentral Gyrus (44)

Table 4.5 A sample list of activated clusters following noxious heat stimulation (BrainVoyager QX auto generated) Talairach Coordinates, the 't' value signifying measure of signal and 'p' the statistical probability of the voxel being a true activation

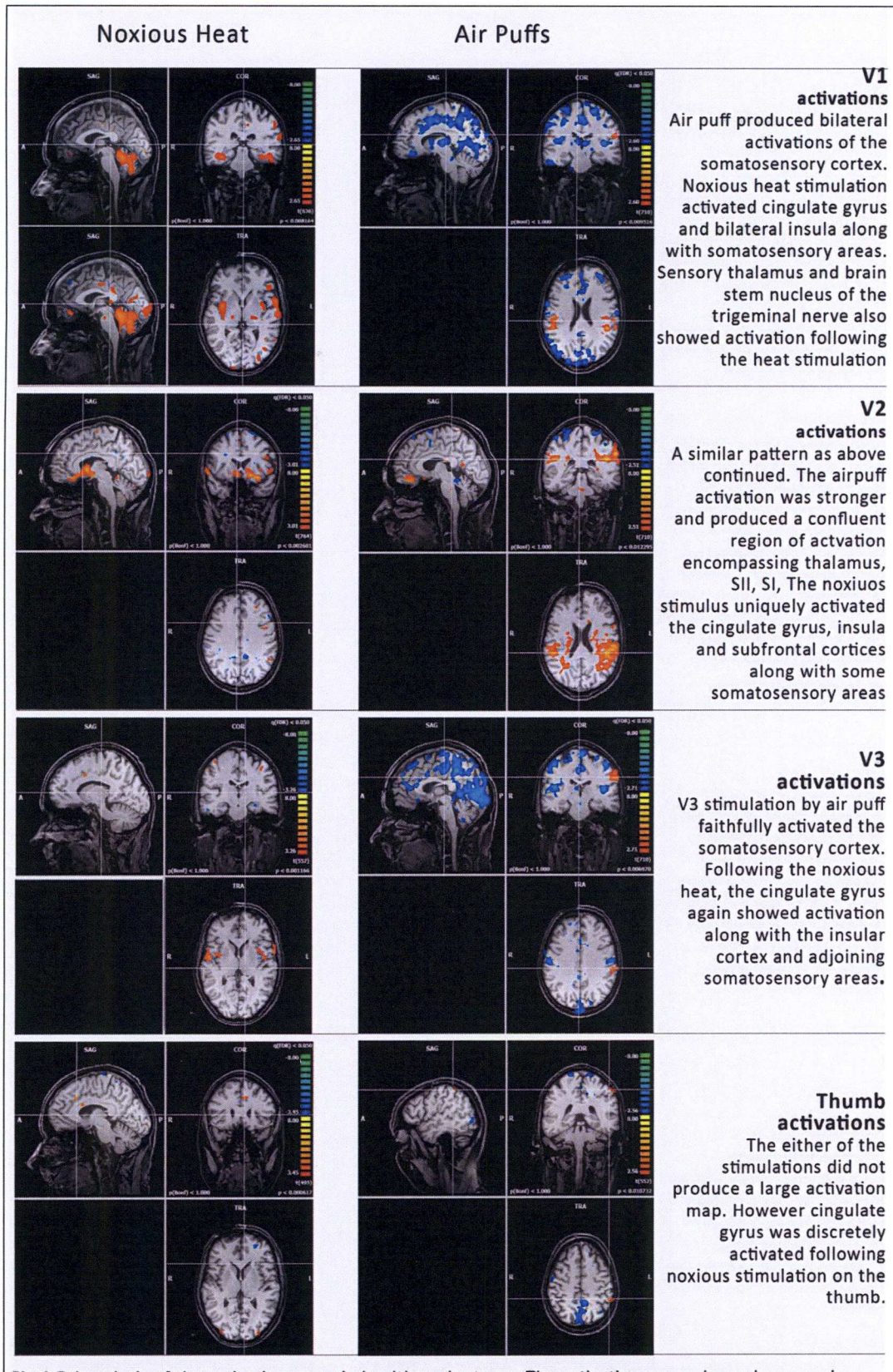

Fig 4.5 Ananlysis of the activation maps in healthy volunteers. The activation maps shown here used a default q value of <0.05. However to demonstatre brainstem activations, in two groups, the parameter was relaxed but within a cluster corrected p value of <0.05. The p value is available in each block of slices.

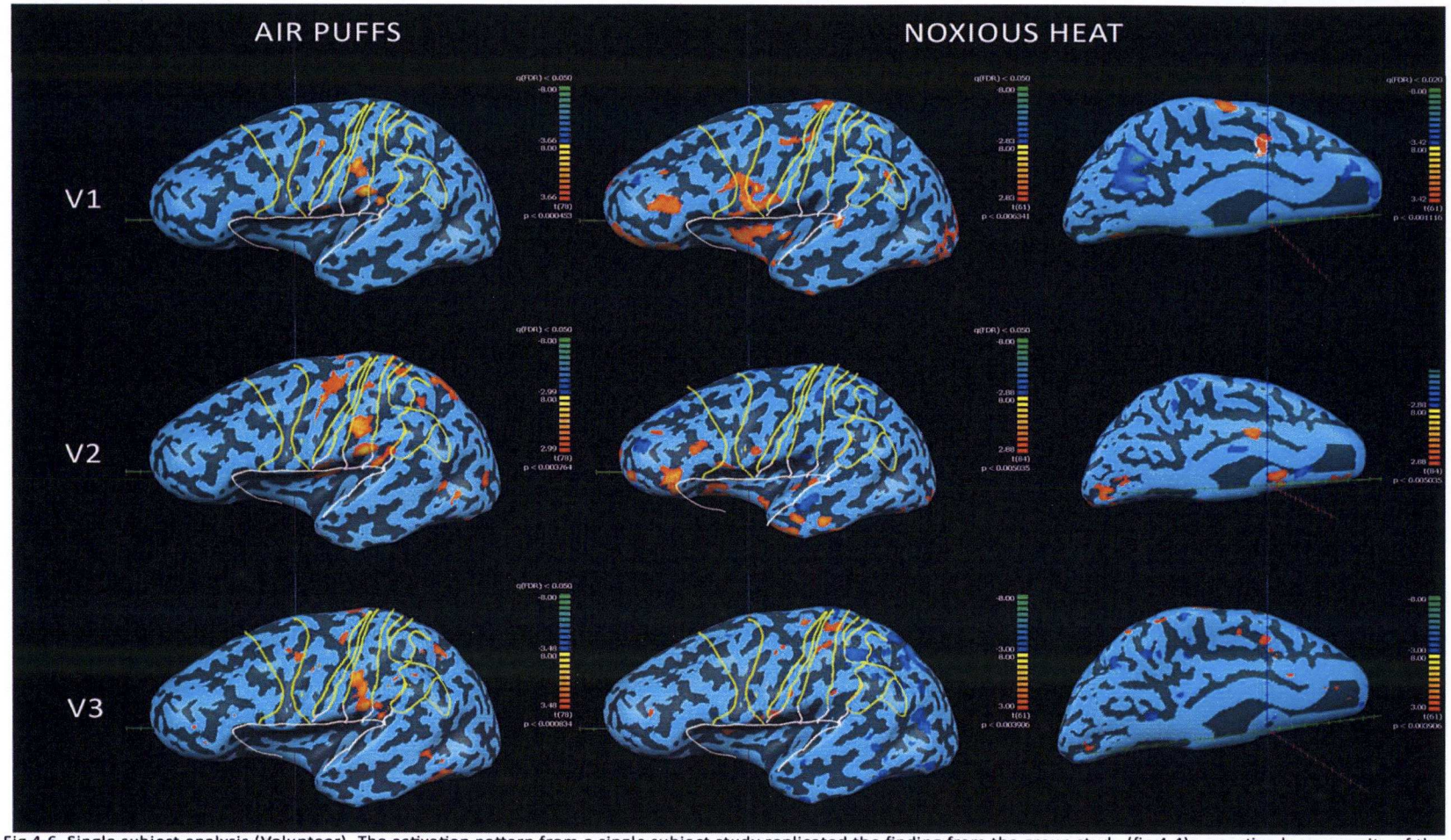

Fig 4.6 Single subject analysis (Volunteer). The activation pattern from a single subject study replicated the finding from the group study (fig 4.4)suggesting homogeneity of the data within the group. The activations following noxious heat stimulation matched that of air puff in S I area but more anteriorly located, corresponding to area 3a. Anterior cingulate and anterior insular activations were a constant feature following noxious heat stimulation. The tactile stimulation activated area 3b of SI and spreded into SII, PV near the posterior boundary of the insula.

Volunteer: single subject analysis: air puffs and noxious heat

The study looked into a random volunteer sample from the database to verify whether a single subject analysis was plausible. The experimental paradigm and use of a 3T platform theoretically had improved the data acquisition and signal to noise ratio. However it was necessary to determine that the single subject dataset would stand a strict statistical test FDR $q < 0.05$).

The result of a single subject analysis was summarised in fig 4.6. The activations could be seen in the ipsilateral trigeminal brainstem nucleus at the level of pons (main sensory nucleus of trigeminal nerve for fine touch and tactile sensation), the contralateral thalamus and contralateral primary somatosensory cortex in following thermal pain and tactile stimulation. The cortical activation maps, represented over the subject's own inflated hemisphere demonstrated activation in primary and secondary somatosensory cortex with somatotopy. The analysis of fMRI dataset following thermal pain demonstrated the cingulate and insular activations in all the three runs from the trigeminal dermatome.

The areas of activations from the dataset (V2 air puff) were further matched with the time course data. This demonstrated good fitting of the HRF with the predicted response in every visible cluster. The HRFs were synchronous and showed an overall pattern of HRF amongst the activated clusters. This response from the ROIs, further validated the activation map. (Please refer to Fig 4.7)

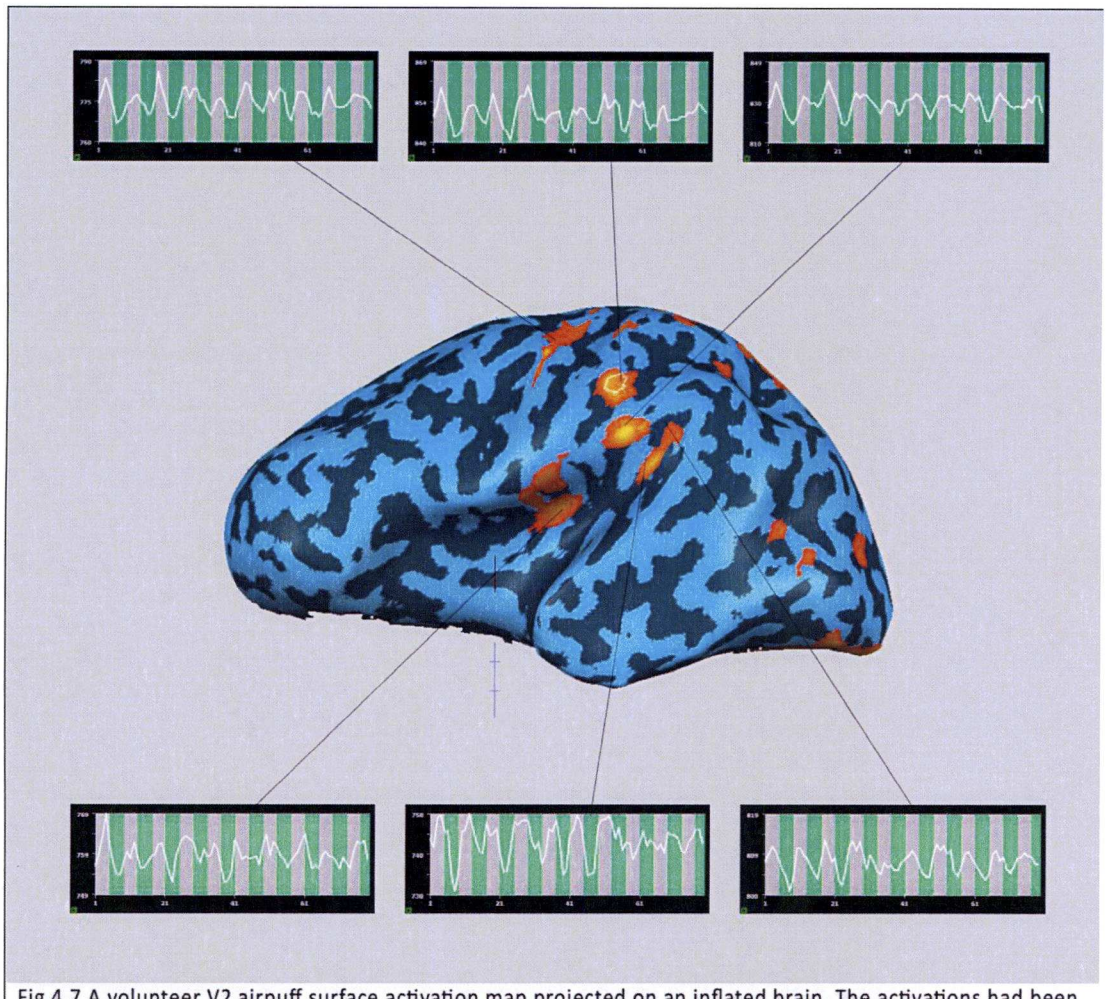

Fig 4.7 A volunteer V2 airpuff surface activation map projected on an inflated brain. The activations had been t tested and corrected for multiple comparisons by False Detection Rate analysis ($q < 0.05$). For this single subject analysis, a time course analysis were undertaken to further check the validity of the data.

Summary from volunteer (group and single subject analysis) study

The findings from the volunteer study is summarised in table 4.6

Volunteers	SI				SII		Insula		Cingulate
	3a	3b	Area1	Area2	PV	SII	Ant	Post	Ant
Pain									
Tactile									

Table 4.6 Summary of differential activation pattern seen in healthy volunteers following thermal pain and innocuous tactile stimulation to the face and thumb. The differential activations, specially in insula, SII, PV, cingulate, and area 3a of SI were noted consistently through the group analysis and single subject study. ***Red*** *signifies activation noted in the location,* ***White*** *signifies an absent activation in the area.* ***Pink*** *denotes borderline areas.*

Analysis of activations in patients

Patients formed a variant group of subjects. Out of eleven patients whose data could be used for analysis, nine had a diagnosis of trigeminal neuralgia and two suffered from neuropathy. One patient developed an attack of acute neuralgic episode during the experiment. Three patients reported tactile allodynia or unpleasantness following air-puff stimulation of the face.

For the purpose of analysis, the patients were divided into following groups (Fig 4.8) according to response following airpuff experiment to achieve some 'pathology homogeneity' to enable group study and further 'single state single subject analysis'.

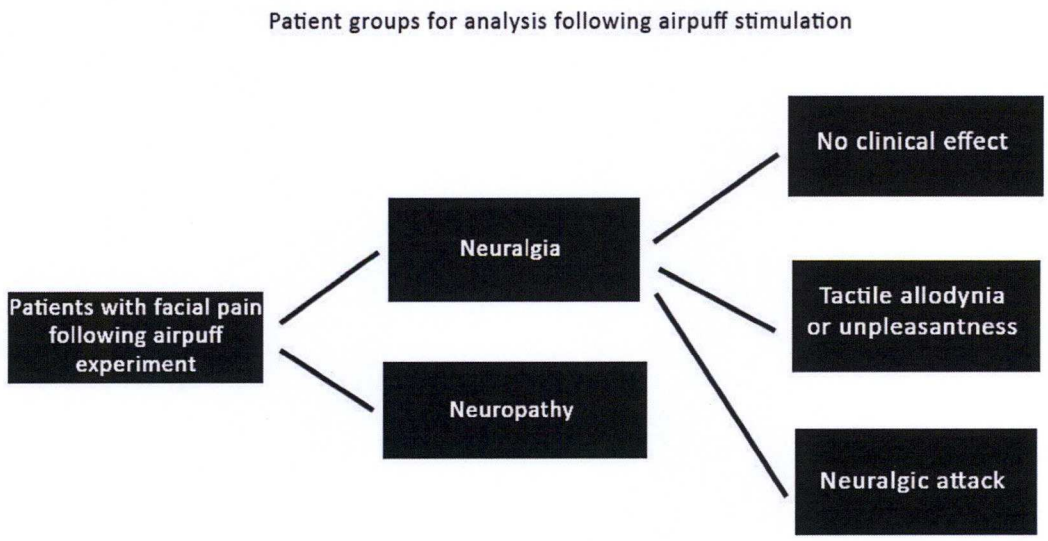

Fig 4.8 Patient groups for analysis.

Patients: Trigeminal neuralgia with air puffs

fMRI data from patients with the diagnosis of trigeminal neuralgia were first analysed as a group. This included three patients who had reported an allodynic or unpleasant response and one patient with an acute neuralgic pain. The activation maps were significantly less populated at high threshold and high confidence interval following air puff stimulation. Small clusters of activations were demonstrated in bilateral SI, SII and insular cortex with appropriate time course data at a lower threshold. Due to scanty activation, observation on somatotopy following air puff stimulation could not be made. However insular activity was significantly more forward than what would be expected from air puff stimulation of face in the healthy volunteers. The brain stem and thalamic activation were not demonstrated in the group studies at FDR $q < 0.05$. At a lower threshold and without correction for multiple comparisons, ipsilateral brainstem, thalamus and cortical activations could be isolated (Fig 4.9). When comparing the activation patterns, activation of cingulate gyrus during innocuous tactile stimulation of the trigeminal somatosensory network was noted with interest. Fig 4.11 a demonstrate an atypical insular activation.

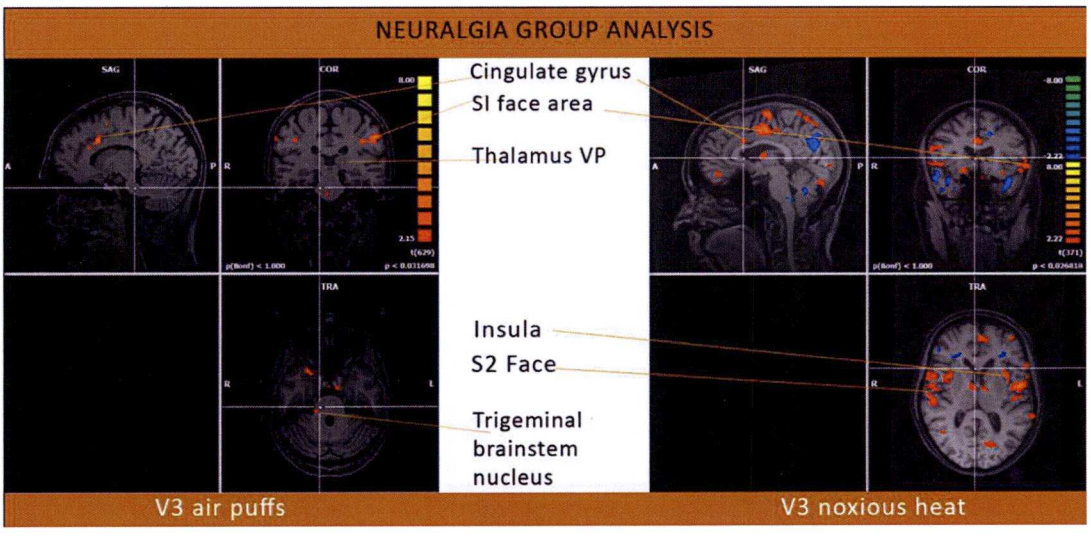

Fig 4.9 Group analysis of the activations from the air puff stimulation and noxious heat stimulation of the face. *Note the low threshold value for air puffs. Activations were not cluster corrected and only a 4mm spatial smoothening was used. The time courses of the clusters match the predicted model well. The ipsilateral brain stem activation was at the level of entry of the trigeminal nerve and would correspond with the main sensory nucleus*

of trigeminal brain stem nucleus complex. Another cluster of activation visible in the brain stem in the medulla would correspond with the spinal trigeminal nucleus. The identification and labelling of the activations in the brain stem being done with respect to the position of the entry of the trigeminal nerve at the pons and vide classical sectional anatomy. Of note was anterior insular activation, which would be atypical following air puff stimulation. Bilateral SI and SII activations are also seen as routine.

The single subject analysis following air puff stimulation was remarkably similar to the group data. (Fig 4.11 a,b &C)

Patients: Trigeminal neuralgia with noxious heat (thermal pain)

Compared to the activations following the tactile stimulation, the thermal pain stimulation produced significantly florid response in the group analysis as well as the single subject analysis.

The activation of contralateral SI corresponding to the face area was seen along with the adjoining part of SII cortex. Anterior insular activation and cingulate activation were also demonstrated. Of note was activation within the posterior insular area which would be an atypical activation for this mode of stimulation when compared with healthy volunteers data. The single subject analysis demonstrated all the activations of the group data and was congruent with the key atypical findings of the posterior insular activation and typical finding of the cingulate gyrus activation. The activations following thermal pain stimulation showed somatotopy. In the SI area the (between V1 and V3 activations) distinct somatotopy of rostra-caudal orientation of the face was maintained.

Patients: Trigeminal neuropathy with air puffs and noxious heat

Two patients with the clinical diagnosis of trigeminal neuropathy was analysed as a group. However due to incomplete datasets, in some runs only one patient's information was used. The activations following the air puffs remained within SI area (area1 & 2 of the SI). The anterior cingulate gyrus was not activated during air

puff stimulus but show strong activation during noxious heat. This was more like the activation pattern of the healthy volunteers group. Trigeminal neuropathy patients responded vividly following thermal pain stimulation unlike all other groups with maximal stimulation of anterior insular cortex. Here, again the loci of activation was appropriate for a painful sensation (when compared with healthy volunteers) but the proportional cluster size was biggest. The insular activation remained confined to the anterior area only (Fig 4.11a, b &C). A synopsis of various activation patterns observed so far in the two different pathology and its variance from that of healthy volunteers are summarised in table 4.7

Neuralgia	SI				SII		Insula		Cingulate
	3a	3b	Area1	Area2	PV	SII	Ant	Post	Ant
Thermal pain			→	→	→	→	→	→	
Innocuous tactile			←	←			←	←	+
Allodynia/ unpleasant feel									
Neuralgic attack									
Neuropathy									
Thermal pain							++		++
Innocuous tactile									

Table 4.7 Summary of the activations in patients with neuralgia and neuropathy. *The* ***red*** *blocks indicate what would be expected in a healthy volunteer for the modality of sensation. The* ***purple*** *blocks denote areas where stimulation has been observed in variance to the healthy volunteer study for the modality. The arrows denotes the way the activation moved when compared with equivalent healthy volunteer study. ++ denotes very busy activation in the area when compared to healthy volunteers*

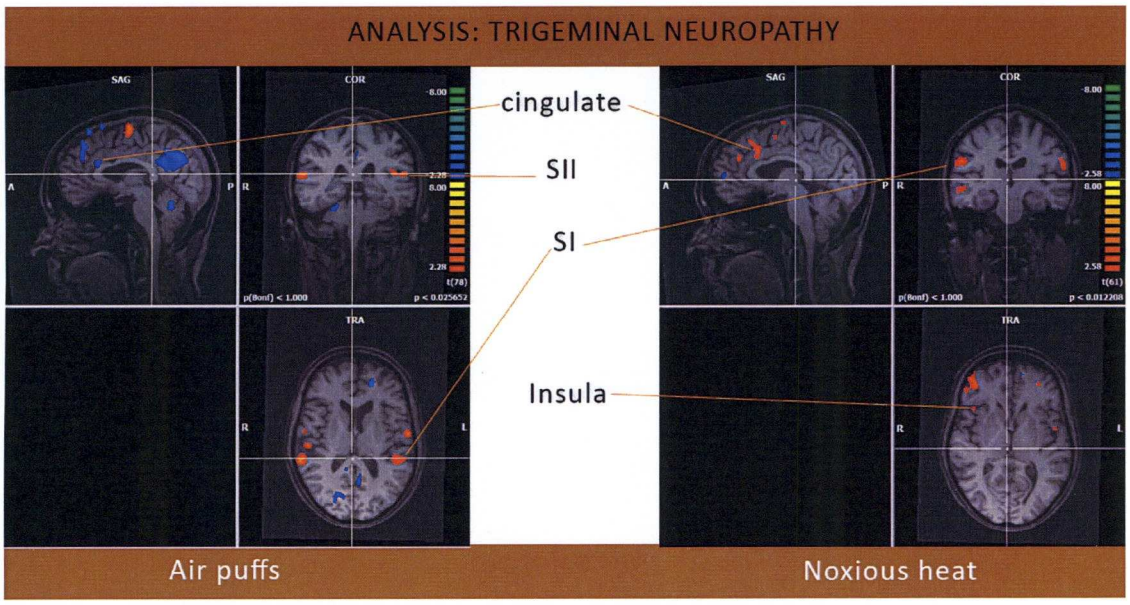

Fig 4.10 Activation following thermal pain and innocuous tactile sensation in Trigeminal Neuropathy. The stimulations caused activation in most of the synaptic stations in the trigeminal somatosensory pathway. Eg Bilateral SI and SII, Insula, Cingulate gyrus. The activation patterns were similar to that of healthy volunteer group except disproportionate response to heat in V3 dermatome.

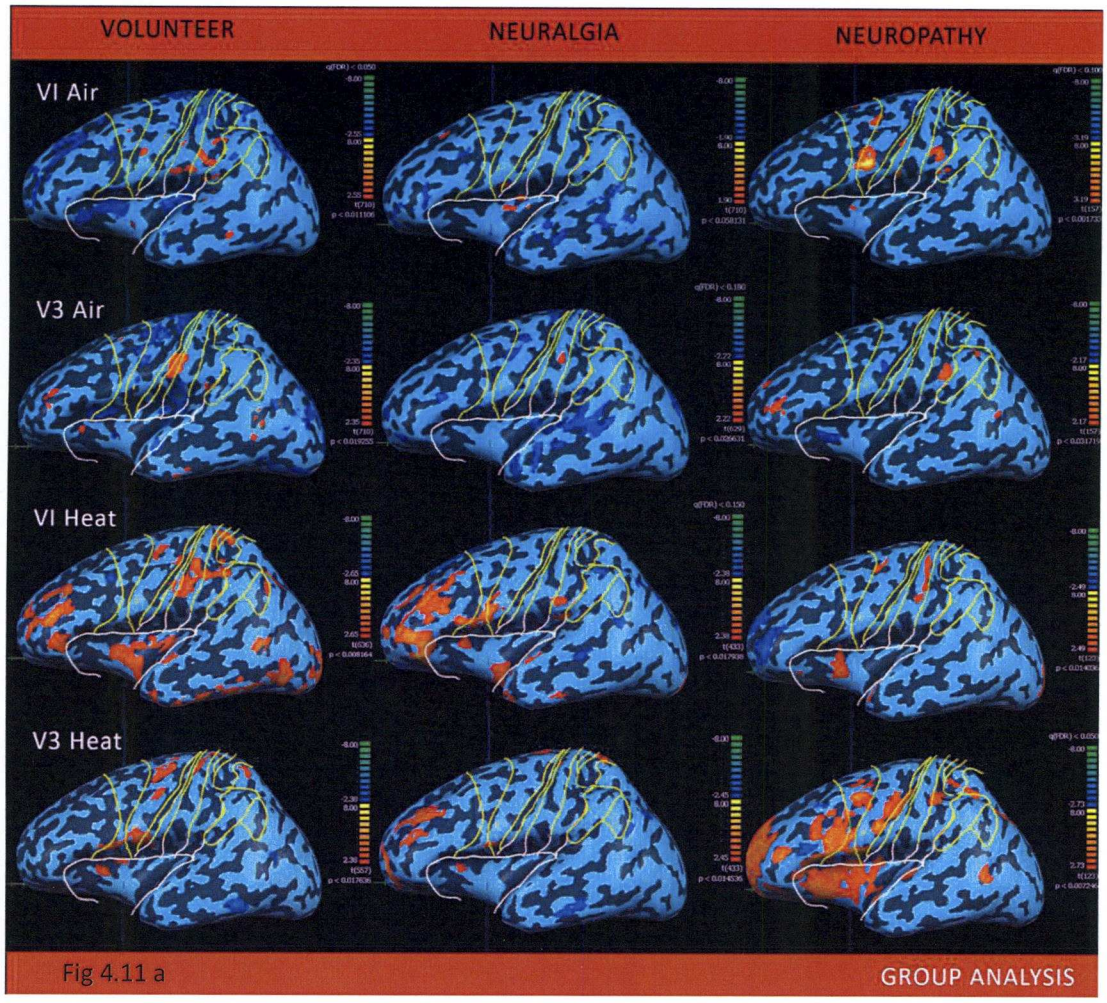

Fig 4.11a,b&c Demonstration of differential activity between healthy volunteers, and patients with trigeminal neuralgia and neuropathy. The maps were presented on inflated contralateral brain to show the activities in cortical areas hidden within a sulcus. The Group and Single subject studies have similar activation pattern. The Brodman areas Fig 4.11b are presented here for quick reference for identifying the location of an activation clusters.

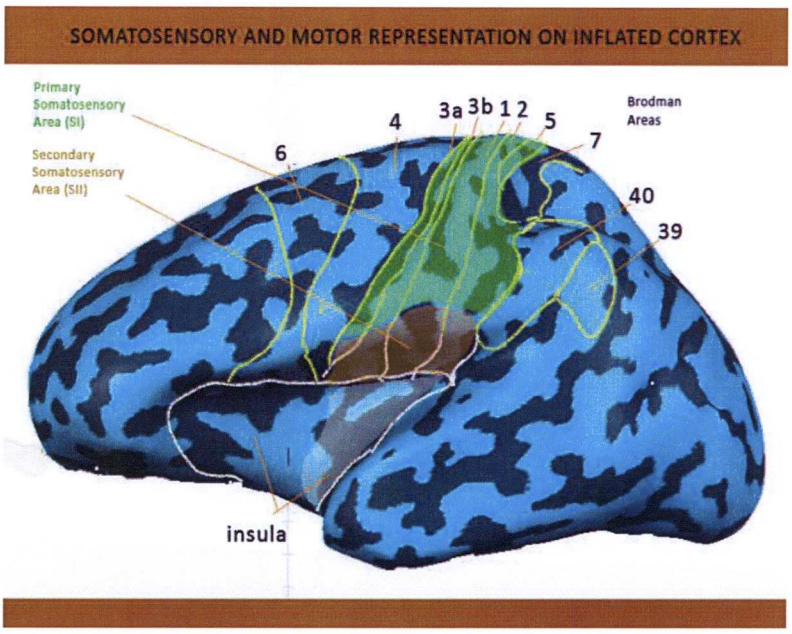

Fig 4.11 b

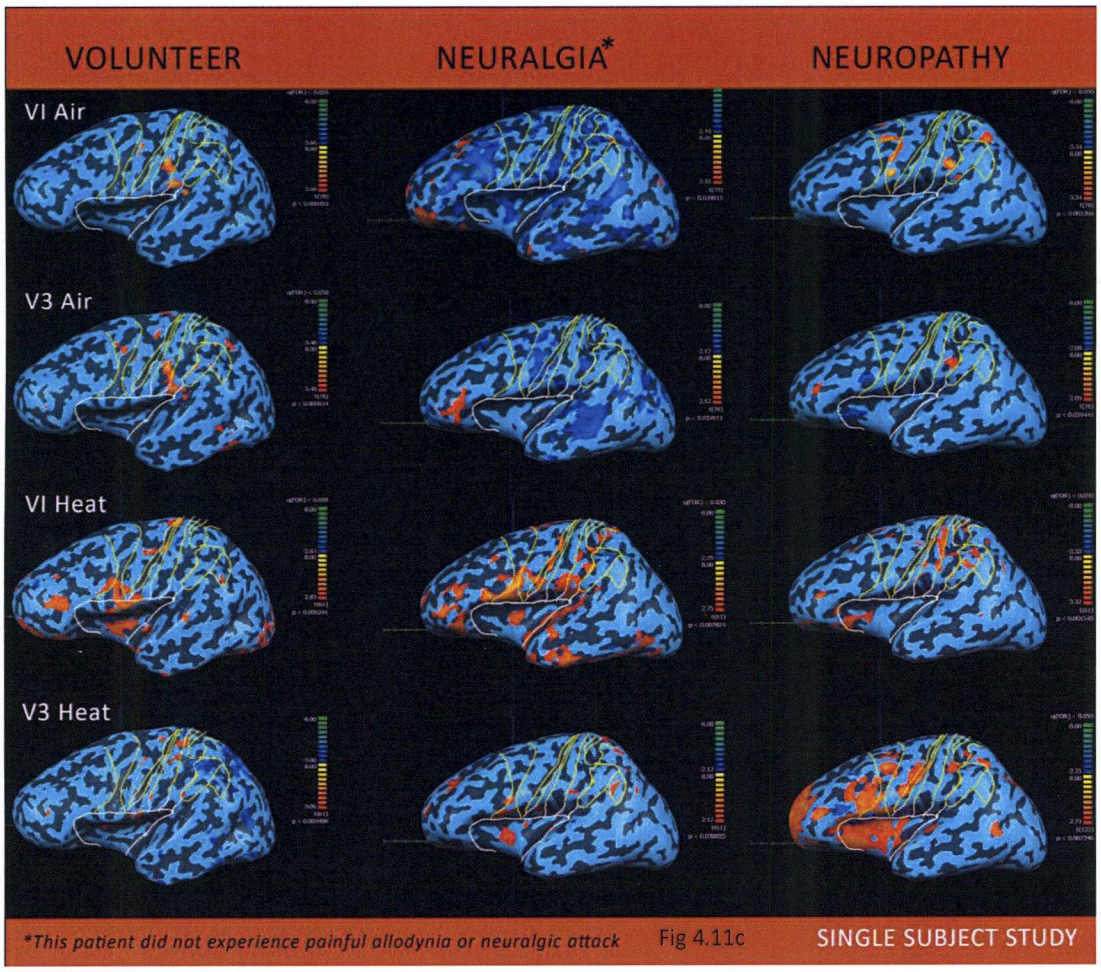

Fig 4.11 a,b&c continued. These diagrams were to facilitate comparison between activation patterns. During air puff experiment, the neuropathic group and volunteers had a similar activation in contralateral areas of SI and SII cortex spilling into very posterior insula. No activation in anterior part of insula during this innocuous stimulation was seen. With V3 air puff stimulation, the volunteer group had more activation clusters on the cortex compared to the patients. Neuropathic patients maintained a close similarity to healthy volunteer's activation pattern. Neuralgia group and single subject both had activation clusters appearing in the mid-anterior insula or adjoining parietal ventral area during innocuous stimulation, which was an atypical finding. During the noxious heat experiment, the activation cluster content of the maps was very dissimilar. However a pattern was observed between neuropathic patients and the volunteers. In spite of vivid activation following the pain stimulus, activations of the insula were confined to the anterior part only. In the neuralgia group, insular activation was mid-anterior with activation of posterior part of SII and parietal operculum, the loci that would usually get activated during tactile stimulus.

Analysis of fMRI runs of trigeminal neuralgia patients classified by 'micromotion'

The trigeminal neuralgia patients were sorted into three unequal groups. Patients who experienced a neuralgic attack formed a group, the second group was formed by patients who felt an unpleasant tactile allodynia from the air puffs but did not proceed to a neuralgic attack. The third group was patients who did not feel any allodynic or neuralgic episodes during the experiment. Fig 4.12 looked into the three groups and their activation patterns following air puff stimulation. This was a subgroup study of the trigeminal neuralgia patients.

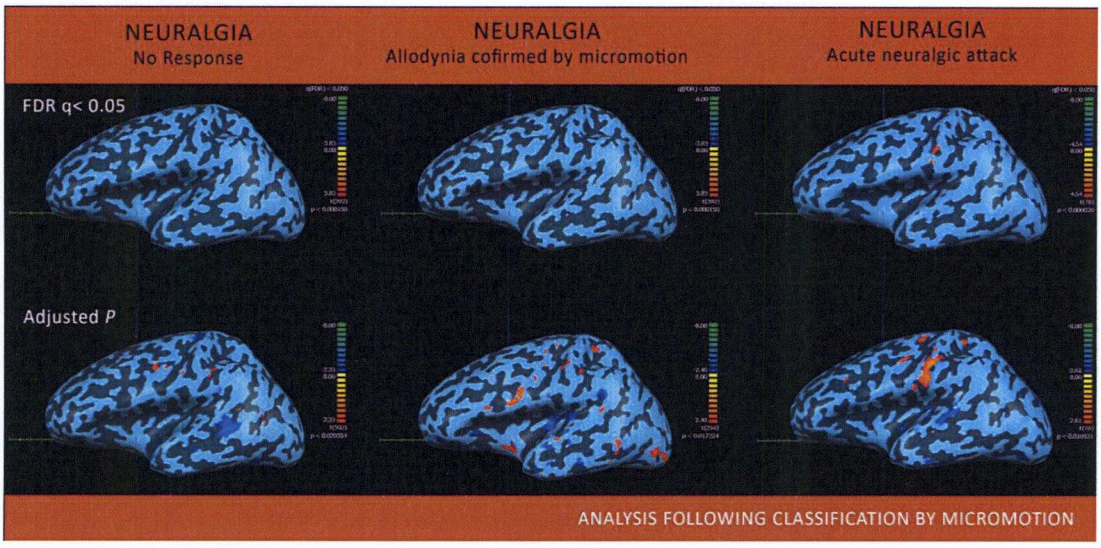

Fig 4.12 The post scan patient report and micromotion analysis helped to look in to the trigeminal neuralgia group in further detail. The above was an analysis of V2 air puff stimulation of the three groups presented on a contralateral inflated map. At FDR q< 0.05 only the patient who had a neuralgic attack demonstrated a discrete activation in the SI area. However on lowering the threshold to a still respectable p<0.001, separate activation maps began to emerge from the three groups. The patients who did not feel any unpleasant sensation had the minimal activation. The face area of SI corresponding to area 3b/area1 was activated in this map with a further activation in area2 and corresponding motor cortex activation. However no other cortical areas, insula or cingulate did activate. In the group who had complained unpleasantness or allodynia, the activations of the somatosensory cortex became more prominent. There was a larger cluster of activation on the face area but most importantly, an activation cluster appeared in the anterior basal part of the insula. During the neuralgic attack, a larger activation map appeared in the SI, corresponding the topography of area 1 spreading into area 3b towards the upper bank of the lateral sulcus. There was a corresponding motor cortex

response which was smaller than the SI response. The activations from the rest of the visible cerebral cortex were wiped out in this map when compared with the allodynia picture which had more clusters of activations. An anterior insular activation or cingulate gyrus activation was not identified during this analysis of the fMRI dataset acquired during a neuralgic attack.

A single patient study through allodynia – neuralgia phase and correlation with micromotion

The allodynic response

Patient 7, suffered a single neuralgic attack during the experiment with air puff stimulation to the V3 segment of the face. She also reported an allodynic response during experiment on the V2 segment and no response while the air puff was applied on the V1 segment. Hence there was a unique opportunity to study the three clinical states in a single patient. Specially an opportunity to identify the transformation of fMRI activity when a neuralgic attack struck.

The fMRI data sets were analysed and micromotion were identified in the reported runs of V2 air puffs and V3 air puffs. Fig 4.13a summarises the V2 allodynic response in this subject. It was observed from the micromotion that patient had a sharp movement in the scanner. The HRF response analysis of the ROI showed the time course of the micromotion matched with a sharp rise in the HRF curve in all the ROIs suggesting abrupt increase in neuronal activity. However patient had not complained of a neuralgic attack during this run of the experiment.

The activation map was particularly informative. There was demonstrable activation of the brain stem trigeminal nucleus complex on the ipsilateral side, contralateral thalamus, and contralateral somatosensory cortex. The highest peak of HRF was demonstrated at the brain stem complex and the rest of the system replicated the response faithfully. No amplification of HRF was seen beyond brain stem complex or thalamus. Thalamic activation was bi lobed suggesting multiple nuclei were involved in thalamic processing. The somatosensory cortex also had a significant cluster at FDR $q<0.05$. Other activations outside somatosensory connections were in contralateral insular cortex and cingulate gyrus.

Tactile Allodynia : Activation Maps, Micromotion and HRF Time Course : to Investigate interaction within the network
A
1
2
B
C
D
1
2
3
D1
Brain stem activation and HRF
D2
Brain stem activation and HRF
D3
Brain stem activation and HRF
A1
Thalamic activation and HRF
A2
Thalamic activation and HRF
3 D Motion Correction time course : showing micromotion
B
Cingulate cortex activation and HRF
C
S1
Cortical activation and HRF
3 D Motion Correction time course : showing micromotion

Fig 4.13a

Fig 4.13a Summary of activation following an allodynia report. *The micromotion confirmed the presence of allodynia. The HRF response corroborated. Three activations were identified in the trigeminal brainstem nucleus complex, the main sensory nucleus, as being located above root entry zone of trigeminal nerve D1, and laterally placed activations were termed D2 and D3. The main sensory nucleus showed maximum activity and HRF spike. The peak in HRF died down upstream specially in the thalamic activations (A1 and A2). The S I cortex also had a damped activation pattern compared to the activity in the brain stem. To note, this patient did not report a neuralgic attack. Importantly, the main sensory nucleus showed an extremely congruent and equivalent activation HRF curve with the anterior cingulate gyrus suggesting a very strong connectivity between them.*

Fig 4.13b The representation of cortical activation following a tactile allodynia on an inflated brain. The centre of gravity of the cluster was based on Area 1 of the primary somatosensory cortex (SI). The activation took the shape of facial representation of the homunculus along area 1 architectonic boundaries and reached SII. Corresponding motor cortex activations were seen. No insular activation was noted.

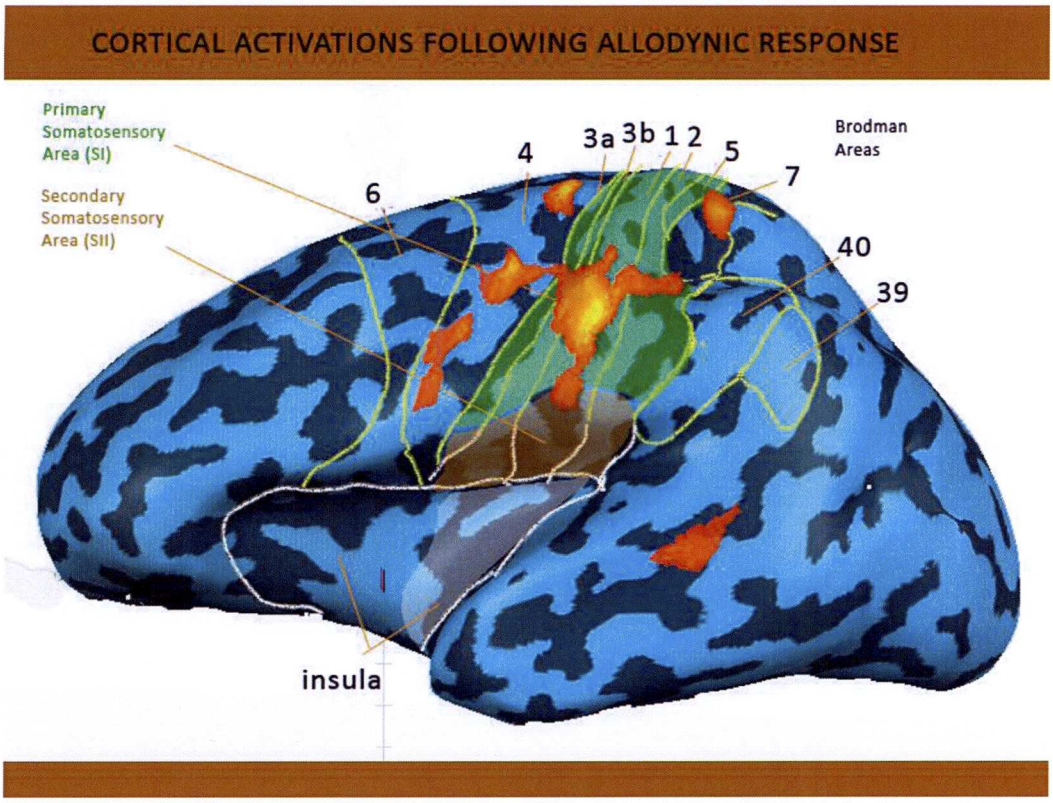

The neuralgic event

The above patient suffered an acute sharp shooting pain of trigeminal neuralgia in the next stage of the experiment. The event happened about 10 seconds before end of the session. The patient completed the scanning session and reported the attack on completion of the scan. The trigeminal neuralgic attack was evoked by the air puff stimulation. Only one patient of the whole group suffered this type of pain.

The 3D motion correction data identified the micromotion and validated the patient report. Following creation of an activation map, the time course data of the HRF was matched with the time course of the 3D motion correction graph and onset of the micromotion was found to correlate and coincide with an accentuated spike in the HRF response throughout the trigeminal somatosensory system. However the HRF spike of the peak activation voxel in contralateral S I seemed to precede the rest of the network. (Fig 4 .14 see row A).

The density of activated clusters following a neuralgic attack at equivalent threshold (FDR $q< 0.05$) was significantly less when compared to the allodynia state. The effect of a neuralgic attack on the cortical activation map seemed to be that of more circumscribed activation. Other than activation of SI and corresponding motor cortex at area 4, the rest of the brain remained devoid of any activation cluster. The lack of activation extends to brain stem, insula, cingulate cortex and thalamus. At lower threshold some brain stem activations were noticed.

The anatomical locations of the ROIs at the brainstem corresponded with the main sensory nucleus of the trigeminal nerve (dorsal to trigeminal root entry zone and away from the midline), and spinal nucleus of the trigeminal nerve (below the level of trigeminal root and towards midline). The HRF from these two activations were compared in Fig 4.15. Unlike during allodynia, the brainstem activations did not have congruent HRF configuration with the rest of the network, specially the activations in the SI cortex. The laterally placed nucleus had a muted peak that fits into the time line of the peak activation voxel's HRF curve but the fit was not as good as was seen during allodynia.

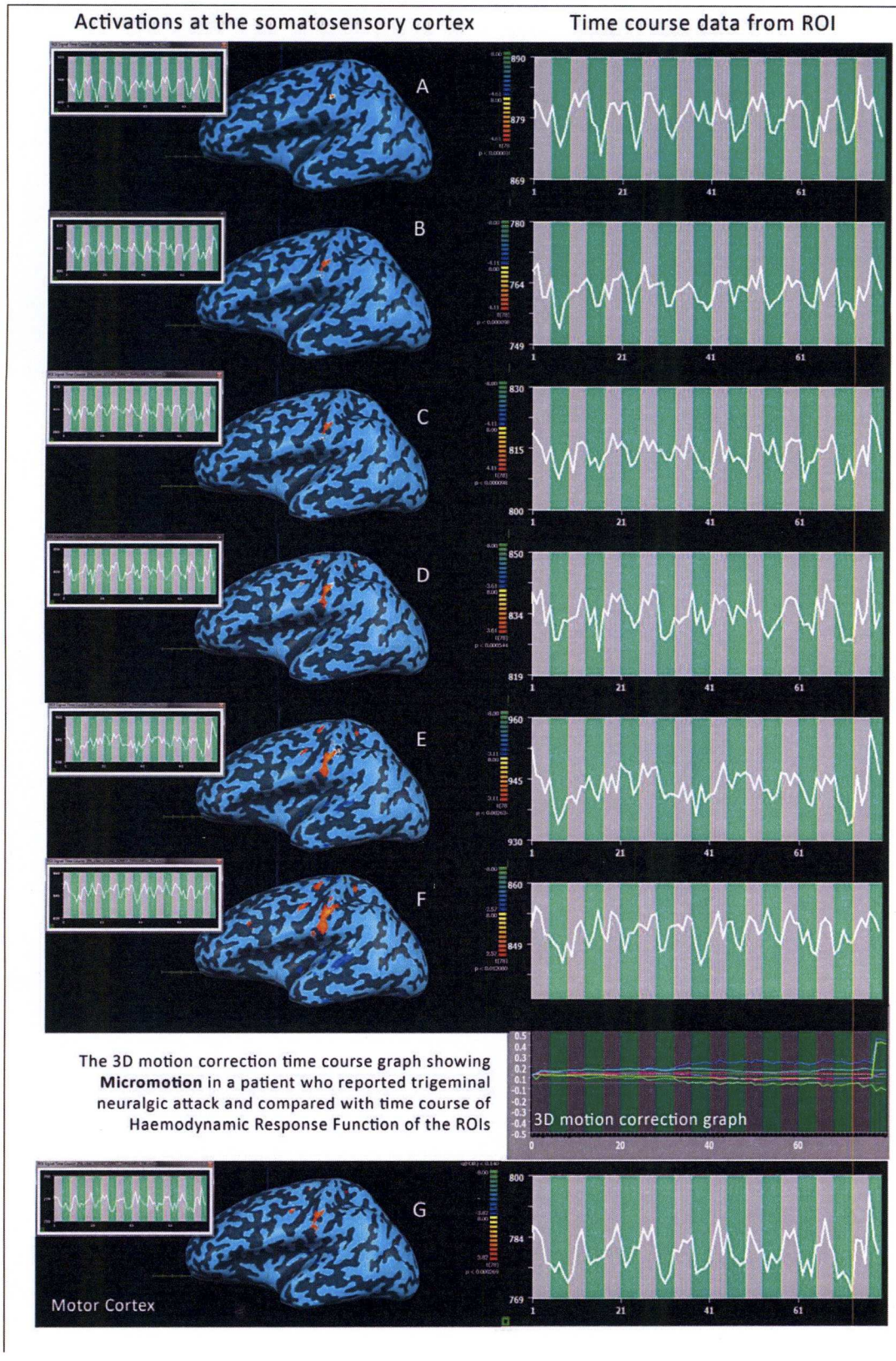

Fig 4.14 The activation of the somatosensory cortex following an acute trigeminal neuralgia attack and the hemodynamic response function of the activated regions of interest were correlated with the micromotion identified during 3D motion correction. The micromotion was a confirmatory guide that a neuralgic attack had happened and its temporal location on the time course of the HRF. The onset of micromotion coincided

accurately with the activation on the motor cortex, and with the clusters in the SI except for the peak activation voxel with highest confidence of a true activation (row A). Here the spike of the HRF graph had stared few moments earlier than rest of the activated area. It is to be noted that the subsequent rows B,C,D.etc were activations from the surround of the peak activation voxel, identified by allowing the peak voxel to grow by relaxing the threshold of the statistical parameter. Row F signifies a ROI at the edge of the activated cluster where the HRF no longer showed the spike of neuralgic attack. Row G is the activation in the motor cortex which just precedes the movement identified by 3D motion correction algorithm. The activation of the peak activation voxel preceding the rest of the cluster is suggestive of a cause effect relationship akin to centre surround activation seen in around epileptogenic focus.

In an effort to locate the possible source of the second peak seen in the HRF described above, activations in the brain stem were investigated. The result is demonstrated in Fig 4.15

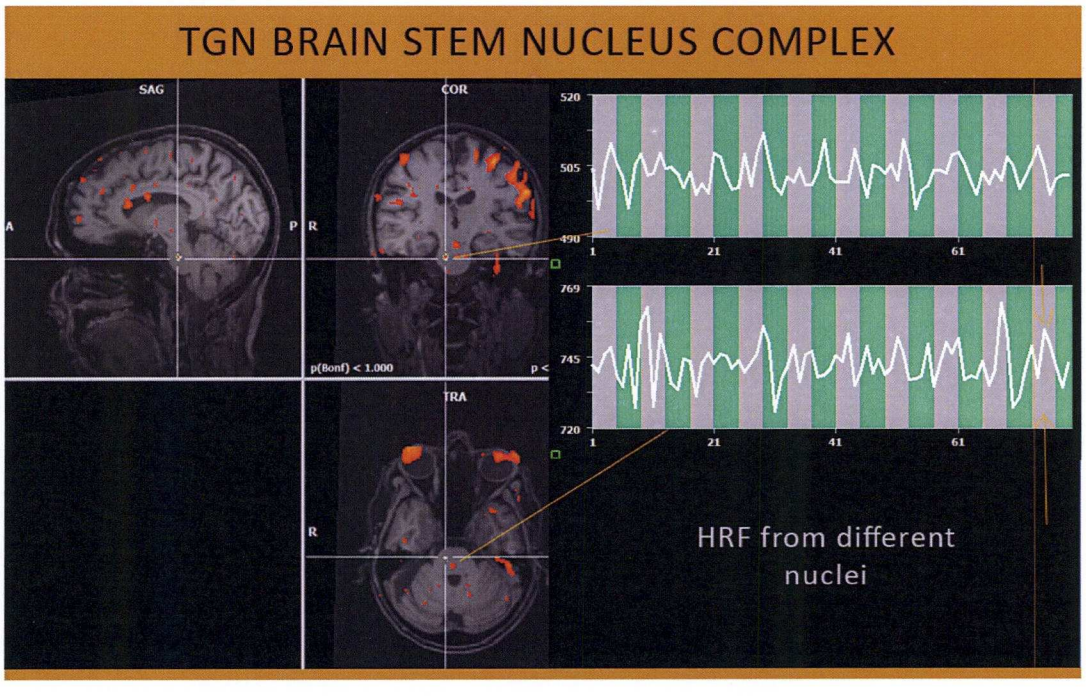

Fig 4.15 The hemodynamic response function curve from two different nuclei at the brain stem. The lateral placed nucleus had an earlier and one spike 'peak' following the marker line. While the medial and lower paced nucleus had a slightly delayed peak. The HRF of the first nucleus fitted well with the time line of the spike seen in the peak activation voxel at SI (Fig 4.14 row A). The HRF of the second nucleus fitted with the smaller subsequent spike in the HRF of the peak activation voxel. The fit is not as good as in the case of allodynia.

Further analysis of the trigeminal neuralgic attack data set using different predictor model (second analysis)

Our experiment with air puffs caused tactile stimulation to the face. The HRF predictor model reflected the 'on' and 'off' stages of the tactile stimulation in its block design. Patients, who felt unpleasantness with each epoch of the air puffs experiment, also fitted well with the model. However when a neuralgic attack was triggered after an initial quiet period , the 'predictor model' would have failed to predict the model HRF. The model should reflect the event of the neuralgic attack. Keeping this in mind, a new predictor model was designed to interrogate the neuralgic episode (Fig 4.15a). This predictor model utilised information from the micromotion observation to predict the time of onset of the neuralgic pain (attack).

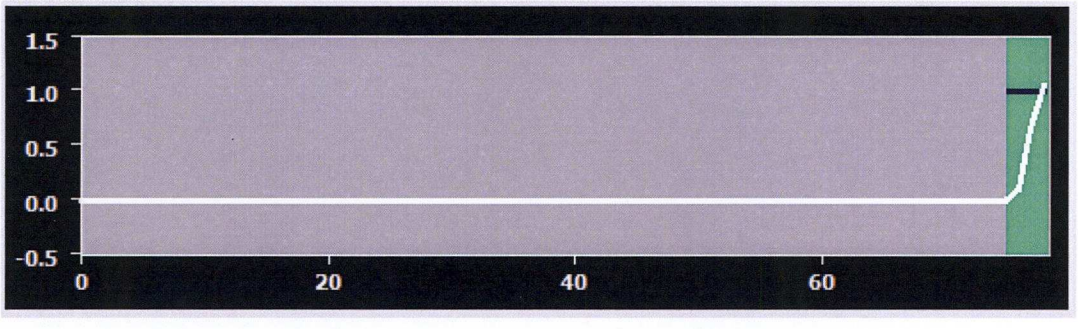

Fig 4.15a *Alternative 'Predictor model' for the analysis of 'triggered neuralgic pain'. This model is akin to event related fMRI analysis and considers the information from micromotion time line to identify the onset of the event of the painful neuralgic attack.*

The activation map following the second analysis demonstrated the brain areas active at the point of neuralgic attack. The activation clusters were profuse and spread along the whole of the area 1 of the primary somatosensory cortex (S I), involving whole of the face area and the rest of the body representation. Strong activity was identified in anterior part of cingulate gyrus (the part which was active during allodynic phase), subfrontal area, but the strongest activity at the onset of the neuralgic attack was identified in bilateral subgenual area of the cingulate gyrus (Broca's area 25). The HRF of these ROIs showed that they were comparatively dormant during the initial part of this airpuff run till the neuralgic attack happen. The brain stem activation was conspicuous by its absence and so was the thalamic activity even from this second analysis. Fig 4.15b summarises the activations during the neuralgic attack with the revised predictor model.

Activation Map following micromotion directed alteration of predictive HRF model to reflect the event of a Neuralgic Attack

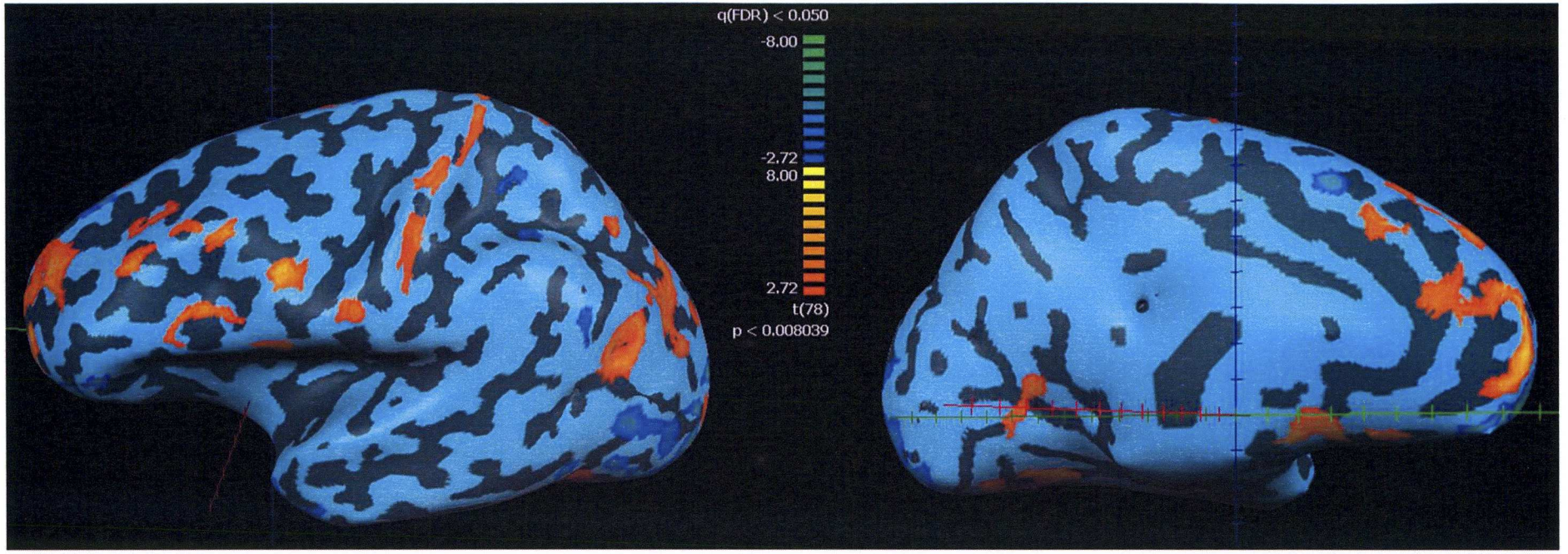

Fig 4.15b The modification of the predictive model unveiled an extensive activation during the neuralgic attack which was not visible before. The activation along area 1 of somatosensory cortex involved whole of the face area, extending into adjacent anatomic aareas. Activation of the frontal areas, subfrontal cingulate and perigenual areas were notable. Notable absence was insular activation.

The activation clusters from one patient following airpuff stimulation through the spectrum of clinical presentations

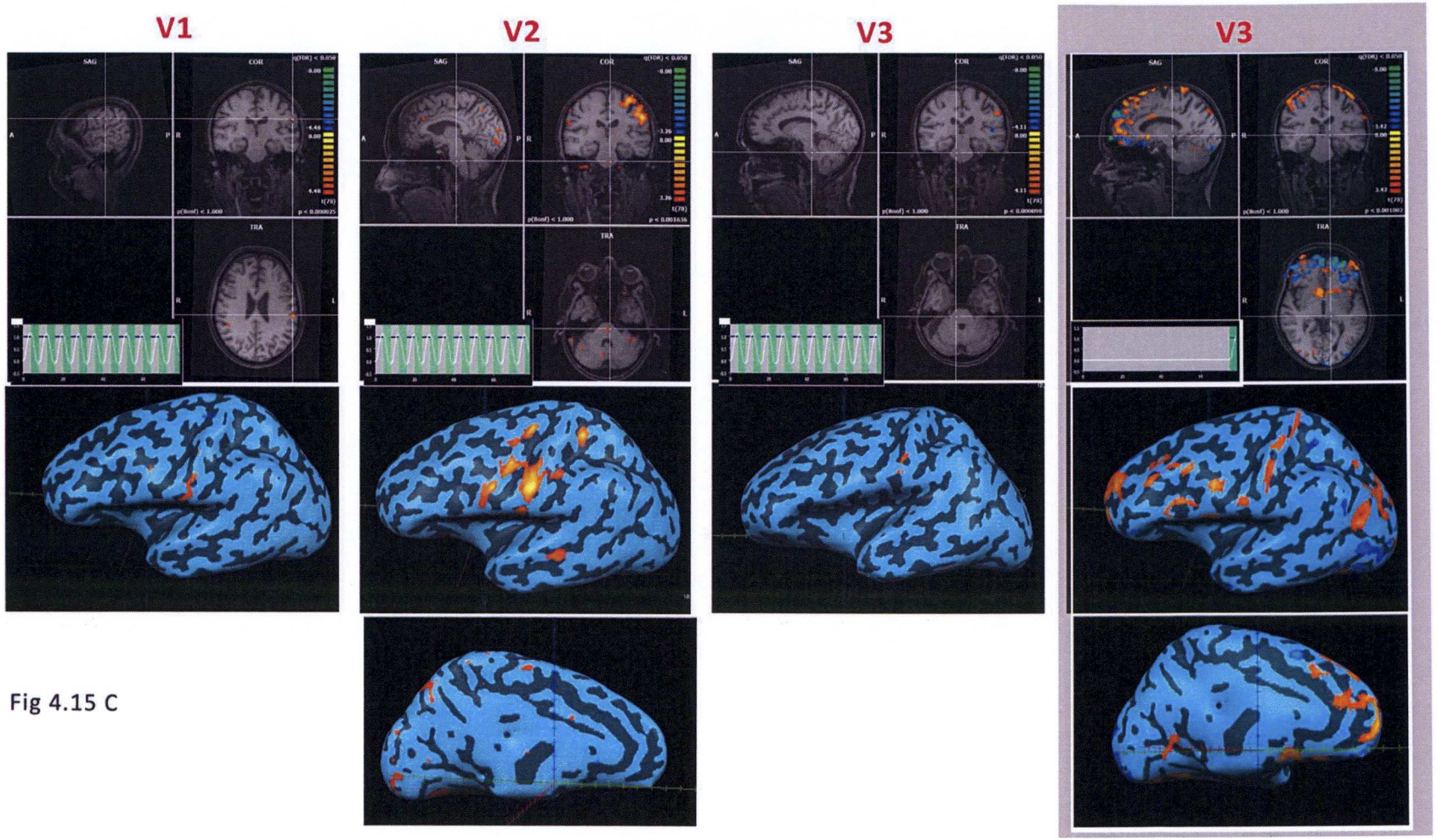

Fig 4.15 C

Fig 4.15 C *Summary of the activation clusters from airpuff stimulation at V1,2,3 of the trigeminal dermatome. These activations were from a single patient who experienced a neuralgic attack during stimulation of the V3 segment. This patient also reported unpleasant, painful sensation (allodynia) during stimulation of the V2 segment. No pain was complained during V1 stimulation. The shaded part of the diagram showed revised analysis of the activation during neuralgic attack using an event related predictive model. Note the extensive activations in the area 1 of the whole of the primary somatosensory cortex along with frontal, subfrontal, subgenual and cingulate activations in the revised analysis when compared to V2(allodynic response) and V1 (no response). The original predictive model failed to unveil the full extent of the activation during a neuralgic attack.*

The activation following thermal pain (noxious heat) and comparison of the activation pattern following allodynic response.

The activations during these two painful states, that the patient experienced during the experiment, on the same day, were compared. The similarity of the experimental environment and scanner condition made this comparison very robust. Fig 4.16 summarises the observation made from these comparison.

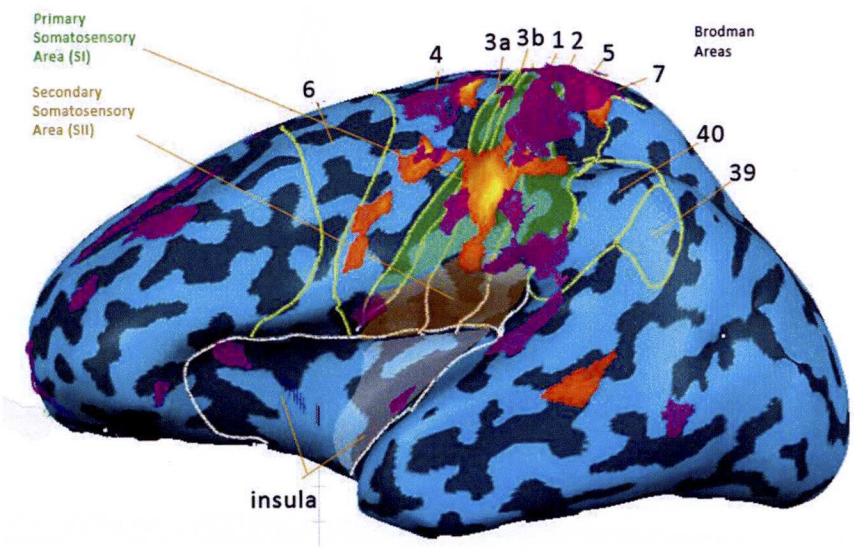

Fig 4.16 Observations were made following comparison of the activation patterns between thermal pain from a noxious heat stimulation and experience of allodynic pain following an innocuous tactile sensation imparted by air puffs. Activations in SI and SII were observable at high threshold of FDR $q<0.05$. The activation in primary somatosensory cortex were similarly located in the face location but in adjacent architectonic areas. The thermal pain activation straddled area 3b and area 2 of SI while allodynic pain caused SI activation in area 1. The

thermal pain caused activation of SII, anterior part of parietal operculum (PV), anterior insula and cingulate gyrus. The allodynic pain activations, remained confined to area 1 , extending to lateral border of SII. There was hardly any overlap of activation areas in the somatosensory cortex. **Orange** activations are from allodynic response and **Purple** activations are during thermal pain.

Chapter 5: Discussion

We have demonstrated through a set of evoked sensations in an fMRI based experiment, that patients suffering from trigeminal neuralgia and trigeminal neuropathy have characteristic patterns of brain activations, which are distinct and different from those of healthy volunteers. We have also demonstrated that it is possible to identify these characteristics on a single subject analysis from a 3Tesla MRI platform.

The key findings from our experiment are tabulated below:

1. Results show consistency and gross congruency with published research in the area. There are new concepts in analyses used in this research.
2. Micromotion detection is a useful and valid tool for identifying patient events and a surrogate for 'timed patient- event data'. The concept of micromotion detection and its successful application is new in this field of research.
3. The analysis of generic brain activations observed in patients and healthy subjects agree with published research, while the detailed analyses of the activation patterns confirm our hypothesis of existence of a differential pattern of activation in trigeminal nerve mediated pain. The results

demonstrated in this field are novel and add to the existing knowledge in the field.

4. The successful use of all available time course data in a single patient through the symptom cycle provides a putative novel explanation for the pathophysiology of trigeminal neuralgia.

Since description by Ogawa (Ogawa et al.,1990), fMRI has been used extensively to investigate pain conditions. Many fMRI studies (Treede et al.,1999; Peyron et al.,2000; Borsook et al., 2004; Apkarian et al., 2005) in healthy volunteers have established the basic components of the conceptual 'pain matrix' (Melzack 1990). The generally accepted components of the 'pain matrix' are primary somatosensory cortex (S I), secondary somatosensory cortex (S II), anterior insula, parietal ventral area of operculum (part of SII), anterior cingulate gyrus, prefrontal area, and deep grey nuclei of the thalamus & brain stem. The activations of S I, SII, Insula, thalamus are often bilateral. Though the concept of 'pain matrix' has recently been critically appraised (Iannetti and Mourax, 2010), the anatomical connectivity between these regions exists and there is compelling evidence that these brain regions show activity following experimental pain in healthy volunteers with or without pre-sensitisation. The trigeminal system has been investigated by several researchers (Fitzek et al., 2004; Borsook et al., 2004; Mainero et al.,2007; Moulton et al., 2007) as trigeminal neuralgia has been recognised as an 'ideal pathological model' for chronic neuralgic pain conditions. Most of these studies were confined to the identification of activation clusters in brain through tactile stimulation or thermally evoked pain sensation. However chronic pain conditions are associated with changes to the nervous system. This phenomenon is variously described as reorganisation, sensitisation, and neural plasticity. Hence the pain matrix elicited by evoked pains in healthy volunteers is not expected to be the same as in a chronic pain state and one can expect to see a change if reorganisation has happened. It is indeed that some authors have reported such variations (Moisset and Bouhassira, 2007) while others

have been able to demonstrate activations of the classical pain matrix in pathological pain (Schweinhardt et al.,2006).

This work originated from the hypothesis that a difference will exist in the fMRI measured brain activation patterns between a physiologial reponse to tactile and noxious stimuli in healthy subjects and those with trigeminal nerve-mediated pain. Moreover, it was hypothesied that there exist a differential brain activation pattern between types of trigeminal pain. Because of multiple documented changes in cerebral activation in various chronic pain conditions, no further hypotheses regarding the exact nature of the alterations were set a priori, except that they were to be found in the cerebral network forming the 'pain matrix'.

The experiment and analysis

Our result show consistency and gross congruency with reports by other researchers in this field (Fitzek et al., 2004; Borsook et al., 2004; Mainero et al.,2007; Moulton et al., 2007; Moisset et al.,2010). While in most studies the investigators had used a mechanical brush, automatic or manually operated as the tactile stimulation medium, in this research we used air puffs. Air puff stimulation has been used before in humans to elicit a startle response in fMRI experiments (Nuener et al.,2010). Airpuffs provide a simple tactile stimulus with a desired frequency and single uniform direction. It has a distinct advantage over a brush as a tactile stimulator. A brush stimulation not only imparts a tactile sensation, but also generates pressure, texture and surface information which can produce multiple areas of activation in the somatosensory cortex, and the noise of such additional activation can submerge that directly linked to the stimulus under study. Using the air puff method, we demonstrated reproducible and precise Area 2 activation in the primary somatosensory cortex along with area SII of secondary somatosensory cortex in healhy volunteers. Area 2 is known to deal with directional tactile stimulus in primates in studies involving direct cortical recording (Hyvarinen and Poranen 1978) which is still taken as the gold standard method for assigning cortical functions. We also used a standardised thermal pain stimulation. This approach provided ample data from single subject analysis following multiple comparison correction in most of the fMRI experiments using False Discovery Rate (FDR) approach (Benjamini and

Hochberg, 1995). In all our single subject analysis, we have used a FDR $q < 0.05$, which denotes a confidence that 95% of the discovered voxels are true activations, as the starting point for building the activation map. When a lower threshold is used, the activation map is checked for congruency in relation to the time course data. The consistency of our results, the overall agreement of the activation maps with conventional neuroanatomy and, broadly speaking, findings by other researchers, can be seen as a justification for the decision to analyse the results obtained from a small number of subjects (10 volunteers and 11 patients). Similarly, it was deemed justified to divide the patients further into two groups of 9 and 2 according to pathology.

Identification of micromotion and its application to enrich data analysis

3D motion correction using rigid body transformation with respect to a reference volume (the first acquired volume in most cases of fMRI data) is an integral part of fMRI data pre-processing to reduce noise. The algorithm for 3D motion correction is inbuilt within most software packages developed for fMRI data analysis. The 3D motion correction algorithm has sub-millimetre sensitivity to identify motion of the volume scanned by comparing movement of self generated reference points in 6 axes of motion; 3 translations and 3 rotations. Thus motion correction time course graph is at least as sensitive to detect motion as the 'video' of 'video telemetry EEG' used for investigation of epilepsy.

The detection of motion in the time course graph was useful in this experiment on patients with trigeminal neuralgia. It is maintained here that a true unpleasant tactile allodynia or a full triggered neuralgic attack would definitely cause a reflex and protective movement of the head. Though the patients were warned of the movement and were asked to try not to move in the scanner during the experiment, a minor millimetre movement would be unavoidable if a sudden undeclared pain or unpleasantness strikes. We used the signature of this movement on the motion correction graph to corroborate a patient report of tactile allodynia or attack of neuralgia. We have called this 'micromotion' and it is a surrogate representation of

an evoked response from a sensory stimulus. It may be slightly less precise than electromyography (EMG) that a group recently used in conjunction with fMRI to time an evoked response (Nuener et al.,2010). However the temporal resolution of the motion correction time course graph showing micromotion is precise enough to mark the onset of physical motion and match it with the experimental paradigm considering fMRI response has a lag of around 2 seconds (Goebel, 2007) from a change in field potential. This means that, in real time, change of potentials in the ROI for the observed activity had happened 1 volume. The micromotion is used for two purposes in this research.

First, it is used to categorise fMRI runs in trigeminal neuralgia patients into three groups. The nine patients in the neuralgia group were heterogeneous. There was a mix of patients who felt no unusual sensation from the tactile stimulation, while others felt allodynia and one patient went on to develop a neuralgic attack. Such distinct precepts are likely to reflect different neural activations. This information might be otherwise lost if a simple group analysis was undertaken. Micromotion corroboration coupled with patient report allowed us to identify the fMRI runs which would have this information and categorize the set into three subgroups for analysis. The result in fig 4.12 when compared to group analysis of fig 4.11a exemplifies the use of micromotion in data classification and outcome.

Second, the use of micromotion analysis provides a surrogate marker for the time of onset of an evoked response from the sensory stimulus. Once the time of onset of the response was identified on the time course, that point was referenced in each ROI time course data to analyse how the HRF in them has responded to the stimulus around that point of time. This allowed us to investigate functional connectivity and temporal relationship between the ROIs in effort to understand the functioning of the network. Fig 4.12, 4.14.4.15 exemplifies the use of micromotion for this purpose. To our knowledge, this approach has not been used or described before.

Activation map analysis

We have demonstrated a variance in the fMRI activation pattern of brain in patients with trigeminal neuralgia and trigeminal neuropathy from that of healthy volunteers when stimulated by a set of thermal pain and innocuous tactile stimulation.

In healthy volunteers, we demonstrated a modality specific segregation of the activation areas within primary (S I) and secondary (S II) somatosensory cortex. Modality specific sensory subregions are well established in other cerebral sensory fields like visual cortex and auditory cortex. Different visual cortical areas are known to subserve perception of linearity, acceleration, color etc (Zeki et al.,1991). The segregation of functions in somatosensory cortex in humans and non human primates had also been described. Hyvarinen and Poranen in 1978 showed that Area 2 of S I contains around 40% of the direction sensitive neurons from the hand area in a monkey (Hyvarinen and Poranen, 1978). Another group showed the presence of parietal ventral (PV) area in the previously known region S II, thus dividing the previous SII into two areas (Disbrow et al., 2000). PV is known to take part in complex information processing from a moving stimulus. Area 3b and Area1 of the primary somatosensory cortex (S I) deal with primary sensation from the cutaneous areas. (Please refer to table 2.1 for complete list of functions of the somatosensory areas).

In the same group we found that air puffs induced a discrete area 1 and area 2 activation which is different from our previous pilot experiment on healthy volunteers in 1.5 T MRI when a brush was used; (published in abstract form only). The activation was bilateral. We also found that the stimulation from thermal pain at T_{pain} caused activation medial anterior to that of tactile stimulation, in the area 1 and 3b spreading to 3a. However activation from this stimulation did not encroach on the activities of air puff on the contralateral primary sensory cortex.

Segregation was also seen in the insular cortex. Thermal pain resulted in activation of the anterior insula only. The cingulate gyrus was activated only during painful stimulation with heat. The diagram below summarises activation maps following innocuous tactile and thermal pain stimulation in the healthy volunteers (results

shown are in the regions comprising the 'pain matrix', including the relevant somatosensory and affective areas).

Volunteers	SI				SII		Insula		Cingulate
	3a	3b	Area1	Area2	PV	SII	Ant	Post	Ant
Thermal pain									
Innocuous tactile									

Fig 5.1 Schematic diagram summarising the activation pattern on cortical areas following the fMRI experiments on healthy volunteers. Red indicate areas where activation was noted.

Activation of primary and secondary sensory cortical areas described above had been extensively reported following stimulation of the trigeminal areas in healthy volunteers (Fitzek et al., 2004; Borsook et al., 2004; Mainero et al.,2007; Moulton et al., 2007), We report the same activations with further detail regarding the segregation of the activations within a region.

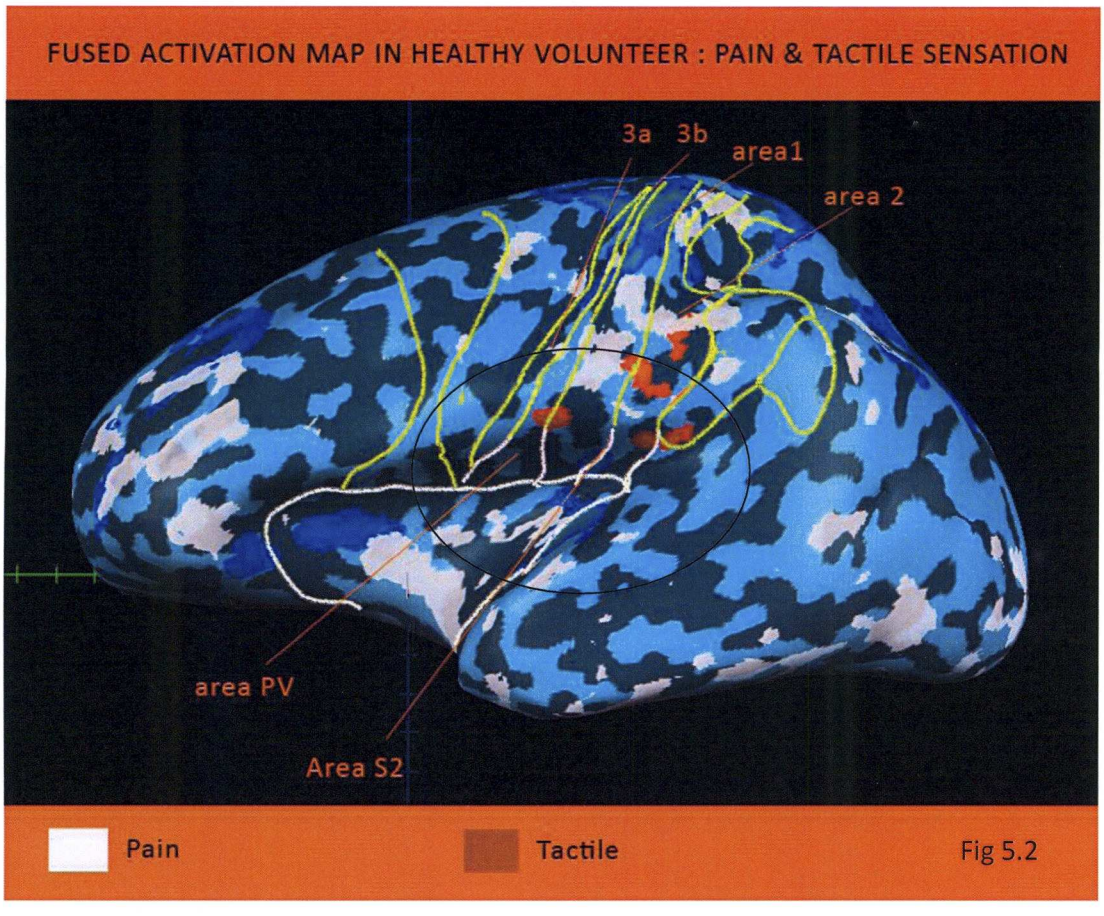

Fig 5.2 Superimposed thermal pain and innocuous tactile stimulation activations - activation maps from the healthy volunteers. Segregation of activity is demonstrated with tactile activations are confined around area 2 of primary somatosensory cortex (SI) , and PV and area S2 of secondary somatosensory cortex (S II). Activations in the medial surface and deep structures are described in chapter 4

In patients with trigeminal neuralgia, the above described modality specificity of the activation is lost specifically within the insular cortex, area 2 of primary somatosensory cortex and cingulate gyrus. In the group analysis as well as in single subject analysis with a high threshold value (FDR $q< 0.05$), the activations following thermal pain encroached extensively into area2 of the S I region and into posterior insula. Tactile stimulation caused activation of the cingulate gyrus and insula. The overall impression from the activation maps suggested that the sensitivity to thermal pain has been comparatively more and there has been activation of areas by innocuous tactile stimulation that would be otherwise activated from a pain stimulation. This observation forms a pattern as all patients had previosly felt the thermode at T_{pain} to be more painful on the face compared to the thumb, contrary to

the observation in volunteer group, who felt otherwise (Fig 4.1b). Taking the thumb as reference, it would mean that patients with neuralgia had a lower threshold for $_{Tpain}$ representing a subclinical hyperalgesia, and this is reflected in the fMRI activation maps. In summary, the neuralgia patients, as a group, and when not showing an allodynic response or having a neuralgic attack demonstrated a near crossover of the activation map for the modality (with healthy volunteers as reference).

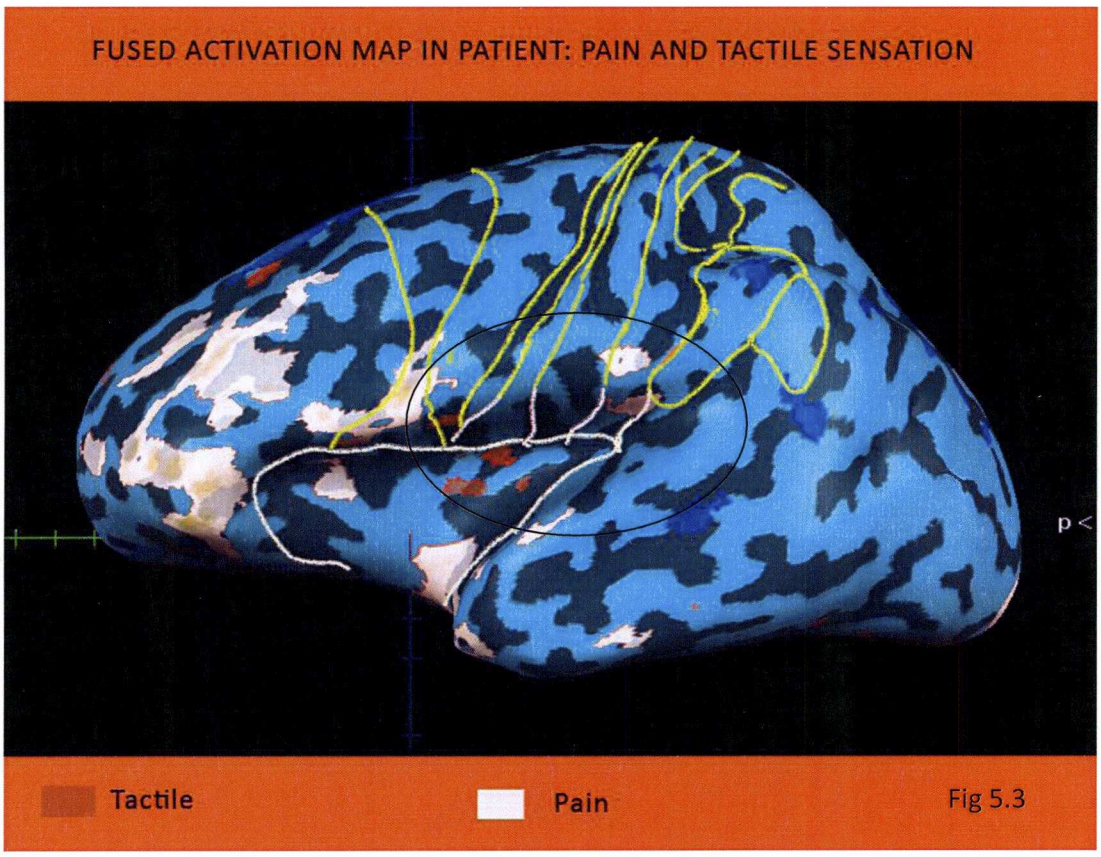

Fig 5.3 Superimposed activation maps of V1 thermal pain and innocuous tactile stimulation in trigeminal neuralgia patients (group analysis). The reversal of activation areas to be noted. Pain activated area 2 while insular cortex being activated by tactile stimulation (compare with Fig 5.2)

Micromotion assisted analysis

As previously mentioned, micromotion assisted categorisation of fMRI data and analysis has not been reported before. The analysis described in fig 4.12 used micromotion to categorise the trigeminal neuralgia group of patients into three.

Broad fMRI group analysis is not very logical in chronic neuropathic patients or in any pathology where the pathophysiology could involve neural structure in a random fashion. Neural plasticity or reorganisation is the basis of chronic neuropathic pain. It cannot be assumed a priori that such reorganisation will happen in a uniform or stereotyped way in every individual. This fact reduces the chances of any group assessment to reveal a consistent pattern of abnormal activations. In a neuropathic condition there could be a common area in an activation map that is shared by both patients and healthy volunteers, accompanied in patients by a spread of the activation from there, which is reorganizational and random. It is the second feature that signifies the underlying disease and not the activation that is common with the healthy volunteers. If it is so, a robust single subject analysis would seem preferable to group analyses in neuropathic pain conditions. The crucial issue is of course the reliability of the data obtained from a single patient. The results of this study give support to the contention that such an analysis is possible, as comparing fig 4.11a and 4.11c, suggests. In fig 4.11c, with a high threshold, the activation map of brain activations following thermal pain is much more populous than in group study, uncovering involvement of a wider area of insula and primary somatosensory cortex in the area 2. Micromotion analysis can help in validating single subject analysis time course graphs by identifying the 'marker event related HRF' in ROIs and increase the confidence of declaring a voxel as active and a cluster as important component of the network. Event related fMRI or recent EMG coupled fMRI (Nuener et al., 2010) can also serve the same purpose.

The above logic also holds true in a group of patients with varied symptoms. A group fMRI analysis would yield a better representative activation map if the homologous symptoms are sub grouped and analysed. We used micromotion to subgroup neuralgia patients. The subgroup analysis showed logical representative progression of activation pattern, which was masked by group analysis. Similar segregation, based on patient's report, had been reported by others (Moisset et al, 2010). We used a further corroborative evidence in the form of micromotion for assisting the segregation.

We found that as a patient moved from being symptom free following a tactile stimulus through to a allodynic phase to a neuralgic attack, the activation map on the somatosensory cortex, which was active in the face area only initially spreads to involve adjoining areas but more importantly the cingulate gyrus as allodynia sets in, a neuralgic attack then cause a discrete and very intense activation in the face area of primary somatosensory cortex with virtual wipe out of the activations clusters from other neighbouring regions except the motor cortex. (fig 4.12)

This sequential finding fits into our current concept of neurovascular coupling and fMRI response. fMRI response is proportional to the LFP to a limit (Logothetis NK. Wandell BA, 2004), and severe pain is known to cause surrounding inhibition (Apkarian et al., 2000).

The schematic representation below summarises the fMRI activation maps in trigeminal neuralgia and trigeminal neuropathic patients.

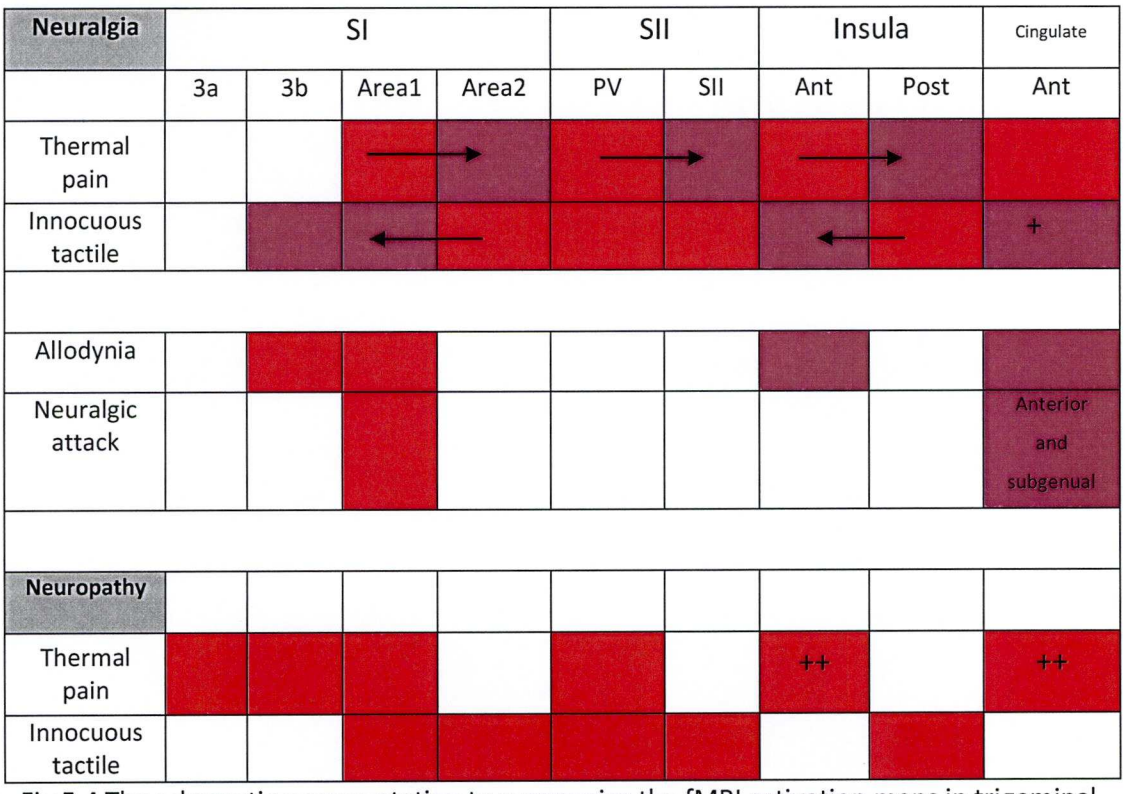

Fig 5.4 The schematic representation to summarise the fMRI activation maps in trigeminal neuralgia and trigeminal neuropathic pain. Red areas are locations where an activation is expected for the modality of the sensation and purple areas are those where it has moved to in the condition. ++ denotes major increase in activity in the area when compared to healthy volunteers.

Trigeminal neuropathy

Activation maps of the patients suffering from trigeminal neuropathy demonstrated a specific activity , when compared with the neuralgia group or healthy volunteer. The fMRI activations of the brain in response to thermal pain was comaparatively more populus on observation (Fig 4.11 a,b&c). This result supports the view that trigeminal neuropathy is associated with a C fibre dysfunction. Unlike neuralgia group, activation pattern did not show a reversal or encroachment in areas of the cortex designated as subserving other modalities of sensation. Thermal pain produced a relatively disproportionate fMRI response, but all activations were within the classical pain matrix. The tactile stimulation activated the S II area, as in healthy volunteers and the cingulate gyrus got activated after thermal pain stimulus.

Multiple time course data assisted single patient analysis through a spectrum of clinical presentations

The above patient provided us an unique opportunity to investigate an acute trigeminal neuralgic attack, triggered during the experiment. The patient report, 3D motion correction time course data, the fMRI experiment protocol time course and the HRFs of the activated voxels were combined to accurately time the neuralgic attack on a time line. Thus we made a simple block design fMRI paradigm to an effective event related fMRI dataset. As a further step, we re-analysed the neuralgic attack data set with a revised event corrected predictor model to unearth the areas which matched activity during the neuralgic attack only. To our knowledge, this is the first report of use of 3D motion correction dataset to 'event mark' a block design paradigm. In subsequent analysis the path of the neuronal activity was traced from brain stem nuclei to the somatosensory cortex (fig 4.13a, 4.14, and 4.15) and elucidate when and why an 'allodynia' became a 'neuralgic' attack. The micromotion confirmed the patient reports. The analysis are summarised in fig 4.13, 4.14 and 4.15 a,b,c.

Evidence over the years have suggested that in trigeminal neuralgia, trigeminal nerve or the trigeminal dorsal root ganglia probably are the pain generator rather than the central nervous system (Gass et al.,1997). Our evidence points to the fact that may be only partly true.

In fig 4.13a, the generation of an allodynic sensation was mapped. An activation peak, which synchronised with the reported allodynia and the micromotion graph was retraced back from the somatosensory cortex to the brain stem, through threshold activation clusters that had emerged from the analysis. The activations with a 95% confidence had appeared at conventional locations in the previously described pain matrix by several authors (Fitzek et al., 2004; Borsook et al., 2004; Mainero et al.,2007; Moulton et al., 2007; Moisset et al.,2010).

We isolated three brain stem nuclei which were active corresponding to a congruent time course graph. The medial most of these, which was also most rosral, fitted with the location of the main sensory nucleus. This nucleus showed a strong high activation peak, compared to the other two, which were at slight caudal and lateral location compared to the main sensory nucleus.

The activation from the brainstem main sensory nucleus of the trigeminal nerve was not reciprocated upsrteam in thalamic nucleus or the somatosensory cortex. In fact in this case of allodynia, that did not progress in to a neuralgic attack, the activation in the thalamus and somatosensory cortex were damped. This damped brain stem activity as it climbed upstream however did produce a cluster on the primary somatosensory cortex in the area 1

In the affective circuit, the anterior cigulate demonstrated an exquisite time matched high activation peak that matched the high activity nucleus of the brain stem.

As mentioned earlier, this patient only repoerted unpleasant allodynic response and no neuralgic attack.

It is thus logical to conclude that the medial 'high activity nucleus' relayed to the affective circuit and in this case the anterior cingulate gyrus. The activities from this nucleus was not relayed to thalamus, as thalamic and S1 activities did not mirror its

response. On the other hand, the lateral activities in the brain stem matched the thalamic activity better. The concept of the existence of an affective and discriminatory circuit in the pain matrix had been proposed and cingulate gyrus activity had been associated with pain before (Rainville et al.,1997). But a non invasive tool, fMRI, had never been used before to demonstrate its existence and activity in a single patient analysis.

The fMRI activations (Fig 4.14) from the neuralgic attack paradoxically show very scanty activation clusters. However the demonstrated activities were discrete, anatomically appropriate and had a congruent time course. The HRF showed the signature of the neuralgic attack with a peak activation, which matched the micromotion time course data.

On relaxing the threshold below FDR $q < 0.05$ some activities become apparent in the brain stem. We thus used an activation mask from the allodynia dataset to query the same anatomic locations for activity information for cingulate gyrus and the thalamus. The brainstem had an activity at the same voxel in the neuralgic attack as during allodynia. The consistency of this voxel suggested it to be one of the main location of trigeminal sensory relay. The HRF analysis of this voxel did not match the most of the peak activity of the other ROIs during the neuralgic attack . The HRF from laterally placed brain stem activation however had a good fit with the activity of the peak activation voxel in primary somatosensory cortex without the very distinguished spike of the neuralgic attack. This may suggest that the laterally placed brain stem nucleus was more actively connected to the lateral (discriminatory system) than the medially placed activation. The mask analysis showed no matching activation cluster in the sensory thalamus or in the anterior cingulate area.

The HRF data of the peak activation voxel in S1 was the only voxel in the activation cluster following the neuralgic attack to have a slightly incongruous activity from the rest of the clusters when compared with micromotion time line. If we accept this voxel as the seed of the activation cluster, then it had to be inferred that the activation from this voxel had spread to the rest of the activated area in S1 by

summation of activity from a suceeding wave of activity or this voxel ignited the rest of the S1 like an epileptic focus.

The re-analysis of the neuralgic attack dataset with the revised predictor model (Fig 4.15a) to unmask the areas that were activated only at the point of neuralgic attack returned a more extensive activation cluster map (Fig 4.15b and c). The fact that the whole of contralateral primary somatosensory cortex in the area1 was activated with the strongest correlation in the face area gave more credence to the hypothesis of an activation wave starting from the peak activation voxel and spreading to the rest of the face area and beyond (Fig 5.5). The activation in the somatosensory cortex following this revised analysis remained confined to the area1 (a single architectonic area). The inability of the initial predictor model to demonstrate these activations was due to the fact that these areas had no activity during the initial part of the experimental fMRI run and came alive when neuralgic attack struck. The second predictor was modelled around the neuralgic attack only with the help of micromotion analysis.

The areas that got actvated as neuralgic attack struck were bilateral area 1 of primary somatosensory cortex (the ipsilateral activity was smaller), anterior cigulate gyrus and neighbouring medial frontal cortex, subfrontal areas and strongest activity being at the subgenual cingulate area on either side (Fig 4.15b). No activation clusters were visible in the brainstem or in the thalamus.

The subgenual cingulate is not described routinely as a part of affective pain neuromatrix. However the result from this single patient analysis of the neuralgic attack showed a very strong activity at this area. In the neuropsychology literature, this area is described to be associated with negative mood and sadness (Helen S et al.,1999). Our study indicated that acute painful experience of a neuralgic attack either evoked these experiences or the interpretation of an acute neuralgic sensation to be painful needed involvement of these areas of the subgenual cingulate as well as more conventionally described anterior cingulate areas.

The strong brain stem upstream correlation that was evident in the allodynia activation map, was not evident during the neuralgic attack. Was this a chance

occurance or was it that all the activity that was observed on S1 area during a neuralgic attack was a locally generated cortical activity triggered by a seed ? The 'light up' of a seed (peak activation voxel) may explain the lack of congruent brain stem and absent thalamic activity during a neuralgic attack. The other explanation for lack of equivalent brain stem activity (as seen during allodynia) or thalamic activity could be surround inhibition following an acute pain (Apkarian et al., 2000). Recently (Moisset et al., 2010) conducted an fMRI study on patients with trigeminal neuralgia and demonstrated the activation of most of the loci on trigeminal somatosensory and affective loci in patients suffering from pain. The activation pattern was similar to the allodynic activation map described in this study. On closer analysis it was evident that none of the patients in the study of Moisset et al experienced a fullblown neuralgic attack. Our study thus is in agreement with the results described by Moisset et al, as it applies to the allodynic part of our analysis.

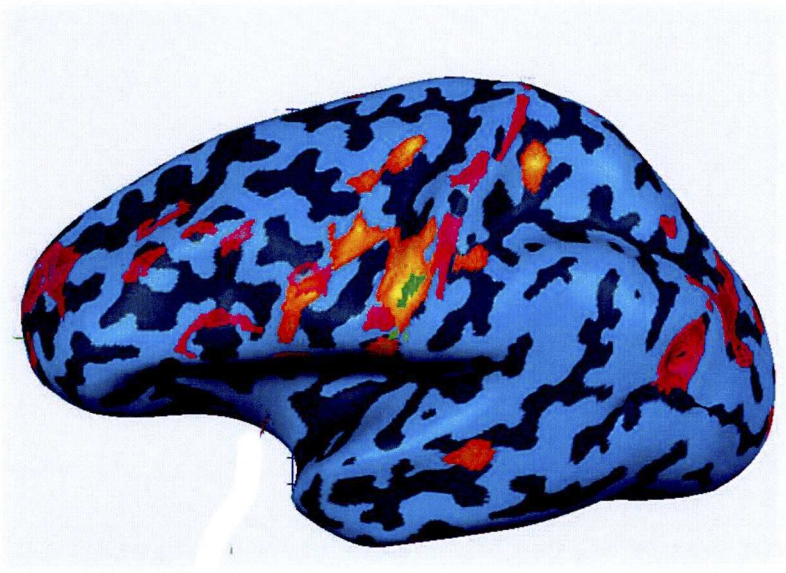

Fig 5.5

Superimposed activation maps of allodynia (orange), neuralgic attack (green) and activations during neuralgic attack following revised predictive protocol (purple). The green cluster , which corresponded to the peak activation voxel during an allodynic response as well, was the initial cluster visible during uncorrected analysis of the neuralgic attack data. It acted as a seed around which the activation during neuralgic attack had spread (purple) along the area1 of the primary somatosensory cortex.

This demonstration also highlights the shortcomings of a fMRI study using 'universal box car design' when elicitation of pain (or any other function) following each epoch of stimulation on – off is not guaranted and only happens during some epochs. This study identified the problem and the solution of the problem for the facial pain studies.

The observations made in this study can be explained by the present knowledge of changes that could happen in the nervous system following a peripheral nerve injury. Trigeminal neuralgia can be described as a chronic constrictive injury (CCI), In CCI, the upregulation of HCN type 1 channels in the cell body of the affected neurons at the dorsal root ganglion and at the site of constriction has now been implicated as the cause of spontaneous firing of these neurons (Chaplan et al., 2003; Jiang et al., 2008). Aberrant excitability of the dorsal root ganglia and dorsal horn has been demonstrated following peripheral nerve damage (Wolf and Mannion, 1999). Obata et al showed that around 12- 25% of the fibres of a nerve (with CCI) is needed to be damaged to sustain a tactile allodynic symptom (Obata et al,. 2003). Changes have been demonstrated in the unconstricted fibres as well.

Changes also happen in the dorsal horn following CCI. The present evidence points to increase in size and number of microglia in proximity of the damaged neuron followed by microglia mediated neurogenic inflammation involving chemokines, cytokines,purinergic receptors in a complex glial neural interaction. In a sciatic nerve inury (SCI) model, these changes would result in hyperalgesia, allodynia and spontaneous pain (Gao and Ji, 2010). Such a response from microglia is local to the dorsal horn and the damaged neuron, and because of the very nature of inflammation, involves the neighbouring neurons as well. This is well exemplified in SCI, when the receptive area of hyperalgesia becomes regional rather than radicular.

Trigeminal neuralgia is an unique pain condition with sharp shooting intense symptom. No other cranial nerve neuralgia is similar and no peripheral spinal nerve injury produces neuralgic symptom akin to trigeminal neuralgia. It is important to appreciate an anatomical speciality that is unique of the trigeminal nerve that may

have caused it to stand apart. Trigeminal nerve is the only peripheral (cranial) sensory nerve where some pain, temperature,crude touch sensation are relayed (in spinal nucleus of trigeminal nerve) in close proximity of the relay centre of highly myelinated fibres of tactile discrimination (in main sensory nucleus) Fig 2.1. In other peripheral sensory nerves, the synaptic relay centre of these two modalities of sensations are anatomically wide apart, with tactile discrimination relaying at the dorsal nuclei in the medulla (nucleus gracilis and cuneatus) and pain and temperature relaying at the dorsal horn (lamina I). The main sensory nucleus of trigeminal nerve is a continuation of the spinal nucleus at its rostral end and there is no anatomical boundary between the two. Hence a microglia mediated neurogenic inflammation at the central terminals of the highly myelinated tactile fibres at main sensory nucleus of trigeminal nerve can theoretically sensitise the neighbouring temperature and nociceptive neurons or vice versa. This is the only location in the central nervous system (other than dorsal root ganglia, which is outside CNS) where a microglia mediated neurogenic inflammation or astroglial activation can potentially cause the degree of thermal hyperalgesia or cross over of modality seen in trigeminal neuralgia. Anywhere upstream from the brain stem will cause spread of symptom into area beyond face, which is not the case in trigeminal neuralgia. CCI causes changes in the dorsal root ganglia and on the axon, at the point of compression.This is also a place where sensitisation of the nociceptive C fibres could happen.

The suggested explanation of the observations made here would be that, CCI of trigeminal nerve sensitise neighbouring neurons at the brain stem relay centres. At main sensory nucleus (which most often gets activated in fMRI studies). This can cause increased sesitivity to thermal experiment seen by us, and cross sensitivity as seen by our crossing of modality in the activation of fMRI maps in neuralgia patients.

The neurogenic inflammation down stream (brain stem) can change sensitivity of the cortical neurons. For example the temperature, crude touch, and the pain sensitive parts of the cortex (area 1 of primary somatosensory cortex) can be sensitised by neuronal inflammation at spinal nucleus of the trigeminal nerve by a CCI affecting afferent fibres to these areas. It is this part of the cortex thats gets activated first in neuralgic patients, sufferring from allodynia or a neuralgic attack.

The proof of hightened sensitivity of the nociceptive system was also found from the synchronus brain stem and anteror cingulate activity demonstrated in allodynia response. During an allodynia, the peripheral stimulus caused the network to activate in harmony, activating the sensitised parts rather than the normal area attributed to the modality. The pain of the allodynia could be attributed to the activation of the anterior cingulate gyrus.

The neuralgic attack could be described as a progression from an allodynic activity. This study suggested that the neuralgic attack involved spread of the activation to the surrounding parts of the area 1 of the primary somatosensory cortex around the peak activation area identified during the allodynic response. This sudden spread of activation was not mirrored in the brain stem or thalamus. Hence it was logical to conclude from the present evidence, that the spread of activation in the cortical areas, that was demonstrarted during a neuralgic attack, was a cortical phenomenon. The peak activation voxel, which showed strong activity during an allodynic response acted like an epileptic focus, with activity spreading over the sensitised part of the cortex. The peripheral representative of this 'seed area' could be the clinical trigger point on the face. This also explained the shooting nature of trigeminal pain, suggesting rapid spread of cortical activity from a specific location.The cortical spread was restricted to the area of the cortex that had been probably sensitised by neurogenic inflammation. As in epilepsy, this event could be spontaneous or triggered. However the maintenace of the activity at the 'seed area' was dependant on peripheral stimulus, which would go a long way as an explanation of therapeutic benefit of microvascular decompression and other surgical procedures for trigeminal neuralgia. The clinical responsiveness of trigeminal neuralgia to antiepileptic medications gave credence to the above interpretation of the findings as well.

Chapter 6: Summary and Conclusion

This research has demonstrated that fMRI based single subject analysis can be used in clinical scenario to aid in the diagnosis of pathological conditions.

The prerequisite for such a clinical application was to define criteria for diagnosis and understanding of the aetiopathological background of those criteria.

The research had used innovative adaptation of the air puff as tactile stimulator, which was a key for the generation of near pure tactile stimulation and fMRI activation maps. The concept of identification of micromotion as a surrogate event marker in facial pain studies and its application to enrich data analysis was also a new addition to the methodology of this type of research.

The result demonstrated distinct difference of fMRI activation maps in patients suffering from trigeminal neuralgia and trigeminal neuropathy when compared with that of healthy volunteers. Distinct pattern of fMRI activation were identified for trigeminal neuralgia and an acute neuralgic attack, which was backed by an

aetiopathological reasoning from current accepted knowledge of generation of pain in chronic constrictive injury of peripheral nerves, astroglial response and microglia mediated neuronal inflammation. The thermal sensitivity and activation area shift in somatosensory cortex in patients suffering from trigeminal neuralgia had not been demonstrated before.

A further insight into events leading to an allodynia -neuralgic attack cycle and demonstration of the change in activation during a neuralgic attack with fMRI is a new a contribution to the chronic pain research.

In conclusion the research proposes that the following criteria could be used to help in the clinical diagnosis of trigeminal neuralgia in situations where a diagnostic dilemma exists.

A comparative criteria with respect to trigeminal neuropathy has also been provisionally proposed, but sufficient number of patients with the diagnosis of neuropathy has not been studied here to be able suggest a firm criteria.

	Neuralgia	Neuropathy
Assessment of thermal sensitivity	Relative hypersensitivity over face compared to palm of hand	Equivocal
fMRI assessment of cortical activation from innocuous Tactile sensation	Shift of activation pattern to contralateral Area 1 of S1 instead of Area2 of S1. , Anterior cingulate activation. Extended activation of S I and additional activation of subgenual cingulate in case of a neuralgic attack	Contralateral activation in Area 2
fMRI assessment of cortical activation from thermal pain sensation	Contralateral activation in area 2 Parietal operculum, Contralateral anterior and posterior Insula, cingulate	Contralateral activation in area 1, PV, anterior insula, cingulate gyrus Vivid activation

Bibliography

Adriaensen H, Gybels J, Handwerker HO, Van Hees J. (1983). Response properties of thin myelinated (A-delta) fibres in human skin nerves. *J Neurophysiol , 49*, 111-122.

Amir R, Michaelis M, Devor M. (1999). Membrane potential oscillation in dorsal root ganglion neurons : Role in normal electrogenesis and neuropathic pain. *Journal of Neuroscience , 19* (19), 8589-8596.

Apkarian AV, Bushnell MC, Treede RD, Zubieta JK. (2005). Human brain mechanisms of pain perception and regulation in health and disease. *Eur J Pain , 9*, 463-484.

Apkarian AV, Shi T, Bruggemann J, Airapetian LR. (2000). Segregation of Nociceptive and Non-nociceptive Networks in the Squirrel Monkey Somatosensory Thalamus. *Journal of Neurophysiology , 84* (1), 484-494.

Araque A, parpura V, Sanzgiri RP, Haydon PG,. (1999). Tripartite synapses: glia the unacknowledged partner. *Trends in neurosciences , 22*, 208-15.

Baliki MN, Geha PY, Apkarian AV, Chialvo DR. (2008). Beyond feeling : chronic pain hurts the brain, disrupting default mode network dynamics. *Journal of Neuroscience , 28* (6), 1398-403.

Barker FG, Jannetta PJ, Bissonette DJ, Larkins MV, Jho HD. (1996). The longterm outcome of microvascular decompression for trigeminal neuralgia. *New Engl J med , 334*, 1077-83.

Baumgartner U, Iannetti GD, Zambreanu, Stoeter P, Treede RD, Tracey I. (2010, Aug 25). Multiple somatotopic representation of heat and mechanical pain in the operculo insular cortex: a high resolution fMRI study. *J Neurophysiology* , Epub.

Beaver DL. (1967). Electron Microscopy of the Gasserian ganglion in trigeminal neuralgia. *J Neurosurg , 26*, 138-50.

Benjamini Y, Hochberg Y. (1995). Controlling the false discovery rate: a practical and powerful approach to multiple testing. *Journal of the Royal Statistical Society , 57* (1), 289-300.

Bingel U, Tracey I. (2008). Imaging CNS modulation of pain in humans. *Physiology , 23*, 371-80.

Borsook D, Burstein R, Becerra L. (2004). Functional Imaging of the Human trigeminal system: Oppurtunities for new insights into pain processing in health and disease. *Journal of Neurobiology , 61* (1), 107-125.

Borsook D, DaSilva A, Ploghaus A, Becerra L. (2003). Specific and Somatotopic Functional Magnetic Resonance Imaging Activation in the Trigeminal Ganglion by Brush and Noxious Heat. *The Journal of Neuroscience , 23* (21), 7897-7903.

Bouhassira D, lanteri-Minet M, Attal N, Laurent B, Touboul C. (2008). Prevalence of chronic pain with neuropathic characteristics in the general population. *Pain , 136*, 380-87.

Bowler JV. (2000). Cerebral Blood Flow. In H. R. Crockard A (Ed.), *Neurosurgery: scientific basis of clinical practice* (3 ed., Vol. 1, pp. 127-141). Blackwell Science.

Bowsher D, Miles JB, Haggett CE, Eldridge PR. (1997). Trigeminal neuralgia, a quantitative sensory perception threshold study in patients who have not undergoneprevious invasive procedures. *J Neurosurg , 86*, 190-2.

Brooks JCW, Nurmikko TJ, Bimson WE, Singh KD, Roberts N. (2002). fMRI of thermal pain: Effects of stimulus laterality and attention. *Neuroimage , 15*, 293-301.

Brown AG, Iggo A. (1967). A quantitative study of cutaneous receptors and afferent fibres in the cat and rabbit. *J Physiol , 193*, 707-733.

Buckner RL, Andrews-Hana JR, Schacter DL. (2008). Brains default network: anatomy, function and relevance to disease. *Ann N Y Acad Sci , 1124*, 1-38.

Bullock TH. (1997). Signals and signs in the nervous system: the dynamic anatomy of electrical activity is probably information rich. *Proc. Natl. Acad. Sci. , USA 94*, 1-6.

Bushnell MC, Duncan GH, Dubner R, He LF. (1984). Activity of trigeminothalamic neurons in medullary dorsal horn of awake monkeys trained in thermal discrimination task. *Journal of Neurophysiology , 52*, 170-187.

Cain DM, Khasabov SG, Simone DA. (2001). Response properties of mechanoreceptors and nociceptors in mouse glabrous skin: an in vivo study. *J Neurophysiol , 85*, 1561-1574.

Catalano SM, Shatz CJ. (1998). Activity dependant cortical target Selection by thalamic axons. *Science , 281*, 559-562.

Caterina MJ, Leffler A, Malmberg AB, Martin WJ, Trafton J, Petersen-Zeitz KR, Koltzenburg M, Basbaum Al, Julius D. (2000). Impaired nociception and pain sensation in mice lacking the capsaicin receptor. *Science , 288*, 306-313.

Chaplan SR, Guo HQ, LeeDH, Luo L, Liu C, Kuei C, Velumian AA, Butler MP, Brown SM, Dubin AE. (2003). Neuronal Hyperpolarisation -activated pacemaker channels drive neuropathic pain. *J Neurosci , 23* (4), 1169-78.

Chiapparini L, Ferraro S, Grazzi L,Bussone G. (2010). Neuroimaging in chronic migraine. *Neurological Science , Suppl 1*, S 19-22.

Cohen-Tannoudji M, Babinet C, Wassef M. (1994). Early determination of mouse somatosensory cortex marker. *Nature , 368*, 460-3.

DaSilva AFM, Becerra L, Makris N, Strassman AM, Gonzalez RG, Geatrakis N, Borsook D. (2002). Somatotopic activation in the human trigeminal pain pathway. *Journal of Neuroscience , 22* (18), 8183-8192.

Disbrow E, Roberts T, Krubitzer L. (2000). Somatotopic organisation of cortical fields in the lateral sulcus of Homo Sapiens: evidence for SII and PV. *Journal of Comparative Neurology , 418*, 1-21.

Duvernoy HM, Delon S, Vannson JL. (1981). Cortical Blood Vessels of Human Brain. *Brain Research Bulletin , 7*, 519-79.

Engel SA, Glover GH,Wandell BA. (1997). Retinotopic organisation of human visual cortex and the functional precision of functional MRI. *Cerebral Cortex , 7*, 181-192.

Erzurumlu RS, Murakami Y, Rijili FM. (2010). Mapping the face in the somatosensory Brainstem. *Nature Review , 11* (4), 252-263.

Fitzek S, Fitzek C, Huonker R, Reichenbach JR, Mentzel HJ, Witte OW, Kaiser WA. (2004). Event related fMRI with painful electrical stimulation of the trigeminal nerve. *Magnetic Resonance Imaging , 22*, 205-209.

Fukuchi-Shimogori T, Grove EA. (2001). Neocortex patterning by the secreted signalling molecul FGF8. *Science , 294*, 1071-4.

Gao YJ, Ji RR. (2010). Chemokines, neronal-glial interactions, and centra processing of neuropathic pain. *Pharmacol Ther , 126* (1), 56-68.

Gardner WJ, Miklos MV. (1959). Response of trigeminal neuralgia to decompression of sensory root: discussion of cause of trigeminal neuralgia. *JAMA , 170*, 1773-6.

Gass A, Kitchen N, Macmanus DG, Moseley IF, Hennerici MG, Miller DH. (1997). Trigeminal Neuralgia in patients with multiple sclerosis: lesion localisation with magnetic resonance imaging. *Neurology , 49*, 1142-4.

Gelnar PA, Krauss BR, Szeverenyyi NM, Apkarian AV. (1998). Finger tip representation in the human somatosensory cortex: An fMRI study. *Neuroimage , 7*, 261-283.

Genovese CR, Lazar NA, Nichols T. (2002). Thresholding of statistical maps in functional neuroimaging using the false discovery rate. *Neuroimage , 4*, 870-8.

Geyer S, Schormann T, Mohlberg H, Zillies K. (2000). Area 3a, 3b,and 1 of human primary somatosensory cortex. *Neuroimage , 11*, 684-696.

Gitton Y, Cohen-Tannoudji M, Waseef M. (1999). Role of thalamic axons in the expression of H-2Z1, a mouse somatosensory cortex specific marker. *Cerebral Cortex , 6*, 611-20.

Goebel R. (2007). Localisation of brain activity using functional magnetic resonance imaging. In S. C (Ed.), *Clinical Functional MRI* (pp. 11-49). Berlin: Springer.

Hammeke TA, Yetkin FZ, Mueller WM, Morris GL, Haughton VM. (1994). Functional Magnetic Resonance Imaging of somatosensory stimulation. *Neurosurgery , 35*, 677-681.

Helen S, e. a. (1999). Reciprocal limbic cortical function and negative mood: Converging PET findings in depression and normal sadness. *American Journal of Psychiatry , 156*, 675-682.

Hodge LK, Klassen MP, Han BX, Yiu G, Hurrell J, Rousseau G, Lemaigre F, Tessier- Lavigne M, Wang F. (2007). Retrograde BMP sigmnalling regulates trigeminal sensory neuron identities and the formation of precise face maps. *Neuron , 55* (4), 572-586.

Hunt PS, Mantyh PW. (2001). The molecular dynamics of pain control. *Nature reviews: neuroscience , 2*, 83-91.

Hyvarinen J, Poranen A. (1978). Movement sensitive and direction and orientation selective cutaneous receptive fields in the hand area of the post central gyrus in monkeys. *Journal of Physiology , 283*, 523-37.

Iadecola C, Yang G, Ebner TJ, Chen G. (1997). Local and propagated vascular responses evoked by focal synaptic activity in cerebellar cortex. *Journal of Neurophysiology , 78*, 651-59.

Iannetti GD, Mourax A. (2010). From neuromatrix to pain matrix and back. *Experimantal Brain Research , 1*, 1-12.

Iannetti GD, POrro CA, Pantano P, Romanelli PL, Galeotti F, Cruccu G. (2003). Representation of different trigeminal divisions within the primary and secondary human somatosensory cortex. *Neuroimage , 19*, 906-12.

Inan M, Crair MC. (2007). Development of Cortical Maps: Perspective from Barrel Cortex. *The Neuroscientist , 13* (1), 49-61.

Inque K, Tsuda M. (2009). Microglia and Neuropathic Pain. *Glia , 57*, 1469-79.

Jannetta PJ. (1977). Treatment of trigeminal neuralgia by suboccipital trantentorial cranial operation. *clinical neurosurgery , 24*, 538-49.

Jenkinson M. (2001). Improved unwarping of EPI images using regularised BO maps. *Neuroimage , 13* (6), S165.

Jensen KF, Killackey HP. (1987). Terminal arbors of axons projecting to somatosensory cortex of the adult rat The altered morphology of the thalamocortical afferents following neonatal infra orbital nerve cut. *Journal of Neuroscience , 7*, 3544-53.

Jiang YQ, Xing GG, Wang SL, Tu HY, Chi YN, Li J, Liu FY, Wan Y. (2008). Axonal accumulation of hyperpolarisation activated cyclic nucleotide gated cation channels contribute to mechanical allodynia after peripheral nerve injury in rat. *Pain , 137* (3), 495-506.

Kaas JH, Nelson RJ, Sur M, Lin CS, Merzenich MM. (1979). Multiple representation of the body within primary somatosensory cortex of the primates. *Science , 204*, 521-23.

Kacem K, Lacombe P, Seylaz J,Bonvento G. (1998). Structural organisation of the perivascular astrocyte endfeet and their relationship with the endothelial glucose transporter: A confocal microscopy study. *Glia , 23*, 1-10.

Kress M, Koltzenburg M, Reeh PW, Handwerker HO. (1992). Responsive and functional attributes of electrically localised terminals of cutaneous C-fibres in vivo and in vitro. *J Neurophysiol , 68*, 581-595.

Krubitzer L, Clarey J, Tweedale R, Elston G, Calford M. (1995). A redefinition of somatosensory areas in the lateral sulcus of macaque monkeys. *Journal of Neuroscience , 15* (5), 3821-3839.

Kruger L, Perl ER, Sedivec MJ. (1981). Fine structure of myelinated mechanical nociceptor endings in cat hairy skin. *J Comp Neurol , 198*, 137-154.

Kunc Z. (1970). Significant factors pertaining totrigeminal tractotomy in trigeminal neuralgia, pathogenesis and pathophysiology. In W. A. Hassler R (Ed.). Stuttgart: Thieme.

Kuyper H.G.J.M. (1958). Corticobulbar connection to the pons and lower brainstem in man: an anatomical study. *Brain , 81*, 364-368.

Laguardia JJ,Cohr RJ, Gilden DH. (2000). Numbers of neurons and nonneuronal cells in the trigeminal ganglia. *Neurology Research , 22*, 565-66.

Lee J. (2008). Brain Stem. In S. Susan (Ed.), *Anatomical Basis of Clinical Practice* (pp. 280-281). Churchill livingstone-Elsevier.

Lewin GR, Moshourab R. (2004). Mechanosensation and pain. *J Neurobiol , 61* (1), 30-44.

Lin W, Kuppusamy K, Haacke EM, Burton H. (1996). Functional MRI in human somatosensory cortex activated by touching textured surfaces. *J Magn Reson Imag , 6*, 565-572.

Logothetis NK. (2002). The neural basis of the blood oxygen level dependent functional magnetic resonance imaging signal. *Philos. Trans. R Soc. Lond B Biol. Sci. , 357*, 1003-37.

Logothetis NK, Pauls J, Augath M, Trinath T,Oeltermann A. (2001). Neurophysiological investigation of the basis of fMRI signal. *Nature , 412* (6843), 128-30.

Logothetis NK. Wandell BA. (2004). Interpreting the BOLD signal. *Annu Rev Physiol. , 66*, 735-769.

Luo L, Chang L, Brown SM, Ao H, Lee DH, Hiquera ES, Dublin AE, Chaplan SR. (2007). Role of peripheral hyperpolarisation activated cyclic nucleotide modulated channel pacemaker channels in acute and chronic pain models in the rat. *Neuroscience , 144* (4), 1477-85.

Magistretti PJ, Pellerin L,Rothman DL, Shulman RG. (1999). Neuroscience: Energy on demand. *Science , 283*, 496-497.

Mainero C, Zhang WT, Kumar A, Rosen BR, Sorenson GA. (2007). Mapping the spinal and supraspinal pathways of dynamic mechanical allodynia in human trigeminal system using cardiac gated fMRI. *Neuroimage , 35*, 1201-10.

Manger P, Woods TM, Munoz A, Jones EG. (1997). Hand/Face border as a limiting boundary in the body representation in monkey somatosensory cortex. *Journal of Neuroscience , 17* (16), 6338-6351.

Maniero C, Zhang WT, Kumar A, Rosen BR, Sorensen AG. (2007). Mapping the spinal and supraspinal pathways of dynamic mechanical allodynia in the human trigeminal system using cardiac gated fMRI. *Neuroimage , 35*, 1201-1210.

Mathiesen C, Caesar K, Lauritzen M. (2000). Temporal Coupling between neuronal activity and flow in rat cerebellar cortex as indicated in field potential analysis. *Journal of Physiology , 523*, 235-46.

May A, Matharu M. (2007). New insights into migraine: application of functional and structural imaging. *Current Opinion in Neurology , 3*, 306-9.

McMahon SB, Koltzenburg M. (1990). Novel classes of nociceptors: beyond Sherrington,. *Trends Neurosci , 13*, 199-201.

Melzack R. (1990). Phantom limb and the concept of a neuromatrix. *Trends in Neurosciences , 13* (3), 88-92.

Melzack R, Wall PD. (1965). Pain Mechanism: a new theory. *Science , 150* (699), 971-9.

Merskey H, Bogduk N. (1994). Classification of chronic pain. In *Description of chronic pain synderomes and definition of pain terms* (pp. 59-7). Seatle: IASP press.

Meyer RA, Davis KD, Cohen RH, Treede RD, Campbell JN. (1991). Mechanically insensitive afferents (MIAs) in cutaneous nerves of monket. *Brain Res , 561*, 252-261.

Miles JB, Eldridge PR, Haggett CE, Bowsher D. (1997). Sensory effects of microvascular decompression in trigeminal neuralgia. *J Neurosurg , 86* (2), 193-6.

Moisset X, Villain N, Ducrex D, Serrie A, Cunin G, Calade D, Calvino B, Bouhassira D. (2010, Jul 5). Functional Brain imaging of trigeminal neuralgia. *Eur J Pain* , E pub ahead of print.

Moisset X,Bouhassira D. (2007). Brain imaging of neuropathic pain. *Neuroimage , 37* ((suppl 1)), S80-8.

Moulton EA, Pendse G, Morris s, STrassman A, Aiello-Lammens M, Becerra L, Borsook D. (2007). Capsaicin induced thermal hyperalgesia and sensitisation in the human trigeminal nociceptive pathway: an fMRI study. *NeuroImage , 35*, 1586-1600.

Napadow V, LaCount L, Park K, As-Sanie S, Clauw DJ, Harris RE. (2010). Intrinsic brain connectivity in fibromyalgia is associated with chronic pain intensity. *Arthritis Rheum , 62* (8), 2545-55.

Nguyen BT,Tran DT, Hoshiyama M,Inui K, Kakigi R. (2004). Face representation in the human primary somatosensory cortex. *Neuroscience Research , 50*, 227-32.

Nuener I,Stocker T, Kellermann T,Ermer V, Wegener HP, Eickhoff SB, Schneider F, Shah NJ. (2010). Electrophysiology meets fMRI: Neural correlates of startle reflex assessed by simultaneous EMG-fMRI data acquisition. *Human Brain Mapping* (E pub).

Nurmikko TJ, Eldridge PR. (2001). Trigeminal Neuralgia - pathophysiology,diagnosis and current treatment. *British Journal of Anaesthesia , 87* (1), 117-32.

Obata K, Yamanaka H, Fukuoka T, Yi D, Tokunaga A, Hashimoto N, Yoshikawa H, Noquchi K. (2003). Contribution of injured and uninjured dorsal root ganglion neurons to pain behaviour

and the changes in gene expression following chronic constriction injury ofthe sciatic nerve in rats. *Pain , 101* (1-2), 65-77.

Ogawa S, Lee TM, Nayak AS, Glynn P. (1990). Oxygen sensitive contrast in magnetic resonance image of rodent brain at high magnetic fields. *Magnetic Resonance Medicine , 14*, 68-78.

Ogawa S, LeeTM, Kay AR, Tank DR. (1990). Brain Magnetic Resonance Imaging with contrast dependant on blood oxygenation. *Proceeding of National Academy of Science , USA 87*, 9868-72.

Ogawa S, LeeTM, Stepnoski R, Chen W, Zhu XH, Ugurbil K. (2000). An approach to probe some neural systems interaction by functional MRI at neural time scale down to milliseconds. *Proceeding of National Academy of Science , USA 97*, 11026-31.

O'Leary DD, Borngasser D. (2006). Cortical Ventricular zone progenotors and their progeny maintain spatial relationship and radial patterning during preplate development indicating an early protomap. *Cerebral Cortex , 16* (suppl 1), 46-56.

Ostrowsky K, Magnin M, Ryvlin P, Isnard J, Guenot M, Mauguiere F. (2002). Representatation of pain and somatic sensation in the human insula: a study of responses to direct electrical cortical stimulation. *Cerebral Cortex , 12*, 376-385.

Penfield W, Boldrey E. (1937). Somatotopic motor and sensory representation in the cerebral cortex of man as studied by electrical stimulation. *Brain , 60*, 389-443.

Peyron R, Laurent B, Garcia -Larrea L. (2000). Functional imaging of brain responses to pain, A review and meta analysis. *Neurophysiology Clinic , 30*, 263-88.

Peyron R, Laurent B, Garcia-Larrea L. (2000). Functional imaging of brain responses to pain. A review and meta-analysis. *Neurophysiology Clinic , 30* (5), 263-88.

Pons TP, Garraghty PE, Cusick CG, Kaas JH. (1985). The Somatotopic organisation of area 2 in macaque monkeys. *Journal of comparative Neurology , 241*, 445-66.

Rainville P, Duncan GH, Price DD, Carrier B, Bushnell MC. (1997). Pain affect encoded in human anterior cingulate but not somatosensory cortex. *Science , 277*, 968-971.

Ravens JR. (1974). Anastomoses in the vascular bed of the human cerebrum. In C. -N. J (Ed.), *Pathology of Cerebral Microcirculation* (pp. 26-32). Berlin: De Gruyter.

Reina-De l, Rodriguez-Baeza A, Sahuquillo-Baris J. (1998). Morphological characteristics and distribution pattern of arterial vessels in human cerebral cortex: a scanning electron microscope study. *Anat Rec , 251*, 87-96.

Rengachary SS . (1996). *Neurosurgery* (Second ed., Vol. 1). (W. R. SS, Ed.) Mcgraw-Hill.

Sarsam Z, Garcia-Finana M ,Nurmikko TJ, Varma TR, Eldridge P. (2010). The long term outcome of microvascular decompression. *British journal of neurosurgery , 24* (1), 18-25.

Scadding J. (2000). Pian and Painful States. In H. R. Crockard A, *Neurosurgery, Scientific Basis of Clinical Practice* (Vol. 1, pp. 245-261). Blackwell Science.

Schmidt R, Schmelz M, Ringkamp M, Torebjork E, Handwerker H. (1995). Novel classes of responsive and unresponsive C nociceptors in human skin. *J Neurosci , 15*, 333-341.

Schweinhardt P, Glynn C, Brooks J, Mcquay H, Jack T. (2006, 32). An fMRI study of cerebral processing of brush evoked allodynia in neuropathic pain patients. *Neuroimage* , 256-65.

Selman RW, Lust WD, Ratcheson RA. (1996). Cerebral Blood Flow. In R. S. Wilkins RH (Ed.), *Neurosurgery* (2 ed., Vol. 2, pp. 1997-2006). McGraw-Hill.

Servos P, Engel SA,Gati J, Menon R. (1999). fMRI evidence for an inverted face representation in human somatosensory cortex. *Neuroreport , 10*, 1393-95.

Silver IA. (1978). Cellular microenvironment in relation to local blood flow. *Ciba foundation symposium , 56*, 49-67.

Smoliar E, Smoliar A, Sorkin L, Belkin V. (1998). Microcirculatory bed of the human trigeminal nerve. *Anat Rec , 250*, 245-49.

Stohr M, Petruch F. (1979). Somatosensory evoked potential following stimulation of trigeminal nerve in man. *journal of Neurology , 220*, 1393-95.

Talairach J, Tournoux P. (1988). *Co-planer stereotaxic atlas of the human brain.* New York: Thieme.

Tolias As, Smirnakis SM, Augath AS, Trinath T, Logothetis NK. (2001). Motion processing in the macaque: revisited with functional magnetic resonance imaging. *Journal of Neuroscience , 21*, 8594-601.

Tracey I, Bushnell MC. (2009). How neuroimaging studies have challenged us to rethink: is chronic pain a disease. *J Pain , 10* (11), 1113-20.

Treede RD, Apkarian AV, Bromm B, Greenspan JD, Lenz FA. (2000). Cortical representation of pain: functional characterisation of nociceptive areas near the lateral sulcus. *Pain , 87* (2), 113-9.

Treede RD, Kenshalo DR, Gracely RH, Jones AK,. (1999). The cortical representation of pain. *Pain , 79*, 105-11.

Van der Loos H, Woolsey TA. (1973). Somatosensory Cortex: Structural alteration following early injury to sense organs. *Science , 179*, 395-98.

Verkhratsky A, Butt A. (2007). *Glial Neurobiology.* John Wiley and sons, LTD.

Wan Y. (2008). Involvement of hyperpolarisation activated cyclic nucleotide gated cation channels in dorsal root ganglion. *Sheng Li Xue Bao , 60* (5), 579-80.

Weidner C, Schmelz M, Schmidt R, Hansson B, Handwerker HO, Torebjork HE. (1999). Functional attributes discriminating mechano-insensitive and mechano-responsive C nociceptors in human skin. *J Neurosci , 19*, 10184-10190.

Wiesendanger M, Miles TS. (1982). Ascending pathways of low threshold muscle afferents to the cerebral cortex and its possible role in motor control. *Physiology review , 62*, 1223-1270.

Wolf CJ, Mannion RJ. (1999). Neuropathic pain, Aetiology, symptoms,mechanisms and management. *Lancet , 353*, 1959-64.

Woolsey CN, Erickson TC, Gibson WE. (1979). Localisation in somatic sensory and motor areas of human cerebral cortex as determined by direct recording of evoked potentials and electrical stimulation. *Journal of Neurosurgery , 51*, 476-506.

Zeki S, Watson JD, Lueck CJ, Friston KJ, Kennard C, Frackowiak RS. (1991). A direct demonstration of functional specialisation in human visual cortex. *Journal of Neuroscience, 11*, 641-49.

stimulation. This was specially confirmatory as the frequency of the movement did not relate to any physiological cause.

The tactile allodynia and unpleasantness short of a full blown neuralgic pain is a common finding in patients with trigeminal neuralgia. Trigeminal neuralgia or 'tic douloureux' as it is also known, is associated with movement in facial muscles when the pain strikes. Unpleasantness or pain generated by air puffs can cause small movements of the head by reflex action during the scan. As air puff generator or the air-tubes had no physical contact with the patient, any movement noticed was a direct result of this reflex micromovement of the head.

The movement seen was validated by 'patient reporting' of pain or unpleasantness. The movement had high sensitivity in trigeminal neuralgia patients in our experimental set up. It was present 100% of the times when a neuralgic patient had reported a response following the fMRI run. Micromotion was also seen in the run where patient reported triggering of a neuralgic attack.